World Conference on Interventional Oncology (WCIO) 2018

June 7–10, 2018, Boston, Massachusetts

Paper 1: Inhibition of PI3K/mTOR/AKT Signaling in Combination with Thermal Ablation Decreases Tumor Growth in a Mouse Model of Hepatocellular Carcinoma

D.E. Jondal[1], S.M. Thompson[1], K.A. Butters[1], B.E. Knudsen[1], J.L. Anderson[1], L.R. Roberts[2], M.R. Callstrom[1], D.A. Woodrum[1]; [1]*Radiology, Mayo Clinic, Rochester, MN;* [2]*Gastroenterology and Hepatology, Mayo Clinic, Rochester, MN.*

Objectives: Prior studies have shown that PI3K/mTORC2-dependent AKT signaling is a critical mediator of hepatocellular carcinoma (HCC) cell survival to thermal ablation induced heat stress. The aim of the present study was to test the hypothesis that inhibition of PI3K/mTOR/AKT pathway increases thermal ablation induced HCC tumor killing in vivo.

Methods: In an IACUC-approved study, athymic nude mice bearing subcutaneous N1S1 HCC tumors (10mm maximum diameter) were randomized to receive the oral PI3K/mTOR inhibitor NVP-BEZ235 (50mg/kg) or vehicle control (NMP/PEG) on a single or two-dose schedule: 1 hour prior to ablation ± 24 hours post-ablation. Mice were then randomized to receive an intentional subcurative laser thermal ablation at 1.5W for 45s (N≥ 9 per group) or sham ablation (N≥ 9 per group). Tumor growth was monitored by caliper measurements up to 7 days post-ablation. Tumor volumes were compared between treatment groups (vehicle + sham, vehicle + ablation, BEZ235 + sham, BEZ235 + ablation).

Results: There was a significant decrease in HCC tumor volume by day 7 post-ablation in the BEZ235+ablation (696±164mm^3) group compared to vehicle + sham (1689±153 mm^3), vehicle + ablation (1040±143 mm^3) and BEZ235 + sham (1121±165 mm^3) groups ($p<0.001$, $p<0.05$, $p<0.05$, respectively). However, there was no significant difference in tumor volume in the BEZ235+ablation group between the single and double BEZ235 dosing schedule ($p=0.81$). There was a significant decrease in tumor volume in the vehicle+ablation and BEZ235+sham compared to vehicle+sham ablation ($p<0.02$, both). There was no significant difference in tumor volume between the vehicle+ablation and BEZ235+sham groups ($p=0.87$).

Conclusions: These data suggest that single-dose adjuvant PI3K/mTOR/AKT pathway inhibition prior to thermal ablation decreases post-ablation HCC tumor growth. Further pre-clinical studies in other HCC models are needed to determine the generalizability of these findings and to optimize the drug dosing and schedule prior to translation to clinical trials.

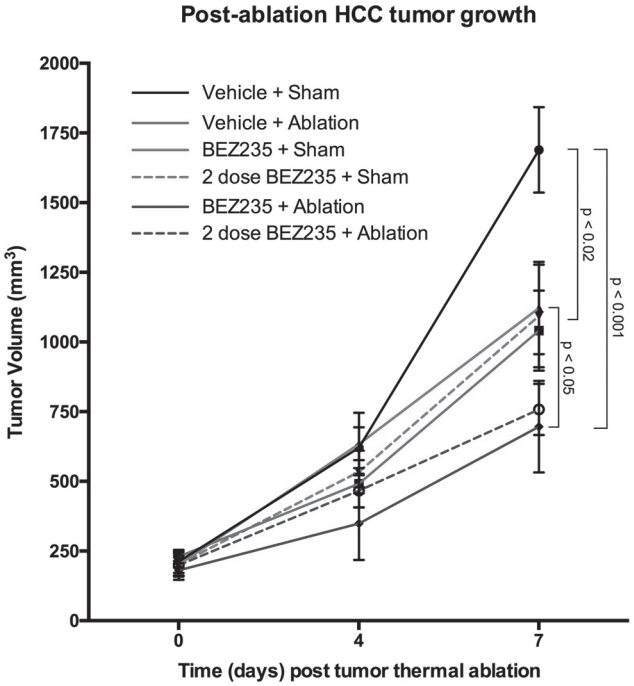

Paper 2: Safety and Feasibility of Integrating Yttrium-90 Radioembolization with Capecitabine-Temozolomide for Grade 2 Liver-Dominant Metastatic Neuroendocrine Tumors (CapTemY90) - Final Report

M.C. Soulen[1], U.R. Teitelabum[2], D. van Houten[1], G. Deitrick[1], N. Damjanov[2], K. Cengel[3], D. Metz[4]; [1]*Radiology, University of Pennsylvania, Philadelphia, PA;* [2]*GI Oncology, University of Pennsylvania, Philadelphia, PA;* [3]*Radiation Oncology, University of Pennsylvania, Philadelphia, PA;* [4]*Gastroenterology, University of Pennsylvania, Philadelphia, PA.*

Objectives: Advanced tumor grade portends poorer disease control with both systemic and liver-directed therapies. An integrated treatment protocol combining capecitibine-temozolomide with yttrium-90 radioembolization (CapTemY90) for patients with liver-dominant grade 2 metastases was designed in the hopes of achieving synergistic improvement in liver disease control with no more than additive toxicities. This report describes the feasibility and safety of this integrated loco-systemic regimen.

Methods: The NET Tumor Board identified 21 patients with unresectable Grade 2 neuroendocrine tumor liver-dominant metastases without contraindications to radioembolization or to CapTem. Initial therapy consisted of capecitabine 600 mg/m2 twice daily for 14 days and temozolomide 150-200 mg/m2 in two divided doses on Days 10-14, with 14 days between cycles. During the initial cycle of CapTem, simulation angiography was performed to measure the hepatopulmonary shunt fraction and exclude non-target hepatoenteric vessels. The dominant lobe was radioembolized on Day 7 of the 2nd cycle of CapTem. For patients with bilobar disease, the other lobe was treated on Day 7 of the 3rd or 4th cycle of CapTem.

Results: 19/21 patients completed the prescribed therapy. Two did not have their planned second lobe radioembolization due to post-embolization toxicities. Adverse events were as expected for each therapy alone, including thrombocytopenia, fatigue, nausea, post-embolization pain and hepatic dysfunction. ORR was 74% in the liver and 55% for extrahepatic tumor. Median PFS was not reached at a mean follow-up of 27 months. PFS at three years was 67%, with 74% progression-free in the liver.

All WCIO abstracts and posters are selected by WCIO coordinators, and are graded via blind peer review based on scientific merit, originality, relevance and clarity.

Conclusions: CapTemY90 is a feasible and safe integrated therapeutic regimen for intermediate-grade liver-dominant NETs. Toxicities were additive. Oncologic outcomes suggest synergy and provided the basis for design of a multicenter Phase 2 trial.

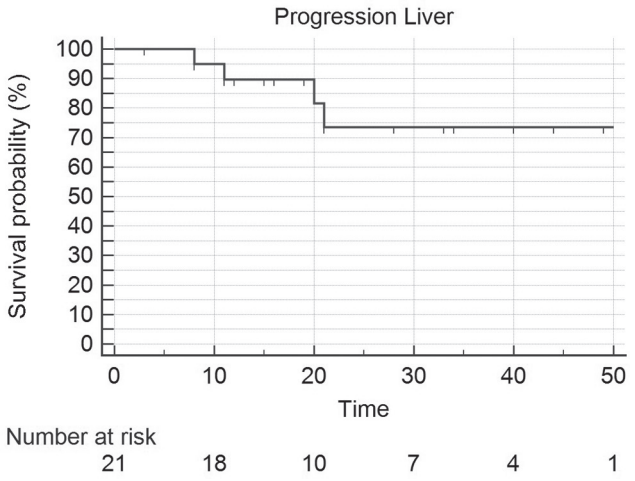

Paper 3: Study of Mobilizable ^{125}I Seed Chain Coaxial Drainage Catheter Placement for Intraluminal Brachytherapy of Malignant Obstructive Jaundice

H. Niu, J. Wang, X. zhang, B. Wang, L. Hao, w. Sun, S. Li; *Minimally invasive surgery, Affiliated Hospital of Shandong Academy of Medical Sciences, Shandong, China.*

Objectives: This retrospective study compared the advantages and disadvantages of mobilizable ^{125}I seed chain coaxial drainage catheter placement and percutaneous transhepatic cholangial drainage (PTCD) in the treatment of malignant obstructive jaundice (MOJ).

Methods: Sixty-three patients with diagnosed MOJ who were randomly assigned to receive treatment with a mobilizable ^{125}I seed chain coaxial drainage catheter placement (experimental group, 35patients) or a conventional PTCD placement (control group, 28patients). The goal of this study was to evaluate total bilirubin(TBIL), direct bilirubin(DBIL), tumor markers (cancer antigen (Ca199), as well as bile duct patency time and survival time in both groups. A p value of less than 0.05 indicated a significant difference.

Results: There were no significant differences between the two groups in terms of baseline characteristics. Mobilizable ^{125}I seed chain coaxial drainage catheter placement and PTCD were successfully performed and well tolerated in 63 patients with MOJ. Serum levels of bilirubin at1 month following the procedure demonstrated no significant difference between the experimental group and the control group. but the decrease of Ca199 in the experimental group was better than those in the control group, the difference was statistically significant (169.9±173.8vs315.9±261.7umol/L). The patency time of bile duct were measured between the two groups after the operation. The median time of bile duct patency was 10±0.53 months (95% CI 8.96–11.04) in the experimental group and 6±0.47 months (95% CI 5.07–6.93) in the control group, respectively. As a result, the bile duct patency of the experimental group was found to be significantly longer than that of the control group($P<0.05$). During follow-up period, none of hematobilia and bile duct injury related to radiation were detected in the experimental after operation. Cholangitis was found in 4 patients in the control group, but controlled after antibiotic treatment. The median survival was significantly longer in experimental group than in control group: 11.05±0.75 versus 7.5±0.42 months, respectively ($P < 0.05$).

Conclusions: Mobilizable ^{125}I seed chain coaxial drainage catheter placement served as a minimally invasive strategy for the prevention of restenosis is feasible and effective for malignant biliary obstruction, and seems to prolong the bile duct patency and survival time.

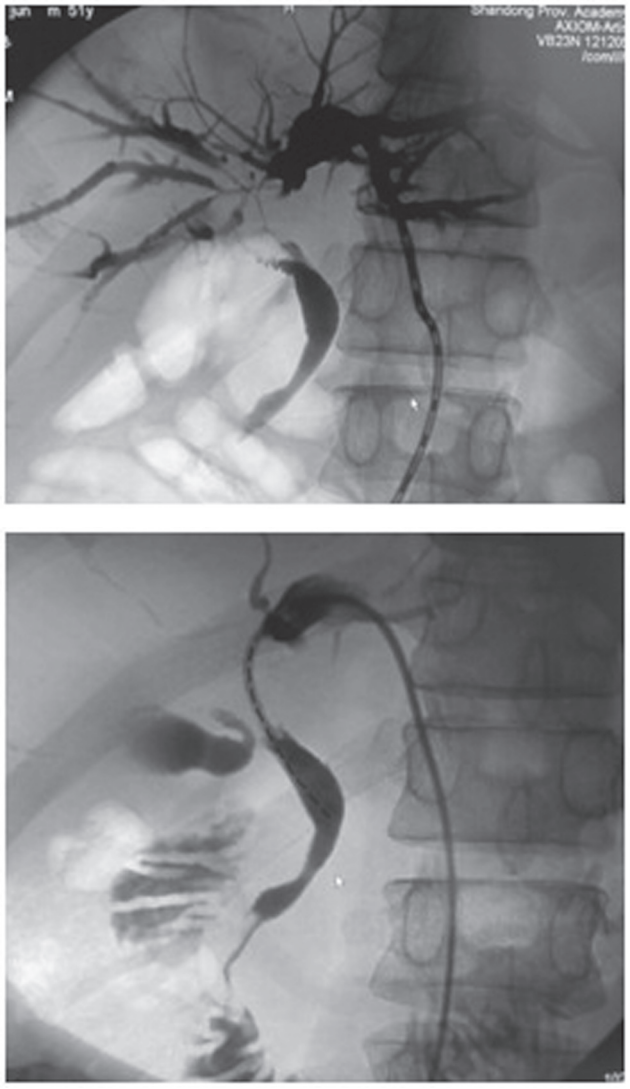

Paper 4: Inflammation Marker as a Biomarker for Overall Survival After Transarterial Chemoembolization: Importance of Neutrophil-to-Lymphocyte Ratio in Hepatocellular Carcinoma

C. Sellers[1], J. Uhlig[1], J. Ludwig[1], J. Pollak[1], T. Taddei[2], S. Stein[3], H.S. Kim[1]; [1]*Department of Interventional Radiology, Yale School of Medicine, New Haven, CT;* [2]*Department of Digestive Diseases, Yale School of Medicine, New Haven, CT;* [3]*Department of Medical Oncology, Yale School of Medicine, New Haven, CT.*

Objectives: To investigate the neutrophil-to-lymphocyte ratio (NLR) as a prognostic biomarker in patients with hepatocellular carcinoma (HCC) treated with transarterial chemoembolization (TACE).

Methods: Patients from the cancer registry diagnosed with HCC from 2005 to 2016 and treated with TACE were investigated. The baseline NLR was calculated within 30 days prior to TACE. ROC curves were used to determine the optimal NLR cut-off point. Patients were then stratified by NLR. Kaplan-Meier curves and Cox proportional hazards models were performed. Tumor and liver reserve parameters were included and analyzed in the MVA.

Results: 155 patients met inclusion criteria. The mean age was 63.5 years (SD 9.1 years). Patients were 83% male (128 patients) and 66% white (103 pts). 67% of patients (103 pts) were Child-Pugh Class (CPC) A. 24% of patients (37 pts) were CPC B, and 9% (14 pts) were CPC C. 61 patients (40%) had AJCC Stage I disease, while 46 patients had Stage II disease (30.1%). 34 patients and 12 patients had Stage III (22.2%) and Stage IV (7.8%) disease respectively. At an NLR cut-off of 3.5, patients in the higher and lower NLR groups did not differ significantly by age, gender, race/ethnicity, CPC score, MELD score, or AJCC stage. Median overall survival (OS) for all TACE patients was 19.7 months (95% CI: 15.9–24.5 mo). Patients with NLR

< 3.5 had an increased median OS (24.5 mo, 95% CI: 19.4–33.9 mo) vs. patients with NLR ≥ 3.5 (median OS 9.6 mo, 95% CI: 6.5-15.9 mo) (p=0.0009). When stratified by AJCC stage, patients with NLR < 3.5 had improved median OS vs. patients with NLR ≥ 3.5 for patients with Stage II (19.7 mo vs. 6.5 mo, p=0.0068) and Stage III (21.0 mo vs. 8.9 mo, p=0.0115) respectively. Baseline NLR did not significantly affect median OS for patients with AJCC Stage I (33.9 mo vs. 23.5 mo, p=0.1603) or Stage IV disease (11.3 mo vs. 6.2 mo, p=0.1942). Univariate analysis demonstrated increased survival for patients with NLR < 3.5 (HR 1.97, 95% CI: 1.30-2.93, p=0.0015) as compared to patients with NLR ≥ 3.5. Multivariate analysis adjusting for age, gender, ethnicity, Child-Pugh score, MELD score, AJCC stage, and alpha-fetoprotein (AFP) demonstrated a survival benefit for patients with a lower baseline NLR (HR 1.83, 95% CI: 1.14-2.90, p=0.0135). Lower AJCC stage and lower AFP were also associated with survival benefits on multivariate analysis.

Conclusions: Higher baseline NLR ratios are associated with decreased survival in HCC patients treated with TACE. Further investigations on inflammatory markers as survival biomarkers with LRT are warranted.

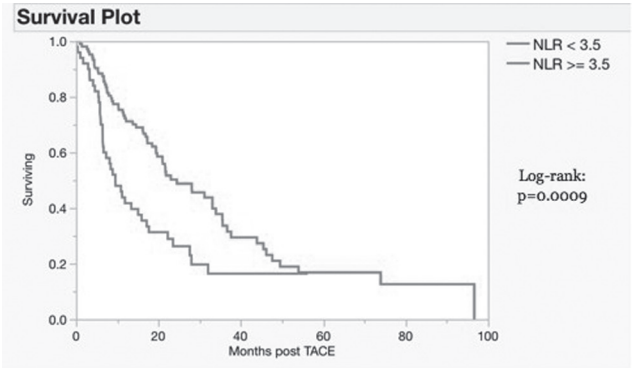

Kaplan-Meier curves for HCC patients with TACE by NLR.

Paper 5: Multicentric Assessment of the Hong Kong Liver Cancer Staging System in Chinese Patients Following Transarterial Chemoembolization as Initial Treatment

B. Zhong[1], G. Teng[1], C. Ni[2], S. Chen[3]; [1]*Center of Interventional Radiology & Vascular Surgery, Department of Radiology, Zhongda Hospital, Southeast University, Nanjing, China;* [2]*Department of Interventional Radiology, First Affiliated Hospital of Soochow University, Suzhou, China;* [3]*Department of Interventional Radiology, Cancer Hospital of Jiangsu Province, Cancer Institution of Jiangsu Province, Nanjing, China.*

Objectives: Recently, the hepatitis B–based Hong Kong Liver Cancer (HKLC) staging system was reported to guide treatment options. We aimed to validate the performance of the HKLC compared with the Barcelona Clinic Liver Cancer (BCLC) staging system in Chinese hepatocellular carcinoma (HCC) patients treated with conventional transarterial chemoembolization (cTACE).

Methods: This retrospective study included patients with HCC who underwent cTACE between January 2008 and December 2016 at three Chinese institutions. Considering no terminal stage patients included, all of the patients were calculated HCC stage using 5-substage HKLC (HKLC-5), 9-substage HKLC (HKLC-9), and the BCLC system. Based on overall survival (OS), these three staging systems' performance on treatment outcome prediction were compared using C statistic, Akaike information criterion (AIC), linear trend chi-square, likelihood ratio chi-square, and calibration plots, respectively.

Results: 715 patients with mean age of 58 years old were included. Of them, 591 (82.7%) were men. The median OS was 10.1 months. Both BCLC and HKLC showed significant OS classification (Fig 1). Compared with the BCLC system, the HKLC system, especially HKLC-9 showed better performance on survival prediction (HKLC-9: C=0.689, AIC=6646.162; HKLC-5: C=0.683, AIC=6662.663; BCLC: C=0.680, AIC=6654.146), homogeneity (likelihood ratio chi-square: HKLC-9=232.38, HKLC-5=215.87, and BCLC=224.39, p <0.001) and calibration (R^2: HKLC-9=0.923, HKLC-5=0.916, and BCLC=0.914) (Fig 2). BCLC showed better performance on monotonicity (linear trend chi-square: HKLC-9=121.641, HKLC-5=117.389, and BCLC=125.752; p <0.001).

Conclusions: Combining survival prediction, discrimination, and calibration, the HKLC, especially HKLC-9 system performed better for Chinese patients treated with cTACE than the BCLC system.

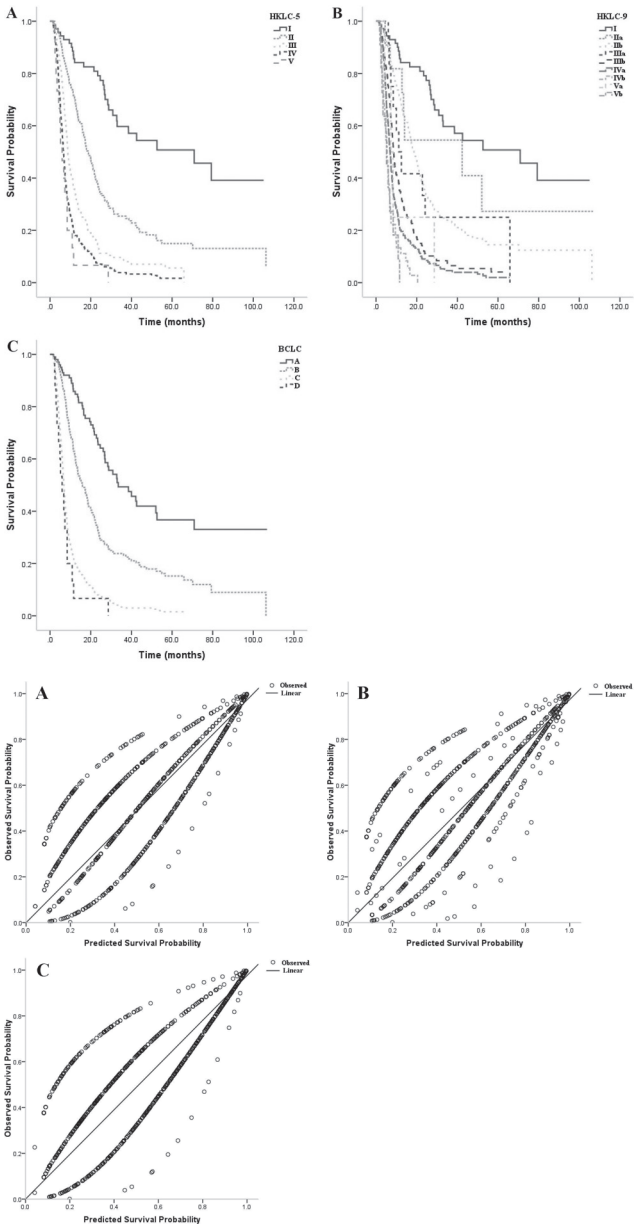

Paper 6: Early Safety From a Phase 1, Multicenter, Open-Label Clinical Trial of Talimogene Laherparepvec Injected Into Liver Tumors

S.S. Raman[1], M. Pless[2], A. Cubillo[3], A. Calvo[4], J. Hecht[5], C. Liu[6], E. Chan[6], J. Chesney[7], A. Prat[8]; [1]*Radiology, UCLA, Santa Monica, CA;* [2]*Kantonsspital Winterthur Department of Oncology, Winterthur, Switzerland;* [3]*HM Universitario Sanchinarro, Madrid, Spain;* [4]*Hospital General Universitario Gregorio Marañón, Madrid, Spain;* [5]*David Geffen School of Medicine, University of California, Los Angeles, CA;* [6]*Amgen Inc, Thousand Oaks, CA;* [7]*James Graham Brown Cancer Center, University of Louisville, Louisville, KY;* [8]*Hospital Clínic, University of Barcelona, Barcelona, Spain.*

Objectives: Talimogene laherparepvec is a genetically modified HSV-1 oncolytic immunotherapy designed to preferentially replicate in tumors, produce granulocyte-macrophage colony-stimulating factor (GM-CSF), and stimulate antitumor immune responses. This study evaluates the safety of intrahepatic injection of talimogene laherparepvec in patients (pts) with hepatocellular carcinoma (HCC) or liver metastases (mets).

Methods: The primary objective is to assess the maximum tolerated dose. Eligible pts were ≥ 18 years old, had progressive HCC or breast cancer (BC), colorectal cancer (CRC), gastroesophageal cancer, melanoma, non-small cell lung cancer, or renal cell cancer with liver mets, with measurable liver tumors suitable for injection. This dose escalation study comprised 2 groups: A (non-HCC) and B (HCC).

Talimogene laherparepvec was given initially at 10^6 plaque-forming units (PFU)/mL followed by up to 4 mL of 10^7 PFU/mL (cohort 1) or 10^8 PFU/mL (cohort 2) every 21 (± 3) days (Q21D), or up to 8 mL of the maximum tolerated concentration (MTC) Q21D (cohort 3). Injection volume was based on lesion size.

Results: Results from cohorts 1 and 2 of group A are reported. Of 14 pts treated, 12 (3 BC, 9 CRC) were DLT-evaluable, with median age of 65.5 years (range: 33-73). Median number of injection was 3, and 1 pt received all 12 injections. MTC was 10^8 PFU/mL. There was 1 DLT, grade 3 aspartate aminotransferase (AST)/grade 2 bilirubin increase after 1 dose. In all treated pts, 4 (28.6%) had grade 3/4 treatment-related adverse events (TRAEs): anemia and increased gamma-glutamyltransferase, alanine aminotransferase (ALT), and AST. There were 2 deaths attributable to disease. Incidence of serious AEs (SAEs) is shown (Table).

Conclusions: The MTC was 10^8 PFU/mL Q21D after initial injection at 10^6 PFU/mL. Repeated intrahepatic injection of talimogene laherparepvec at the FDA-approved concentration for intralesional injection of melanoma was deemed tolerable and feasible in pts with liver mets. Additional investigation in combination with a checkpoint inhibitor is planned.

DLT-Evaluable Pt Incidence of SAEs

	n
Any SAE	6
Any TR SAE	2
Pyrexia	1
AST increase [a]	1
Hernial eventration	1
Syncope	1
ALT increase [a, b]	1
Nausea [a, b]	1
Pneumothorax [b, d]	1
Urinary tract infection [b, d]	1
Liver cholestasis due to hematoma [c]	1
Hepatic hemorrhage [c]	1

a, TR SAEs; b, occurred in 1 pt; c, occurred 1 pt, procedure-related; d, not procedure-related.

Paper 7: Outcomes After Transarterial Embolization Versus Radioembolization of Neuroendocrine Tumor Liver Metastases

R. Zener, H. Yoon, E. Ziv, A. Covey, K.T. Brown, C.T. Sofocleous, R. Thornton, F. Boas; *Interventional Radiology, Memorial Sloan Kettering Cancer Center, Woodside, NY.*

Objectives: To evaluate initial response and overall survival (OS) of neuroendocrine tumor (NET) liver metastases initially treated with transarterial embolization (TAE) versus radioembolization (RE).

Methods: An IRB-approved retrospective review was performed of 186 patients with NET liver metastases initially treated with TAE (n=160) versus RE (n=26). For each patient, we evaluated: initial response by mRECIST, overall survival after initial locoregional therapy, primary site (lung, pancreas, small bowel, or other), tumor grade and degree of differentiation, Charlson comorbidity index, Child Pugh score, ECOG performance status, TAE particle size, angiographic evidence of arteriovenous shunting, whether an extrahepatic vessel was embolized during the initial treatment, presence of extrahepatic tumor, volume of liver disease, degree of selectivity of the embolization, presence of NET-related symptoms, and urgency of the initial procedure.

Results: There was no difference in initial response for NET treated with TAE versus RE (53% vs 59% CR or PR, p=0.66). Initial response was higher for TAE using particles <100 μM versus TAE using only particles ≥100 μM (64% vs 42%, p=0.007). Multivariate logistic regression showed that use of particles <100 μM, and liver <50% replaced with tumor were independent predictors of a better initial response rate. For well to moderately differentiated NET, median OS after initial locoregional therapy was 55 months for both TAE and RE (p=0.91). For poorly differentiated or undifferentiated NET, median OS after initial locoregional therapy was 13 months for TAE and 5 months for RE (p=0.076). There was no significant difference in survival between TAE patients treated with <100 μM versus only ≥100 μM particles. Multivariate Cox proportional hazards model showed that well to moderately differentiated NET, and liver <50% replaced by tumor were the only independent predictors of improved OS.

Conclusions: NET patients treated with TAE have the same initial response and overall survival, compared to RE. NET patients treated with TAE using particles <100 μM had better initial response, but the same overall survival, compared to TAE using only particles ≥100 μM.

Paper 8: Chronic Hepatic Changes in Patients with Metastatic Neuroendocrine Tumors Treated with Y-90 Radioembolization: Single-Center Experience

G. El-Haddad[1], S. Damgaci[5], A. Jung[4], F. Galambo[4], J. Levine[6], B. Morse[1], T. Rose[1], T. Jarmi[3], B. Biebel[7], B. Kis[8], J. Strosberg[2]; [1]*Diagnostic Imaging and Interventional Radiology, Moffitt Cancer Center and Research Institute, Tampa, FL;* [2]*Medical Oncology, Moffitt Cancer Center, Tampa, FL;* [3]*Transplant Medicine, University of South Florida, Tampa, FL;* [4]*University of South Florida, Tampa, FL;* [5]*Cancer Physiology, Moffitt Cancer Center and Research Institute, Tampa, FL;* [6]*Radiology, Ochsner Clinic Foundation, New Orleans, LA;* [7]*Diagnostic Imaging and Interventional Radiology, Moffitt Cancer Center and Research Institute, Tampa, FL;* [8]*Diagnostic Imaging and Interventional Radiology, Moffitt Cancer Center and Research Institute, Tampa, FL.*

Objectives: To evaluate the chronic effects of Y-90 radioembolization on the liver of patients with metastatic neuroendocrine tumors (mNET).

Methods: Retrospective review from 2009 to 2016 of all mNET patients who were treated with Y-90 glass microspheres and had at least 6 months follow up. We compared imaging and laboratory findings from pre-radioembolization to last follow up. We analyzed morphological changes of liver cirrhosis and liver dysfunction based on changes in albumin and bilirubin.

Results: 57 patients (M:34, F:23, mean age 62 ±11 years) with mNET WHO grade 1 (n= 41), grade 2 (n=10), grade 3 (n=1), and unreported (n=5) received sequential whole liver (n=43), and unilobar (n=14) treatment. Most common primary tumor site was in the small bowel (n=23), followed by pancreas (n=15), and other (n=19). The average and median delivered radiation dose was 144±40 and 134±40 Gy, respectively. Mean imaging follow up from the time of first radioembolization for whole liver and unilobar treatment was 29±17 and 28±22 months, respectively. Of the patients who received sequential whole liver treatment, 57% (25/43) developed liver dysfunction, 77% (33/43) developed morphological changes compatible with cirrhosis, of which 67% (22/33) had associated ascites ($p<0.0001$). There was no statistically significant correlation between tumor progression (25/43), systemic chemotherapy prior to Y-90 (15/43), bland or chemoembolization (16/43) and the development of cirrhosis and ascites. None of the 11 patients who had bilobar disease and received unilobar radioembolization developed cirrhotic morphology in the untreated contralateral lobe, despite receiving systemic chemotherapy (n=4), or bland embolization (n=3) to the contralateral lobe ($p<0.0001$).

Conclusions: The majority of mNET patients undergoing bilobar radioembolization with Y-90 glass microspheres developed liver dysfunction, and had radiographic features of cirrhosis; in more than half of those cases this was associated with ascites. In patients with bilobar disease, but received radioembolization to one lobe, none developed radiographic features of cirrhosis in the untreated lobe. These chronic liver changes which could be at least partially related to radioembolization need to be considered in mNET patients who have a longer median life expectancy than patients with other types of liver metastases. Further dosimetry studies are needed to evaluate the appropriate dose for Y-90 treatment of liver mNET.

Paper 9: The Effect of TACE/Ablation to the Change of TAA Specific T Cell Response in Hepatocellular Carcinoma

Y. Zhang; *Beijing Youan Hospital, Capital Medical University, Beijing, China.*

Objectives: Transarterial chemoembolization and thermal ablation have been found to play a very important role in the control of disease progression in the patients with intermediate-stage and early-stage HCC, while it is not clear whether TACE/Ablation could change TAA specific T cell response or not, which is very important in the evaluation of the effects of TACE/Ablation and predication of relapse of HCC.

Methods: PBMCs were collected from the HCC patients before and after TACE/Ablation, and overlapping peptides covered most of current TAA, including SALL, MAGE, NY-ESO, SSX and AFP, which were used in the ELISpot Assay to evaluate the change of TAA specific T cell response.

Results: 1. The frequency of recognition to TAA increased from 52.9% of patients before TACE/Ablation to 88.2% of patients after TACE/Ablation (p=0.024); 2. The magnitude of T cell response to TAA from 105 (SFU/10^6 PBMCs) in patients before TACE/Ablation increased to 197 (SFU/10^6 PBMCs) in the patients after TACE/Ablation. 3. In addition, the T cell response to SALL and AFP changed from subdominant to predominant when comparing the patients before and after TACE/Ablation.

Conclusions: TAA specific T cell response, including the frequency, magnitude and profiles, can be changed after TACE/Ablation, which might be one of mechanism to control the diseases progression of HCC.

Paper 10: Preclinical Evaluation of Locoregional Delivery of Low-Density Lipoprotein Docosahexaenoic Acid Nanoparticles Shows Promise as a Novel Treatment for Hepatocellular Carcinoma (HCC)

P. Sutphin[1], J. Li[2], R.J. Brown[3], I.R. Corbin[2]; [1]*Radiology, UT Southwestern, Dallas, TX;* [2]*Advanced Imaging Research Center, UT Southwestern, Dallas, TX;* [3]*Neurological Surgery, UT Southwestern, Dallas, TX.*

Objectives: Investigate the antitumor activity of low-density lipoprotein-nanoparticles reconstituted with docosahexaenoic acid (LDL-DHA) following transcarotid intrahepatic catheter delivery.
Methods: Orthotopic rat models of HCC (DEN and N1-S1 xenografts) were treated with a single dose of 2 mg/kg of LDL-DHA nanoparticles via transcarotid catheter-based delivery. Three days following LDL-DHA delivery or sham procedure, histologic examination was performed to evaluate for both tumor and normal liver toxicity. Oxidative stress was examined as a potential mechanism of LDL-DHA toxicity through in vitro studies. N1-S1 rat hepatoma cells were treated with LDL-DHA and examined for oxidative stress with glutathione, dihydroethidium fluorescence and thiobarbituric acid reactive species assays.
Results: Histologic examination of sham-treated and LDL-DHA tumors demonstrated evidence of LDL-DHA-induced necrosis in tumor specimens without evidence of injury to the adjacent normal liver. In vitro studies to examine for oxidative stress revealed deviant glutathione metabolism and increased reactive oxidative species in tumor cells following treatment with LDL-DHA, but not in control treatments.
Conclusions: Catheter-based transarterial delivery of LDL-DHA nanoparticles is a feasible approach that more faithfully reflects the treatment strategy used in humans. Metabolism of LDL-DHA nanoparticles disrupts redox homeostasis within tumor cells leading to the antitumor effects.

Paper 11: Influence of Bead Size on Doxorubicin Concentration and Distribution After Transarterial Chemoembolization by Matrix-Assisted Laser Desorption/Ionization- Mass Spectrometry in a Rat Orthotopic Model of Hepatocellular Carcinoma

H. Nishiofuku[1], A.C. Cortes[2], A. Minhaj[2], D.L. Baluya[2], E. Cressman[2], P. Urszula[2], T. Tanaka[1], K. Kichikawa[1], R. Avritscher[2]; [1]*Radiology, IVR Center, Nara Medical University, Kashihara, Japan;* [2]*Interventional Radiology, The University of Texas MD Anderson Cancer Center, Houston, TX.*

Objectives: The purpose of this study was to evaluate the effect of bead size on spatial distribution and relative concentration of doxorubicin in liver tumors after transarterial chemoembolization (TACE) with doxorubicin- eluting beads in a rat orthotopic model of hepatocellular carcinoma.
Methods: Tumor-bearing Sprague-Dawley rats were randomly chosen to be euthanized at three or seven days after TACE with doxorubicin-eluting beads of either 40-60 or 70-150 μm in diameter, using a fixed total bead dose of $4x10^4$ microspheres. Fresh tumor tissues accompanied by surrounding normal liver parenchyma were sectioned along the axial plane. The middle section of the tumors was snap-frozen, and serial sections were prepared. One section was processed for Matrix-assisted laser desorption/ionization-mass spectrometry (MALDI/MS) analysis, and an adjacent section was processed for Hematoxylin and Eosin staining. Data acquisition, and image processing was performed using high definition imaging (HDI) and Waters MassLynx platforms. Mass peak intensities signals were calculated from color intensity maps by drawing regions of interest (ROI) over areas with a positive signal. Complete mass spectrometry profiles within the ROIs were exported and further analyzed using Progenesis QI software. Relative doxorubicin concentration was expressed as abundance or area under the peak. Statistical significance was analyzed using two-sided t-test. GraphPad Prism7 was used for statistical analysis.
Results: Abundance of doxorubicin in liver samples was significantly higher in animals treated with 70-150 μm drug-eluting beads 3 days after chemoembolization with mean abundance of 8.6 ± 0.6, when compared with 7.9 ±0.36 detected in the 40-60 μm bead group; P=0.005. A different pattern was observed 7 days after treatment, where animals treated with 40-60 μm beads showed a relative higher mean abundance of 8.1 ± 0.8, compared to 7 ±1.3 in the group treated with 70-150 μm beads; P=0.05. Thus, a significant decrease in doxorubicin abundance was observed in the group of animals treated with 70-150 μm 7 days after treatment; p=0.02. Abundance remained relatively stable in the 40-60 μm bead group throughout the 7 days. Spatially, our results demonstrated that doxorubicin reached the tumor more frequently in the group of animals treated with doxorubicin-drug eluting beads of 40-60 μm compared with frequency of peak signals observed in normal parenchyma regions. In contrast, doxorubicin in the 70-150 μm group was found preferentially within the peritumoral area and normal parenchyma regions.
Conclusions: Transarterial chemoembolization with 40-60 μm drug-eluting beads more efficiently delivered doxorubicin to the tumor bed, while retaining higher concentrations at 7 days after treatment. Meanwhile, doxorubicin concentration was initially significantly higher in animals treated with 70-150 μm drug-eluting beads 3 days after chemoembolization, but rapidly decreased over time. To the best of our knowledge, the present research explores for the first time the spatial distribution of doxorubicin using Matrix-assisted laser desorption/ionization - mass spectrometry.

Paper 12: Microwave Ablation in Lung Using a Novel Thermal Accelerant Agent: Effect on Ablation Zone Volumes and Comparison of Percutaneous and Endobronchial Delivery Methods

A.W. Maxwell[1], W.K. Park[1], G. Baird[1], D.W. Martin[2], D.E. Dupuy[1]; [1]*Department of Diagnostic Imaging, The Warren Alpert Medical School of Brown University, Providence, RI;* [2]*Division of Pulmonary Medicine, The Warren Alpert Medical School of Brown University, Providence, RI.*

Objectives: To determine the effects of a novel thermal accelerant (TA) on microwave ablation zone volumes in porcine lung, and to compare percutaneous and endobronchial (EB) delivery methods.
Methods: This study was performed following institutional animal care and use committee approval. Eight 40-50 kg castrated male domestic swine were treated with microwave ablation of normal lung tissue under general anesthesia. All treatments were performed with the MicroThermX system (Perseon, Salt Lake City, UT) for ten minutes at 60W and 915 MHz utilizing ST antennae under C-arm fluoroscopic guidance. Radiopaque contrast media was added to the TA agent prior to the procedures to facilitate fluoroscopic visualization. Up to four ablations were performed per animal (maximum two per lung). Ablations performed without TA administration were used as controls. Experimental ablations were performed following percutaneous delivery of 2 cc TA into the lung using a 5 Fr Yueh catheter or after EB TA delivery by a fellowship-trained interventional pulmonologist using a flexible bronchoscope. Following the ablation procedures, animals were euthanized and lung tissue explanted for assessment of treatment volumes as determined by triphenyltetrazolium chloride staining for cell death. Statistical analyses were performed using generalized linear modeling with SAS/GLIMMIX assuming a normal distribution with a priori significance set at α=0.05.
Results: Twenty-two ablations were performed in total (16 TA, six control). Among TA ablations, nine were administered percutaneously and seven via EB delivery. Overall, TA ablation zone volumes were significantly larger than control ablations (mean volume 4.6 ± 1.9 cc TA vs. 1.9 ± 0.9 cc control; p<0.0001). Among ablations with TA, those performed following percutaneous delivery had a significantly larger ablation zone volume than those in the EB condition (mean 5.6 ± 1.8 cc percutaneous vs. 3.4 ± 0.4 cc EB; p<0.0001), while ablation zones created following EB administration were significantly more uniform in size distribution (p<0.0001).
Conclusions: Thermal accelerant use is associated with increased microwave ablation zone volumes in normal porcine lung tissue. Percutaneous TA delivery leads to greater increases in ablation zone volume when compared with EB injection. However, more uniform ablation zone size is observed using the EB approach, which may result in more reproducible treatment outcomes. Further investigations in animals and humans are planned.

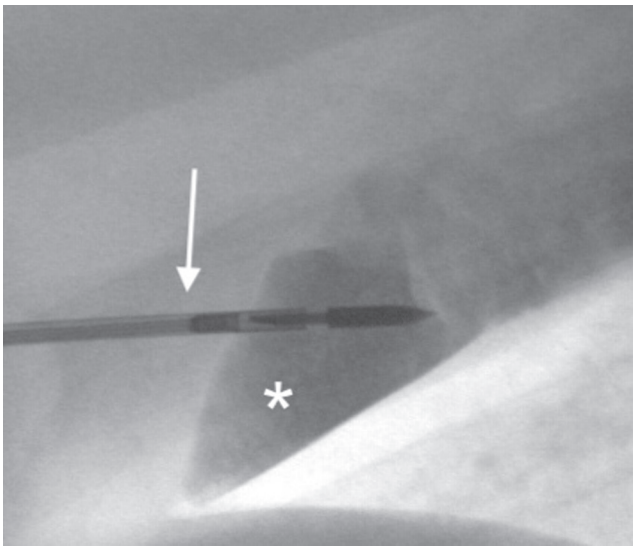

Spot fluoroscopic image demonstrates a microwave ablation antenna (arrow) with feed point positioned within a circumscribed radiopaque collection (asterisk), representing EB-deposited TA.

Paper 13: Histotripsy for Non-Invasive Liver Tumor Ablation in an In Vivo Murine Hepatocellular Carcinoma (HCC) Model

T. Worlikar[1], E. Vlaisavljevich[2], T. Gerhardson[1], S. Kuruvilla[3], J.E. Lundt[1], S. Wan[5], K. Ives[1], F.T. Lee[4], J. Greve[1], T.L. Hall[1], T.H. Welling[5], Z. Xu[1]; [1]*University of Michigan, Ann Arbor, MI;* [2]*Virginia Tech University, Blacksburg, VA;* [3]*Stanford University, Stanford, CA;* [4]*University of Wisconsin, Madison, WI;* [5]*NYU Langone Health, New York, NY.*

Objectives: Histotripsy is a mechanical, non-invasive ultrasonic ablation process that fractionates tissue through the precise control of acoustic cavitation guided by real-time ultrasound imaging. Current liver cancer ablation methods are primarily thermal-based and inherently result in inconsistent tissue ablation because of irregular heat dissipation. This study evaluates the potential, feasibility and tumor volume reduction effects of histotripsy for liver cancer ablation in a subcutaneous in vivo murine HCC model.

Methods: Subcutaneous xenograft tumors were generated by injecting 1-2 million Hep3B cells (human HCC cell-line) into the right flanks of 14 NSG and 7 NOD-SCID mice. The mice were divided into three groups: A (acute, NSG with n=9 treatment and n=1 control), B (chronic, NSG with n=2 treatment and n=2 control) and C (chronic NOD-SCID, with n=6 treatment and n=1 control). Histotripsy was performed when the tumors reached >5mm, using a custom built 1 MHz histotripsy transducer attached to a motorized positioner guided by US imaging system. 1-2 cycle histotripsy pulses at 100 Hz PRF (p- >30 MPa) were delivered to the target and the histotripsy focus was scanned by the positioner to traverse the targeted tumor volume. T1, T2 and T2* weighted MR images were obtained pre and post treatment to assess tumor ablation. Group A was sacrificed within 3 days post treatment. Groups B and C were monitored weekly using caliper measurements and MRI for 3 months or until tumors reached ~1.8cm. Post euthanasia, treated tumor, brain, and lung were harvested for histopathology.

Results: The histotripsy-generated cavitation cloud and the targeted tumor region were visualized on US imaging enabling real-time feedback. In group A, histopathology showed that the targeted region was completely fractionated into acellular debris with a sharp boundary. In groups B and C, MRI monitoring revealed effective tumor volume reduction post treatment as the homogenate and edema were resorbed within 2-3 weeks. However, as this subcutaneous tumor model does not allow sufficient treatment margin and the mice are immune-compromised, residual viable tumor cells developed into tumor regrowth at 3-9 weeks after treatment. Treated mice in chronic groups B and C showed no signs of metastasis in the lung and brain.

Conclusions: This study demonstrates the potential of histotripsy for non-invasive HCC ablation in a subcutaneous model. Additional work is ongoing to study the biological response of histotripsy in immune-competent orthotopic liver tumor models.

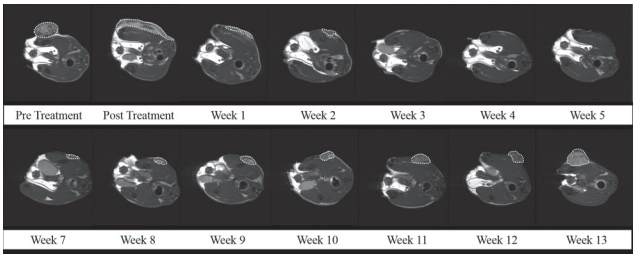

T2-weighted MR images provide an assessment of histotripsy treatment in a group C mouse. The targeted volume appears as a homogeneous, bright area on post-treatment image compared to the pre-treatment image showing a heterogenous tumor with mottled signal. The homogenized tumor volume and edema resulting from the treatment are mostly reabsorbed in 2 weeks post treatment, however regrowth is observed by week 8. The tumor and treated homogenate regions are outlined with yellow dashed line.

Paper 14: Effects of Idarubicin-Eluting Oncozene Microspheres on Pre-Clinical Tumor Microenvironment in Liver Cancer

T. Borde[2], M. Van Breugel[1], J. Chapiro[2], M. Lin[2], L.J. Savic[2], F. Laage-Gaupp[2], T. Shelton[2], L. Adam[2], D. Peters[2], D. Coman[2], J. Walsh[3], M. Miszczuk[2], I. Rexha[2], Q. De Ruiter[2], S. Huber[2], T. Schlachter[2], F. Hyder[3], J. Duncan[3], J. Geschwind[4]; [1]*University Medical Center Utrecht, Utrecht, Netherlands;* [2]*Department of Radiology and Biomedical Imaging, Yale School of Medicine, New Haven, CT;* [3]*Department of Biomedical Engineering, Yale University, New Haven, CT;* [4]*PreScience Labs, Westport, CT.*

Objectives: The main purpose of this study was to evaluate the effect of Oncozene drug-eluting beads with 40 and 100 μm diameters loaded with the antineoplastic agent idarubicin in a rabbit VX2 liver tumor model. Imaging and histopathological analyses of the tumor and liver tissue were performed to investigate embolization effects on the tumor and tumor microenvironment by assessing physiological markers, e.g. extracellular pH (pHe), hypoxia, and vasculature.

Methods: VX2 tumor chunks were implanted into the left liver lobe of 12 New Zealand White rabbits. Animals were subjected to transarterial chemoembolization (TACE) with either 40 (n=5) or 100 μm (n=4) Oncozene microspheres (Boston Scientific, Maple Grove, MN, USA) or assigned as control (untreated, n=3). Multiparametric MRI was performed within 4 days after TACE including dynamic contrast enhanced (DCE) and diffusion weighted imaging (DWI), as well as biosensor imaging of redundant deviation in shifts (BIRDS) for assessment of pHe. Tumors were harvested immediately after MRI. Ex vivo analyses included fluorescence imaging to evaluate idarubicin penetration and immunohistochemistry stainings for proliferation, cell death, and hypoxia (HE, PCNA, TUNEL, HIF-1a, pimonidazol).

Results: DCE showed devascularization of embolized tumors as compared to controls (mean arterial enhancement 8±12 vs. 36±51%, p=0.07). Specifically, the outer tumor rim was less enhanced in treated animals. In controls, DWI revealed significantly lower levels of cellularity in the tumor core than in the tumor rim (apparent diffusion coefficient [ADC] 2.34±0.18 vs. 1.55±0.09 $x10^{-3}$ mm^2/s, p=0.006). Post-TACE, the viable rim could not be discriminated from the necrotic core and ADC values were significantly larger than in liver parenchyma suggesting a loss of tumor cell integrity (1.89±0.18 vs. 1.28±0.21 $x10^{-3}$ mm^2/s, p<0.0001). Regarding pHe BIRDS showed that the tumors were significantly more acidic than liver parenchyma both prior to (mean pHe 6.79±0.08 vs. 7.13±0.08, p=0.02) and after embolization (6.8±0.06 vs. 7.1±0.04, p<0.01). On fluorescence imaging, 40 μm microspheres showed deep vascular penetration and distribution within the tumor as well as in surrounding parenchyma. In contrast, 100 μm beads were found to cause more peritumoral vascular occlusion with less tumor penetration but also no non-target deposition. Idarubicin concentration was measured within 100 μm from embolized vessels with both microsphere sizes. Histopathology revealed matching complete inhibition of tumor cell proliferation, cell death, and enhanced hypoxia within the tumor after embolization in both treatment groups.

Conclusions: TACE with Oncozene beads was feasible in the VX2 rabbit liver tumor model. The study revealed strengths and weaknesses for both 40 and 100 μm Oncozene microspheres, though the clinical applicability needs to be further investigated. mpMRI combining DCE, DWI, and BIRDS could become an important tool in assessing the changes within the tumor microenvironment, and thus could be used for advanced tumor detection, differentiation, and improved treatment response prediction.

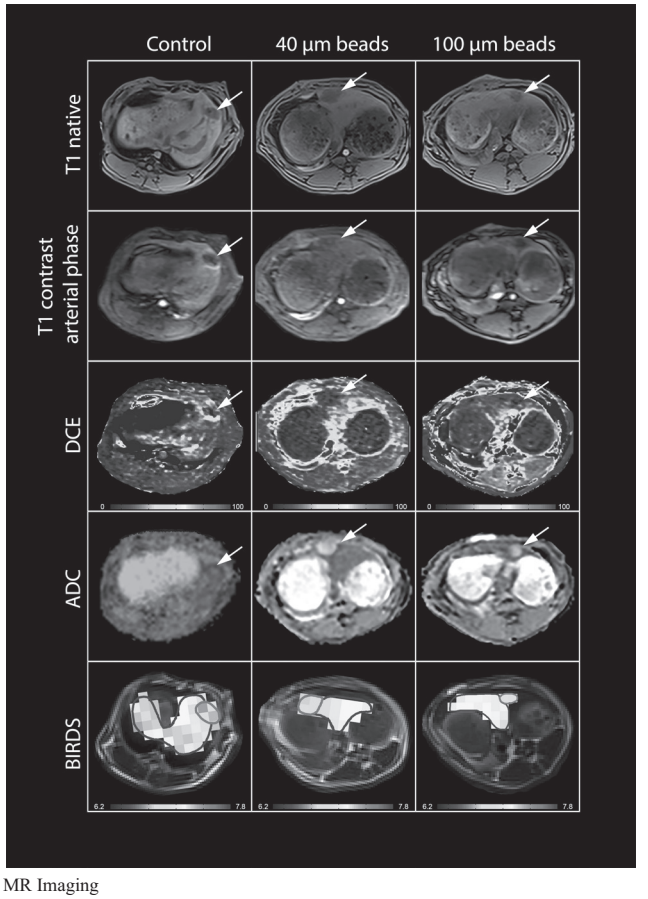

MR Imaging

Paper 15: Radiology Pathology Correlation of Woodchuck Hepatitis Virus-Induced Hepatic Tumors

M. Mauda-Havakuk[1], W. Pritchard[1], A.S. Mikhail[1], M. Starost[2], E. Jones[3], A. Partanen[1], D. Woods[1], J. Esparza-Trujillo[1], I. Bakhutashvili[1], v. Krishnasamy[1], J. Karanian[1], B. Wood[1]; [1]*Interventional Radiology Section, National Institutes of Health, Bethesda, MD;* [2]*Division of Veterinary Resources, National Institutes of Health, Bethesda, MD;* [3]*Radiology and Imaging Sciences, National Institutes of Health, Bethesda, MD.*

Objectives: Define characteristic imaging features and identify corresponding histopathology of viral-induced hepatic tumors in a woodchuck model
Methods: All studies were conducted under a research protocol approved by the Institutional Animal Care and Use Committee. Woodchucks chronically infected with woodchuck hepatitis virus (WHV) developed various hepatic tumors which are similar to human hepatic tumors. Under anesthesia, woodchucks (2-6kg) with and without elevated serum Gamma-Glutamyl transferase (GGT) underwent US and contrast enhanced MRI and multi detector CT. Selective catheterization of the hepatic vasculature, diagnostic angiography and CBCT were performed with 1.7-2.8F microcatheters placed via the femoral artery. Correlative gross pathology and histology were also obtained.
Results: Of the 14 animals studied, 9 had elevated serum GGT. Histological examination of the woodchucks confirmed hepatic tumors including focal nodular hyperplasia, hepatocellular adenoma, and carcinoma (HCC). HCC was the most common hepatic tumor observed. A total of 14 HCCs were observed in 8 different animals. Image-based evaluation revealed longest diameters ranging from 1-6cm. HCC tumors tended to be hypodense on non-enhanced CT and showed heterogeneous enhancement with areas of arterial hyper enhancement of solid areas and hypo enhancement of necrotic areas. The larger HCC tumors with largest diameters of 4.6-6 cm (n=5) tended to be exophytic and hypervascular with large ectatic vessels. The two largest HCC tumors (largest diameter 6 cm) demonstrated high flow arteriovenous shunting. Smaller hepatic tumors (largest diameters of 0.3-0.4 cm, n=6) tended to be isodense on non-contrast images and homogeneously enhancing in the arterial phase. A spectrum of histologies was seen including focal nodular hyperplasia, and in two cases mixed hyperplasia and adenoma. Histopathology of tissue adjacent to HCC typically showed inflammation consistent with viral induced hepatitis.
Conclusions: Woodchucks chronically infected with WHV showed hepatic tumor types with diagnostic imaging and pathology comparable to that in humans. Imaging evaluation of hepatic tumors was correlated with the pathologic characteristics for all tumor types, which offers theoretical advantages compared to the rabbit VX2 model. Woodchucks chronically infected with WHV and bearing hepatic tumors may provide a valuable preclinical model for investigation of natural history, genetic profiles, and translation and validation of novel interventional oncology paradigms.

Paper 16: Towards Improving Thermal Ablation and Chemoembolization for Hepatocellular Carcinoma Through Cancer Stem Cell Inhibition

Y. Huo[2], I. Newton[1]; [1]*Radiology, VA San Diego Healthcare System, San Diego, CA;* [2]*UCSD, San Diego, CA.*

Objectives: Most patients with hepatocellular carcinoma (HCC) are not candidates for transplant or surgical resection. For some with limited disease, a local cure is possible with percutaneous thermal ablation (PTA), which uses thermal energy to destroy tumor tissue in situ. However, incomplete ablation can lead to recurrence. For patients with advanced HCC, noncurative disease control can be achieved through transarterial chemoembolization (TACE) or transarterial embolization (TAE), which disrupt the tumor's blood supply and induce hypoxia. HCC recurrence after PTA, TACE and TAE may arise from surviving cancer stem cells (CSCs). CSCs are rare, self-renewing cells which exhibit resistance to standard cancer therapies including chemotherapy, radiation therapy, PTA/heat stress and TACE/hypoxia/starvation. The PI3K pathway is commonly activated in CSC signaling and serves as a target for CSC inhibition. Adjuvant treatment with HCC CSC inhibitors could improve the efficacy of PTA, TACE, and TAE. Objective: To test the hypothesis that administering HCC CSC inhibitors to HCC cell cultures exposed to conditions simulating incomplete PTA or TAE will decrease HCC CSC enrichment and HCC cell survival.
Methods: An incomplete PTA model was established in vitro by exposing three human HCC cell lines, Hep3B, PLC and HepG2, to a 46.5°C water bath for 10 minutes, with a 37°C water bath as control. TAE was simulated by exposing cells to a 1% oxygen hypoxia chamber and serum-depleted medium for 72 hours. Cultures were treated with PI3K pathway inhibitor LY294002. DMSO served as a control. The surviving HCC cells were analyzed via flow cytometry for the expression level of stem cell markers EpCAM, CD133, and CD44.
Results: Sublethal heat, hypoxia and starvation induced elevated expression of CSC markers including EpCAM, CD133 and CD44. (Fig 1.) Exposure to the CSC inhibitors LY294002 resulted in a depletion of CSC populations. (Fig 2.) Figure. 1. Scatter plots and summary bar graph depicting the effect of heat stress or hypoxia with serum starvation on HCC populations expressing CSC markers. (A) HCC cells demonstrated increases in CSC marker positive populations after 10-minute exposure to heat stress. (B) HepG2 demonstrated a higher EpCAM+CD133+ double positive population after 72-hour exposure to hypoxia and serum starvation. Figure 2. Scatter plots and summary graph demonstrating the expression of EpCAM and CD133 in (A) Hep3B cells and CD44 and CD133 in (B) PLC cells exposed to heat stress without or with LY2940022. LY2940022 administration reduced expansion of the CSC marker positive population.
Conclusions: These data demonstrate that sublethal heat stress or hypoxia plus serum starvation induce an enrichment of HCC CSCs and that inhibition of HCC CSCs reduces the CSC population. Future studies will focus on the mechanisms underlying CSC induction and inhibition in vitro and in vivo. If successful in vivo, adjuvant treatment with HCC CSC inhibitors could improve the efficacy of PTA, TACE and TAE.

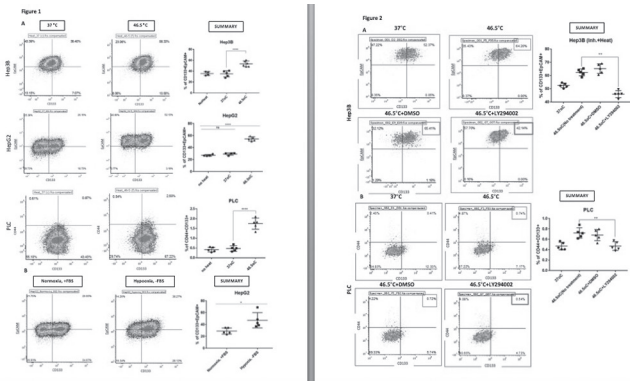

Paper 17: Micelle Paclitaxel Enhanced End-Point Survival in Percutaneous Radiofrequency Ablation of Tumors in a Mouse Tumor Model: Intravenous or Intratumoral Administration?

H. Wu, A. Jiang, S. Wang, W. Yang; *Ultrasound, Peking University Cancer Hospital, Beijing, China.*

Objectives: To determine whether radiofrequency ablation (RFA) combined with intratumoral (MIIT) or intravenous (MIIV) micelle paclitaxel (PTX) administrationresults in greater local drug concentration and achieves better therapeutic efficacy in an animal model.
Methods: Characterization of micelle PTX was performed in vitro. Next, following institutional animal care and use committee approval, 4T1 murine breast tumors were implanted in 131 mice in vivo. Tumor drug accumulation and bio-distribution of major organs for MIIV and MIIT PTX with or without RFA were evaluated at different time points(n = 3/each time point). Drug concentration and intratumoral penetration MIIV and MIIT PTX with or without RFA were evaluated (n = 6/subgroup) after treatment with quantitative analysis orpathologic staining. Mice bearing tumors were randomized into the six groups (n=7/group): control (no treatment), MIIV, MIIT, RFA alone, RFA+MIIV, RFA+MIIT. Kaplan-Meier method was used to estimate end-point survival and log-rank test used for comparison of difference in survival.
Results: PTX encapsulation efficiency was 97.64±1.21 % with favorable cellular uptake capability confirmed in vitro. In vivo, intra-tumoral drug accumulation was always much higher for MIIT PTX than for MIIV PTX within 48hr after injection (P<0.001). Drug deposition within major organs was also decreased for MIIT injection compared to MIIV at 24hoursespecially in the liver ((42.5±1.7 vs 102.9±43.6)×10^9phot/cm^2/s, P<0.001). The MIIT+RFA group (3084.7±985.5 μm) induced greater and deeper drug penetration than the MIIT group alone (881.3±240.1 μm, P=0.001). For end-point survival, the MIIT+RFA group had better survival than MIIV+RFA (20.4±0.3 days vs 15.7±1.8 days, P=0.033, RF alone (20.4±0.3 days vs 14.5±1.3 days, P=0.003).
Conclusions: Direct intratumoral micelle PTX administration improves intratumoral drug accumulation and can further enhance the therapeutic efficacy as well as reduce drug toxicity for major organs, especially in combination with RFA.

Paper 18: Efficacy and Radiation Exposure of an Ultra Low-Dose Chest CT Protocol in CT-Guided Percutaneous Core Needle Biopsy for Small Pulmonary Lesions Using a Third-Generation Dual-Source CT Scanner

C. Li, H. Jia, B. Liu, H. Meng; *Radiology, Qilu Hospital of Shandong University, Jinan, China.*

Objectives: To prospectively investigate the efficacy and radiation dose of an ultralow-dose protocol in computed tomography (ULDCT)-guided percutaneous core needle biopsy (PCNB) for small pulmonary lesions using a third-generation dual-source CT scanner in comparison to standard-dose CT protocol (SDCT).

Methods: In this CT-guided PCNB study, 210 patients were prospectively enrolled and randomly assigned to a SDCT (n = 70; mean age, 66 ± 17 years) or ULD (n = 140; mean age, 61 ± 15 years; 1:2 randomization scheme) protocol. SDCT settings were reference 110 kVp and 50 mAs with automated-attenuation tube potential selection (CARExV and CAREDose4D; Siemens Healthcare). ULDCT settings were fixed at 100 kVp with a dedicated tin filter (100Sn kVp) and 70 mAs. All CT-guided PCNBs in patients with small (≤ 3 cm) pulmonary lesions were performed on a third generation dual-source CT scanner (SOMATOM Force; Siemens Healthcare, Germany). Diagnostic performance, complication rate, and radiation dose were compared between SDCT and ULDCT groups. Subjective image quality was evaluated based on a 5-point scale and was compared.
Results: Technical success rates of 98.5% and 97.1% were obtained in the SDCT and ULDCT groups, respectively (P = 0.522). The sensitivity, specificity, accuracy for diagnosis of malignancy with SDCT were 95.6% (44/46), 100% (19/19), and 96.9% (63/65), respectively. The values were 93.8% (90/96), 100% (35/35), and 95.4% (125/131) with ULDCT, respectively (P > 0.05). Complication rate showed no significant differences between two groups in terms of pneumothorax (18.5% [13/70] versus 21.4% [30/140], P = 0.628) and hemoptysis (5.7% [4/70] versus 7.1% [10/134], P = 0.695). Image quality of ULD satisfied the need for lung interventions. The mean volume CT dose index ($CDTI_{vol}$) and dose-length product (DLP) were significantly lower in the ULDCT compared with the SDCT protocols (0.24 mGy vs 3.3 ± 1.1 mGy and 8.5 ± 0.70 mGy-cm vs 110.5 ± 45.1 mGy-cm; P < 0.001 for both). Mean effective dose for the ULDCT protocol was significantly lower than that for the SDCT protocol (0.15 mSv ± 0.02 vs 1.78 mSv ± 0.76; -91.5%; P < 0.001).
Conclusions: ULDCT protocol with spectral shaping on a third-generation dual-source CT scanner reduces radiation dose significantly when compared with SDCT. ULDCT protocol for CT-guided PCNB is a highly accurate and safe diagnostic method for small pulmonary lesions.

Measurements of scan length and radiation exposure for the SDCT and ULDCT protocols.

Parameter	SDCT protocol	ULDCT protocol	P-value
Scan length, cm	33.6 ± 3.0	35.4 ± 3.6	0.560
CTDIvol, mGy	3.33 ± 1.1	0.24	P < 0.001
DLP, mGy-cm	110.52 ± 45.1	8.57 ± 0.70	P < 0.001
ED, mSv	1.78 ± 0.76	0.15 ± 0.02	P < 0.001

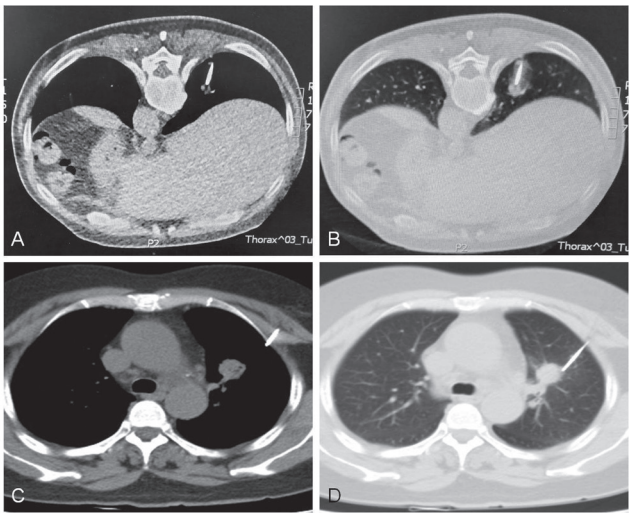

Representative biopsy images using the ULDCT protocol (A, B) at 100Sn kVp and 70mAs (effective dose, 0.14mSv). Representative biopsy images using the SDCT protocol (C, D) at 110 kVp and 50mAs (effective dose, 1.43mSv).

Paper 19: Clinical Application of CT-Guided RFA Combined Immediately Postoperative Biopsy of Pulmonary GGO

Y. Wei; *Radiology, Chinese PLA General Hospital, Beijing, China.*

Objectives: To investigate the effectiveness and safety of an innovative method of CT-guided RFA combined immediately postoperative biopsy of GGO in lung
Methods: 31 patients with 42 pulmonary GGOs had found during October,2015 to October,2017 in our dpartment. 39 lesions had underwent CT-guided RFA combined with immediately postoperative biopsy whereas 3 had history of proven multiple metastatic tumors were excluded. Postoperative 1-,4-,12-,and 24 month follow-up enhanced CT and adjuvant serum tumor markers were performed to evaluate the therapeutic effectiveness of RFA. The endpoints include 2-year local control rate,cumulative disease-free survival and positive incidence of immediate post-op biopsy
Results: All the procedures were completed successfully. 32 of 39(82.1%)lesions got expectative pathologic results. 18 of 39(46.2%)had subtype results. The complications after RFA include 9(22%) pneumothorax with 5(55.6%)needed catheter drainage,1(11.1%)needed air aspiration and 3(33.3%)did not need to deal with. 4(10.3%)patients had suffered local hemorrhage without hemoptysis. Post-op 1-month follow-up showed enlargement and consolidation of the ablation area than Pre-op GGOs((2.41±0.98)cm vs (1.53±0.79) cm, p<0.0001 on CT images whereas 4-month follow-up images showed a shrink of the ablation area than 1-month ones((1.97±0.74) cm vs(2.41±0.98)cm,p=0.0015).2-year local control rate was 96.97%(95%CI,80.38%-99.57%),2-year disease-free survival of non-metastatic malignant GGOs was 96.67%(95%CI,78.60%-99.52%)and 2-year OS was 100%.
Conclusions: CT-guided RFA combined immediately postoperative biopsy of GGO in lung is safe,effective,and minimal invasive. This innovative method can bring clinical benefit to the control and diagnosis of GGO lesions in lung.

Paper 20: Prognostic Value of HMGB1 in Locally High-Risk Prostate Cancer Patients Receiving Primary Cryoablation Therapy

T. Si; Interventional Treatment, Tianjin Medical University Cancer Hospital and Institute, Tianjin, China.

Objectives: To determine the prognostic value of high mobility group box 1 (HMGB1) expression in high-risk prostate cancer (PCa)patients treated with cryoablation.
Methods: The expression of HMGB1 was assessed by immunohistochemistry in cancer lesions from 66 confirmed prostate cancer cases and 20 cases of benign prostate hyperplasia (BPH). Clinicopathological features were compared between positive and negative HMGB1 protein expression groups. We determined the potential association between the expression level and the clinicopathological features and overall patient survival. Kaplan–Meier and multivariate Cox analyses were applied to determine the prognostic value of HMGB1 protein expression on TTP and overall survival for patients with PCa received cryoablation treatment.
Results: The positive rate of HMGB1 expression in PCa was higher than BPH (60.61 % vs 35.00%, P < 0.05). HMGB1 expression were associated with advanced tumor clinical stage (34.48% vs 81.08%, P<0.05), and the prostate specifc antigen (PSA) level (40.00% vs 77.78%). There was no statistical significance of HMGB1 expression rates related with age or Gleason score. Cox regression analyses showed that age, pre-cryoablation PSA level, clinical stage and HMGB1 level were significantly associated with TTP and OS (P < 0.05). Positive HMGB1 immunostaining was significantly associated with poor median TTP (45m vs 58m, P < 0.05), or overall survival (55.5m vs 70m, P < 0.001). Multivariate analysis indicated that HMGB1 protein expression was an independent prognostic factor for overall survival.
Conclusions: Compared to BPH, HMGB1 expression may contribute to the high-risk progression of PCa. HMGB1 presents as a novel prognostic factor for cryoablation in high-risk PCa.

Paper 21: Radiofrequency, Cryo- and Microwave Ablations For T1a Renal Mass: A Comparative Evaluation of Therapeutic Efficacy and Oncologic Outcomes

W. Zhou[2], C. MccCarthy[1], R. Uppot[1], R. Arellano[1]; [1]*Radiology, Division of Interventional Radiology, Massachusetts General Hospital, Boston, MA;* [2]*Tufts University School of Medicine, Boston, MA.*

Objectives: To compare the clinical outcomes of radiofrequency ablation (RFA), cryoablation (CA) and microwave ablation (MWA) for treatment of T1a renal masses.
Methods: A retrospective analysis of 320 patients (mean age 71 yrs, range=22-90 yrs) was performed between October 2006 and December 2017. Mean R.E.N.A.L., PADUA and centrality index score were 6.2, 8.1, and 2.9, respectively. Treatment response, residual disease and survival outcome were compared among the three groups. Local recurrence-free, metastatic -free, and overall survival rates were tabulated using Kaplan-Meier methods and compared with log-rank tests.
Results: 365 T1a biopsy proven RCC measuring 1.2 to 4.0 cm were treated with computed tomography (CT)-guided MWA (n=40, 11%), RFA (n=291, 80%), or CA (n=34, 9%). There were no significant differences in patient demographics or tumor characteristics between the three cohorts. Technical success rate, complication rate and residual disease rate were similar among the three groups (p=0.91, p=0.14, p=0.46 respectively). At two-years follow-up, analysis of the local disease free-, metastatic free,- and overall survival rate showed that MWA is non-inferior to RFA and CA (p=0.60, p=0.93, p=0.75respectively).
Conclusions: CT-guided percutaneous MWA is an effective thermal ablative option, providing comparable therapeutic efficacy and oncologic outcome compared to RFA or CA.

Treatment Response and Oncological Outcomes

	RFA	CA	MWA	P values
Complete response (RECIST criteria)	277 (95%)	29 (85%)	38 (95%)	0.14
Residual tumor	14 (5%)	5 (15%)	2 (5%)	0.14
Locally recurrent disease	1 (0.1%)	0 (0%)	0 (0%)	0.92
Metastatic progression	0 (0%)	0 (0%)	0 (0%)	0.00
Disease-free survival	99%	100%	100%	0.00
Metastatic-free survival	100%	100%	100%	0.00
Overall survival	99%	97%	100%	0.31

Paper 22: The Oncologic Results of Cryoablation in Prostate Cancer Patients with Bone Metastases

T. Si; Interventional Treatment, Tianjin Medical University Cancer Hospital and Institute, Tianjin, China.

Objectives: To explore the role of whole gland cryoablation plus ADT in prostate cancer (PCa) with bone metastases compared with ADT treatment alone in metastatic PCa.
Methods: A total of 30 patients with biopsy-proven PCa with bone metastases underwent cryoablation and ADT treatment. The control group consisted of 30 men who were initially treated with ADT only and who were followed until progression, development of castration resistant PCa or death. Patients were pair matched for age, PSA level, clinical stage, preoperative biopsy Gleason score and bone metastases. Time to clinical progression, time to CRPC, cancer-specific survival and overall survival were analysed using descriptive statistical analysis.
Results: Age at diagnosis, baseline PSA, biopsy Gleason score and ECOG status were comparable between the two groups. Prostate cryoablation was well tolerated and no serious complications occurred. At the last follow-up, patients in the cryoablation and ADT treatment group had a lower median PSA nadir (0.4 ng/ml vs. 0.8 ng/ml, $p < 0.01$) and longer time to CRPC (33 ± 0.9 mo vs. 22 ± 0.8 mo, $p < 0.01$). Further analyses detected the statistically significant benefits of cryoablation treatment not only in PFS (41 ± 1.4 mo vs. 22 ± 0.8 mo, $p < 0.01$), but also in CSS (52 ± 1.9 mo vs. 32 ± 2.4 mo, p ± 0.01) and OS (41 ± 1.5 mo vs. 28 ± 1.7 mo, $p < 0.01$). Moreover, there were fewer palliative procedures for local progression in the cryoablation group than the controls.
Conclusions: Cryoablation plus ADT might be a treatment option in the multimodality management of metastatic prostate cancer. Further investigations are warranted.

Paper 23: Complication and Local Recurrence Prediction of Thermal Ablation for T1b Renal Cell Carcinoma (>4 cm): Is There a Role for the R.E.N.A.L Nephrometry Scoring System?

W. Zhou[2], C. MccCarthy[1], E. Wehrenberg-Klee[1], R. Uppot[1], R. Arellano[1]; [1]*Radiology, Division of Interventional Radiology, Massachusetts General Hospital, Boston, MA;* [2]*Tufts University School of Medicine, Boston, MA.*

Objectives: To investigate the clinical utility of radius, exophytic or endophytic, nearness to collecting system or sinus, anterior or posterior, and location relative to polar lines (R.E.N.A.L) nephrometry scoring system, for prediction of complication and local recurrence in T1b renal cell carcinoma (RCC) following thermal ablation.
Methods: A retrospective evaluation of 68 patients (M:F = 55:13, mean age =77 yrs) was performed between October 2006 and December 2017. Biopsy proven RCCs that were larger than 4 cm are included in this study. The R.E.N.A.L scores were tabulated based on imaging characteristic of the tumor morphology, which were stratify into high risk (R.E.N.A.L score 10-12), moderate risk (7-9), and low risk (4-6). Residual disease and local recurrence rate were compared among the three groups.
Results: Of the 68 biopsy proven T1b RCC (mean R.E.N.A.L score =7.7, SD =1.8) that were treated with percutaneous CT-guided thermal ablation, 19 (30%) are high risk, 29 (36%) are moderate risk, and 20 (34%) are low risk, according to the R.E.N.A.L. scoring system. High R.E.N.A.L risk is significantly associated with higher complication (21%), compared to moderate risk (7%) and low risk (0%) ($p = 0.04$). Local recurrence is more prevalent in the high risk group (16%) in comparison to moderate (10%) and low (5%) risk group, although this trend is not statistically significant.
Conclusions: The R.E.N.A.L nephrometry scoring system could be a useful predicting tool for complication occurs following thermal ablation for T1b RCC.

Analysis of R.E.N.A.L. nephrometry scores for complication and local recurrence

		Low R.E.N.A.L. risk	Moderate R.E.N.A.L. risk	High R.E.N.A.L. risk	p-values
Major Complication					
	Yes	0/20 (0%)	2/29 (7%)	4/19 (21%)	
	No	20/20 (100%)	27/29 (93%)	15/19 (79%)	0.04
Recurrent Disease					
	Yes	1/20 (5%)	3/29 (10%)	3/19 (16%)	
	No	19/20 (95%)	26/29 (90%)	17/19 (84%)	0.39

Paper 24: Safety and Efficacy of Combined Microwave Ablation and Cementoplasty for Painful Extra-Spinal Metastases

R.H. Dunlap, A. Moreland, C. Bailey, K. Hong, M. Khan; *Radiology, Johns Hopkins, Baltimore, MD.*

Objectives: Painful osseous metastases are a common cause of cancer-related morbidity. Many affected patients are not surgical candidates, and up to 40% do not achieve pain relief with radiation therapy. Percutaneous thermal ablation combined with cementoplasty presents an attractive, minimally invasive treatment option in this patient population. While cryoablation is the thermal modality most commonly used in bone in contemporary practice, microwave ablation may offer benefits including decreased procedure times, less susceptibility to heat sink effects, and lack of reliance on bulky gas-cooling systems. We present a retrospective review of patients with painful extra-spinal metastases undergoing combined microwave ablation and cementoplasty to assess safety and clinical efficacy of this treatment.
Methods: Procedures were performed from February 2015 to September 2016 at a single institution under general anesthesia using CT or fluoroscopic guidance for 84 extra-spinal metastases in 72 patients located in the pelvis, femur, humerus, shoulder, and sternum. A single 14g microwave ablation antenna (MedWaves, San Diego, CA) was coaxially inserted into each tumor in a single treatment session per patient. In the same treatment session, polymethylmethacrylate cementoplasty was performed within ablation zone in each case. Pain relief was assessed as a primary endpoint using Visual Analogue Scale pain scores pre- and post procedure. Locoregional tumor control was assessed on follow-up cross-sectional imaging as a secondary endpoint. Procedural complications were recorded to establish safety profile.
Results: Technical success was achieved in ablation of all 84 lesions. Mean maximum axial tumor area was 5.9cm2 (S.D. 3.92). Mean procedure time was 7:43 minutes (range 1:01-14:32) and mean energy dose was 5.40kJ (S.D. 2.94). Mean VAS scores were 6.38 (S.D. 2.07) pre-procedure, 1.81 (S.D. 1.6) at 2-4 weeks and 2.23 (S.D. 1.83) at 3-6 months with statistically significant decreases in pre- versus post procedure pain scores at each time point ($p<0.001$). Follow-up imaging at 6 months demonstrated no local disease progression in 67/72 patients (93.0%). No procedure related complications were reported.
Conclusions: Combined microwave ablation and cementoplasty is a safe and effective, minimally invasive treatment option for symptomatic relief and locoregional control of tumor progression in painful extra-spinal metastases. The degree and duration of pain reduction compare favorably to that of radiation therapy. Further prospective and cost comparative analysis to alternative treatment modalities may be warranted.

Paper 25: Clinical Experience: An Innovative Implant for the Prophylactic Treatment of Impeding Pathological Hip Fracture in Thirty-Seven Patients

F. Deschamps; *Institut Gustave Roussy, Villejuif, France.*

Objectives: To further evaluate the medical device Y-STRUT® (Hyprevention, Pessac, France), designed to provide prophylactic reinforcement of the proximal femur in metastatic patients.
Methods: A first-in-man study (HIPPON) was completed with the first 10 patients implanted with the studied device with a 1-year follow-up. Then an observational post-market study (HIPPON100) was initiated to include the following 100 patients implanted with this innovative device, with a 2-year follow-up. From March 2016, 27 patients were implanted in this study that is still ongoing.
Results: In HIPPON study (n=10), all the patients enrolled (mean 62 yo, 67% male) presented a pertrochanteric lesion shown on imaging with an average Mirels score of 9.42 (8-11). The procedures were performed by interventional radiologists in 97±28 minutes on average, including CT-scan acquisitions, with 9.2±3.1ml of cement injected. Hospitalization duration was 2.3±1.4 days when excluding a patient never discharged. Six patients deceased from cancer progression. One fracture occurred after a median follow-up of 237 days and was attributed to a non-optimal placement of the implant as well as to a rapid tumor progression. Wound healing was achieved in all patients at 6 months, with no case of wound infection, bleeding, leakage, or inflammation. Initial data shows a pain level diminution and an increase in OHS-12 score indicating that both symptomatic and functional conditions of the patients were improved. In HIPPON100 study (n=27), the device was implanted by Interventional Radiologists and Orthopedic surgeons. Results were similar: the patients enrolled had a mean age of 59yo (n=17) with 52% male (n=23), same pertrochanteric lesion and an average Mirels score of 8.6 (8-9) (n=5). The procedure duration was shorter with 86±32 minutes on average (n=23), with 13.2±4.1ml of cement injected (n=13). Hospitalization duration was 2.4±2.3 days (n=7). Two patients deceased from cancer progression (lung). No fracture occurred after a median follow-up of 295days. Results also showed that chemotherapy may not to be stopped before Y-STRUT® implantation and radiotherapy could be done on several patients after the intervention.

Conclusions: This innovative medical device and its associated minimal invasive procedure appear to be a promising consolidation technique for oncologic patients with poor performance status. Further inclusions on the post-market study should confirm these clinical benefits.

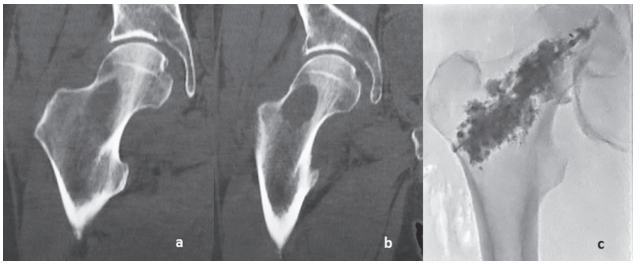

Paper 26: Evaluation of Long-Term Functionality: Percutaneous Trans-Femoral Implantation of Side-Hole Port-Catheter System with Coils-Fixed-Catheter-Tip Methods for Hepatic Arterial Infusion Chemotherapy

J. Hu, X. Wang, G. Cao; *Department of Interventional Radiology, Peking University Cancer Hospital & Institute, Beijing, China.*

Objectives: Hepatic arterial infusion chemotherapy (HAIC) is an effective treatment for liver malignancy. So, we retrospectively investigated long-term functionality and complications of percutaneous trans-femoral implantation of a side-hole port-catheter with a coil-fixed-catheter-tip for hepatic arterial infusion chemotherapy.
Methods: From January 2013 to December 2016, 205 patients (138 men; aged 28-88 years; mean, 59.1±11.2 years) with unresectable malignant liver tumors underwent percutaneous implantation of side-hole indwelling port-catheter into hepatic artery using a fixed-catheter-tip method via the femoral artery. Success, procedure time, duration of port functionality, and complications of port dysfunction were investigated.
Results: Implantation success was 98.5% and the average procedure time was 59.1±10.2 minutes. Predictable functionality of the port-catheter system at 6-, 12-, and 24 months were 97.5%, 89.9%, 70.5%, respectively. Common complications of port irreversible dysfunction were hepatic artery obstruction (4.0%), catheter occlusion (3.5%), and catheter dislocation (0.5%). There was an average of 4.9 HAIC cycles (range: 1-14 cycles).
Conclusions: Percutaneous trans-femoral implantation of a side-hole port-catheter with a coil-fixed-catheter-tip is simple and feasible for HAIC and offers long-term functionality.

Paper 27: Ultrasound-Guided Percutaneous Microwave Ablation of Papillary Thyroid Microcarcinoma: Mid-Term Efficacy Observation

S. Wang, D. Wang, L. Qi, Y. Zhang, S. Yu, Q. Xu; *Ultrasound Medicine, Yantai Affiliated Hospital of Binzhou Medical Uniersity, Yantai, China.*

Objectives: To evaluate the efficacy of ultrasound-guided percutaneous microwave ablation (MWA) for papillary thyroid microcarcinomas during the mid-term follow-up period.
Methods: Between 2009 and 2015, a total of 95 patients (38 males and 57 females; mean age: 40.1±11.2 (19-81)) with 95 tumors of pathologically proven papillary thyroid carcinoma 3.7-10.0 mm in diameter without lymph or distant metastasis were treated with MWA in our department. MWA was carried out using a microwave generator and a microwave antenna (16 G) under local anesthesia. All patients were treated with levothyroxine after MWA to maintain TSH levels below 0.1 mU/L. Follow-up consisted of ultrasonic examination in 95 patients (24~90 months), biopsy in 5 patients, and surgical treatment in 3 patients. The study was approved by ethics committee and all enrolled patients signed informed consent for the treatment.
Results: The mean volume reduction rates of the tumors were -0.28±3.76, 0.48±2.86, 0.91±0.13 and 0.90±0.14 at the 1-month, 3-month, 6-month and the last follow up, respectively ($p<0.05$). And ablated lesions were disappeared completely in 6-14 months after MWA treatment. The patients were not found any lymph recurrence and metastasis during follow up.
Conclusions: Microwave ablation appears to be a safe and effective technique for the treatment of papillary thyroid microcarcinomas during the mid-term follow-up period. Further prospective randomized studies and more experience of MWA are required to expand its clinical application.

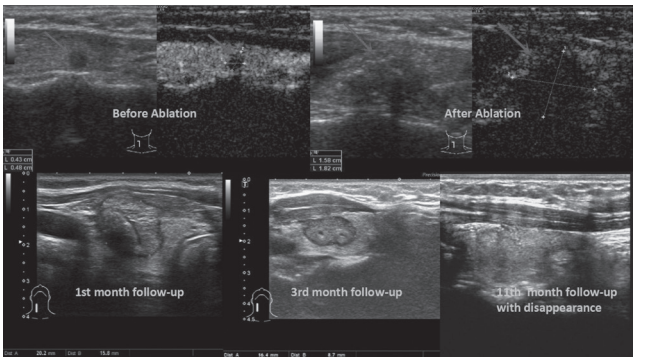

Paper 28: Current State of Palliative Care Training in Interventional Radiology Fellowship: A Survey of Recent IR Trainees

J. Wonderlick, A. Fairchild, D. Rigas, E. Weil, P.J. Patel, S.B. White, S.M. Tutton, E.J. Hohenwalter; *Vascular and Interventional Radiology, Medical College of Wisconsin, Milwaukee, WI.*

Objectives: Palliative care is a requisite skill in the care of patients living with oncologic disease. Interventional Radiologists have assumed a more direct role in the management of oncology patients as the scope and efficacy of treatment has improved, however it is unclear whether palliative training as a component of IR fellowship has kept pace. We sought to understand how training in palliative care is structured within current Interventional Radiology fellowships and whether this training is sufficient to prepare trainees to deal with this patient population.
Methods: An online survey was sent to all former fellows-in-training registered by the Society for Interventional Radiology between 2012 and 2016. The survey consisted of 66 questions over 7 sections which covered fellowship training and experiences, attitudes, and preparation in the context of palliative care as well as respondent characteristics. All survey responses were anonymous. 74 survey responses were received over a one-month period from 1,066 invitations (7% response rate). Survey methods and questions were reviewed and approved by the Institutional Review Board at the Medical College of Wisconsin.
Results: Most respondents report some experience in discussing goals of management with critically ill patients and/or family (98%) and changing goals of care from curative to palliative (85%) during fellowship, however far fewer report direct observation (57% and 48%) or critical feedback (51% and 54%) from attending physicians. Formal teaching in the management of post-procedural complications was high (8.0/10) but the amount of teaching related to management of patients at end of life and communicating end-of-life goals with patients was comparatively low (5.0/10 and 3.2/10, respectively). Further, the quality of such teaching was rated poorly (2.5/10). Respondents report an average level of preparation in caring for patients at the end of life (6.3/10, standard deviation 1.9), however relatively few received explicit teaching in telling a patient that they are dying (9%), determining when to refer patients to hospice (17%), or discussing cessation of anti-neoplastic therapy with patients (21%).
Conclusions: IR trainees are often called on to provide end-of-life care, however formal training in palliative care is lacking during fellowship. Self-reported scores in preparation for dealing with patients at the end of life indicate an opportunity for improvement, particularly in the areas of attending observation and feedback.

Paper 29: Chest Port-Related Venous Thrombosis in Patients with Solid Cancer: Incidence and Risk Factors

S. Jetty, K. Kobayashi, H. Wady, S. Zhang, P. Skummer, D. Zhang, M. Karmel; *Radiology, SUNY Upstate Medical University, Clarence Center, NY.*

Objectives: To retrospectively investigate the incidence of chest port (port)-related venous thrombosis (PVT) and to elucidate the risk factors.
Methods: Between January 2012 and December 2015, a total of 1129 ports were placed in 1129 patients with solid cancers. Patients with port-associated venous thrombosis were identified through chart and imaging review. The patients were divided into two groups based on the records of PVT (PVT group vs non Non-PVT group). More than 20 variables including the patients' demographics, medical history, laboratory data, medication used and port characteristics were compared between groups. To elucidate risk factors for PVT, univariate analysis was performed using proportional hazards regression model for the sub-distribution of a competing risk.
Results: A total of 378,674 catheter-days (median per patient: 250 catheter days) were observed. A total of 28 patients with PVT (2.5%, 0.07/1000 catheter-days) were observed, including 24 symptomatic (85.7%) and 4 asymptomatic (14.3%). Of these, 7 (25%) were on anticoagulants at the time of port placement but only 2 (7.1%) were

at the therapeutic level of international normalized ratio (INR>2.0) at the time of PVT. The median time to thrombosis was 127 days. Location of PVT include superior vena cava (n=7, 17.5%), internal jugular vein (n= 15, 37.5%), brachiocephalic vein (n= 6, 15.0%), subclavian vein (n= 7, 17.5%), and others (n=5, 12.5%). More than one vein was affected in 10 patients (35.7%). No significant difference in patient or port characteristics was seen between groups. In univariate analysis, patients on anticoagulants at time of port placement were at a significantly higher risk of PVT (hazard ratio: 2.73; 95% CI: 1.01-7.51; p=0.02). Other variables were not statistically significant for port-associated thrombosis.

Conclusions: PVT was a relatively rare complication. Patients with anticoagulants at the time of port placement were at a higher risk of PVT and may require close follow-up for PVT.

Poster 1: A Novel Aqueous Liquid Hydrogel Embolic for Tumor Applications: Assessment of Targeted Embolization Performance

S. Ganguli[2], T. DiBartholomeo[3], J. Weintraub[4], R. Lareau[1], H. Claesson[1]; [1]*Instylla Inc., Waltham, MA;* [2]*Massachusetts General Hospital, Boston, MA;* [3]*Advanced Radiology Associates, Shelton, CT;* [4]*Columbia University Medical Center/New York-Presbyterian Hospital, New York, NY.*

Objectives: Currently available liquid embolics are unsuitable for peripheral tumor embolization, and no aqueous-based liquid embolics are commercially available to interventionists[1]. We evaluated relevant in vivo performance of a novel liquid hydrogel embolic. Testing of a biocompatible and in situ forming (independent from blood coagulation parameters) liquid hydrogel embolic was performed to assess effective and precise delivery through conventional microcatheters with avoidance of non-target embolization.

Methods: The hydrogel embolic (Instylla Inc., Waltham MA), formed through a combination of aqueous polyethylene glycol (PEG) polymer solution and initiators, was delivered through microcatheter systems to target areas of the renal arterial vasculature in both New Zealand rabbit and Yorkshire swine. The rabbit renal model was selected as its vascularity and kidney size emulate hepatocellular carcinoma (HCC) tumor in humans. Experimentation in the rabbit included both embolization efficacy via fluoroscopy (ability to achieve stasis and time required for clinically relevant embolization) and 30-day survival with animal health and pathologic assessment of target kidney and non-target organs (lungs, heart, non-treated kidney, and brain). Swine renal segmental embolization was applied to evaluate a model with larger arteries with high flow. The acute swine experimentation focused on ability to achieve selective, clinically-relevant embolization without non-target embolization on fluoroscopy.

Results: Embolic delivery, through a microcatheter system in a rabbit renal artery showed rapid cessation of target area flow in less than a third of the duration required for embolization via conventional technologies[2]. Animals maintained weight and general health during the 30-day survival period, and post-mortem gross evaluation showed target area kidney infarction with necrosis and normal appearance of non-target organs. Swine model demonstrated embolic delivery procedure times that were much less than published for bland bead embolization while delivering discrete embolization to intended areas and avoiding non-target infarction.

Conclusions: An aqueous liquid hydrogel embolic in development offers a rapid, targeted, safe, and effective embolic for potential tumor applications.

References: 1. Poursaid, Azadeh et al. Polymeric Materials for embolic and chemoembolic applications. J Control Release. 2016 Oct 28; 240: 414–433. doi: 10.1016/j.jconrel.2016.02.033. 2. Niu, Huanzhang et al. Application of embolization microspheres in interventional therapy of malignant non-hypervascular tumor of liver. Oncotarget. 2017 Aug 15; 8(33): 55593–55599. doi: 10.18632/oncotarget.16286.

Poster 2: Microwave Liver Ablation: Effects of a Novel Thermal Accelerant Agent On In Vivo Temperature Change and Thermal Energy Deposition

A.W. Maxwell[1], W.K. Park[1], G. Baird[1], D.W. Martin[2], D.E. Dupuy[1]; [1]*Department of Diagnostic Imaging, The Warren Alpert Medical School of Brown University, Providence, RI;* [2]*Division of Pulmonary Medicine, The Warren Alpert Medical School of Brown University, Providence, RI.*

Objectives: To determine the effects of a novel thermal accelerant (TA) agent on ablation zone temperature change and thermal energy deposition during microwave ablation in porcine liver using real-time magnetic resonance thermometry (MRT).

Methods: This study was conducted following institutional animal care and use committee approval. Microwave ablation was performed in castrated adult male domestic swine (40-50 kg) under general anesthesia. The Surblate system (Vision Medical, Santa Clara, CA) was used for all ablation procedures at a power of 100W and a frequency of 2,450 MHz for 10 minutes. Treatments were performed percutaneously with and without injection of 2 mL TA via a 5 Fr catheter within normal liver tissue. Real-time MRT temperature measurements were made on a 3.0 Tesla scanner (Siemens, Erlangen, DE) using a multigradient echo sequence with fat suppression and respiratory gating. Temperature change from baseline within the ablation zone was quantified as the volume of tissue that achieved a cytotoxic temperature greater than or equal to 60°C (V_{60}). Area-under-the-curve (AUC) calculations were also performed using trapezoidal integration to determine thermal energy deposition at a distance of 2.0 cm from the microwave antenna. Finally, AUC data were used to generate energy equivalency plots for TA and control ablations, describing the time for TA ablations to reach the same energy deposition levels as completed control ablations. Data were analyzed with SAS/GLIMMIX using generalized mixed modeling and sandwich estimation assuming a lognormal distribution. Statistical significance was set at α=0.05.

Results: A total of 16 ablations were performed (eight TA, eight control). Overall, ablations performed using thermal accelerant demonstrated significantly greater thermal energy deposition when compared with control ablations (25701 ± 6059 °C*s TA vs. 11161 ± 554 °C*s control; p<0.001). Mean V_{60} was also significantly higher among TA ablations than those performed without TA (27.6 cm^3 vs. 18.6cm^3 and 63.1cm^3 vs. 43.7cm^3, respectively; p<0.01). Energy equivalency between TA and control ablations was achieved following an average treatment duration of 5.8 ± 0.4 minutes.

Conclusions: The use of thermal accelerant is associated with significantly greater thermal energy deposition and higher microwave ablation zone temperatures when compared with control ablations as assessed by MR thermometry. Additional investigations of thermal accelerant performance using animal tumor models and human subjects are planned.

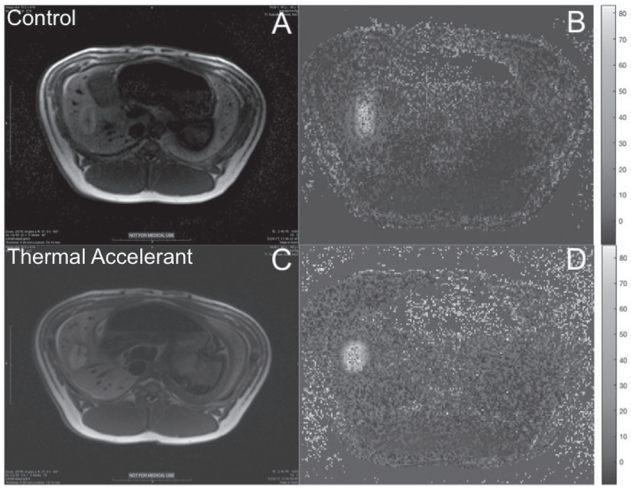

Axial T1-weighted post-contrast and MR thermometry images obtained from microwave ablations performed without (A,B) and with (C,D) thermal accelerant. The use of TA was associated with significantly increased thermal energy deposition and ablation zone temperature. Scale = Δ°C.

Poster 3: Point-of-Care Immunoassay for Rapid Analysis of Tumor Biopsies: Proof-of-Principle

B.M. Currie[1], J. Chen[1], D. Ackerman[2], S. Hunt[1], G. Nadolski[1], T. Gade[1]; [1]*Radiology, Hospital of the University of Pennsylvania, Philadelphia, PA;* [2]*University of Pennsylvania, Philadelphia, PA.*

Objectives: Percutaneous biopsies are playing a more central role in the profiling of malignancies for precision medicine. The success of this strategy hinges on high quality samples, a task complicated by tumor cell heterogeneity and impurity of biopsy specimens. Inaccurate biopsies lead to repeat procedures and can stagnate both treatment and clinical translation of evolving therapies, all of which negatively impacts patient care. A method that confirms the acquisition of cancerous cells at the point-of-care (POC) in the procedural suite while minimizing specimen damage would mitigate these limitations. We demonstrate proof-of-principle for a POC biopsy test that can detect secreted proteins specific to tumor cells.

Methods: This was a preliminary study employing a preexisting IRB-approved observational clinical trial. The protocol was developed for the genomic, proteomic, metabolomic and immunologic profiling of HCC prior to and following TACE and therefore provides an ideal vehicle for the development of a POC test designed to enable these analyses. As part of this prospective cohort study, patients meeting inclusion criteria undergo biopsy prior to TACE. Following biopsy of HCCs from patients (n=4), samples were incubated in 1 mL of biopsy buffer for 5-10 minutes and vigorously shaken and then removed for processing. 50 µL biopsy buffer was applied to a commercial enzyme-linked immunosorbent assay (ELISA) for alpha fetoprotein (AFP). A retrospective analysis was also performed of the operations data related to

all interventional radiology procedures from April 2016 to April 2017 at our institution. The total time for the completion of the biopsy protocol and subsequent TACE (n=13) was compared to the total time for TACE only (n=12) procedures. The TACE only cohort was selected to match the TACE + biopsy cohort to limit factors that could influence differences in procedure time. Statistical analysis was performed with an unpaired Student's t-test, with a p value <0.05 used as the threshold for statistical significance.

Results: No significant difference was observed in the procedure time for patients undergoing TACE + biopsy when adjusted to include readout time required for the proposed immunoassay (104 ± 7.9 min) as compared to TACE alone (88.9 ± 11.4 min, p=0.285). Measurable levels of AFP were only detected in those patients with HCCs staining positive for AFP on immunohistochemistry as assessed by a pathologist (2.6 ± 0.13 vs 0.18 ± 0.024, p < 0.001).

Conclusions: This proof-of-principle study demonstrates the feasibility of integrating the proposed biopsy algorithm into the clinical workflow in terms of procedural time and the ability to accurately identify secreted proteins from HCC as an indication of adequacy.

Poster 4: Robotically Assisted Sonic Therapy (RAST) for Renal Ablation in a Porcine Model: Initial Preclinical Results

E.A. Knott[6], J. Swietlik[6], K. Longo[6], R. Watson[1], C. Green[2], E.J. Abel[5], M. Lubner[6], J.L. Hinshaw[6], A. Smolock[3], F.T. Lee[6], Z. Xu[4], T. Ziemlewicz[6]; [1]*Pathology, University of Wisconsin-Madison, Madison, WI;* [2]*Statistics, University of Wisconsin-Madison, Madison, WI;* [3]*Radiology, University of Pennsylvania, Philadelphia, PA;* [4]*Biomedical Engineering, University of Michigan, Ann Arbor, MI;* [5]*Urology, University of Wisconsin-Madison, Madison, WI;* [6]*Radiology, University of Wisconsin-Madison, Madison, WI.*

Objectives: Robotically-assisted sonic therapy (RAST) is an emerging ablation modality using histotripsy, a non-invasive, non-thermal method to destroy tissue via focused ultrasound. The purpose of this study was to evaluate effects of renal RAST in a porcine model.

Methods: Eleven RAST ablations were performed in 7 female swine: acute bilateral (3 swine, 6 ablations immediately followed by CT and sacrifice), chronic single kidney (3 swine, 3 ablations; CT immediate, 1 week, and 4 weeks after the procedure followed by sacrifice), and chronic bilateral (1 swine, 2 ablations). RAST treatments were performed with a custom therapy transducer (VortxRx, Histosonics, Inc.) and targeted a 2.5 cm diameter sphere in the lower pole of each kidney, intentionally including the central collecting system. Treated kidneys underwent pathologic analysis. CT features were reviewed.

Results: Mean treatment time was 26.4 minutes. Ablations had a mean diameter of 2.4 ± 0.3 cm, volume of 8.5 ± 2.4 cm^3, and were spherical (sphericity index = 1.00). Ablation zone volume decreased by 94% on average over 4 weeks. Histology demonstrated complete lysis with residual blood products/debris inside the ablation zone. Temporary collecting system obstruction by thrombus was observed in 4/11 kidneys (2 acute, 2 chronic), both resolved by day 7. Areas of disrupted urothelium/smooth muscle noted in acute animals demonstrated re-epithelialization by day 28-29. There were no urinary leaks, main vessel thromboses, or adjacent organ injuries on imaging or necropsy.

Conclusions: RAST demonstrated complete histological lysis of the target renal tissue while sparing the urothelium, which is a unique advantage of RAST over thermal ablation modalities. In a porcine model, RAST was well tolerated and not associated with damage to adjacent structures immediately or 4 weeks post-procedure. These results support the continued evaluation of RAST as a potential non-invasive therapy for renal tumors.

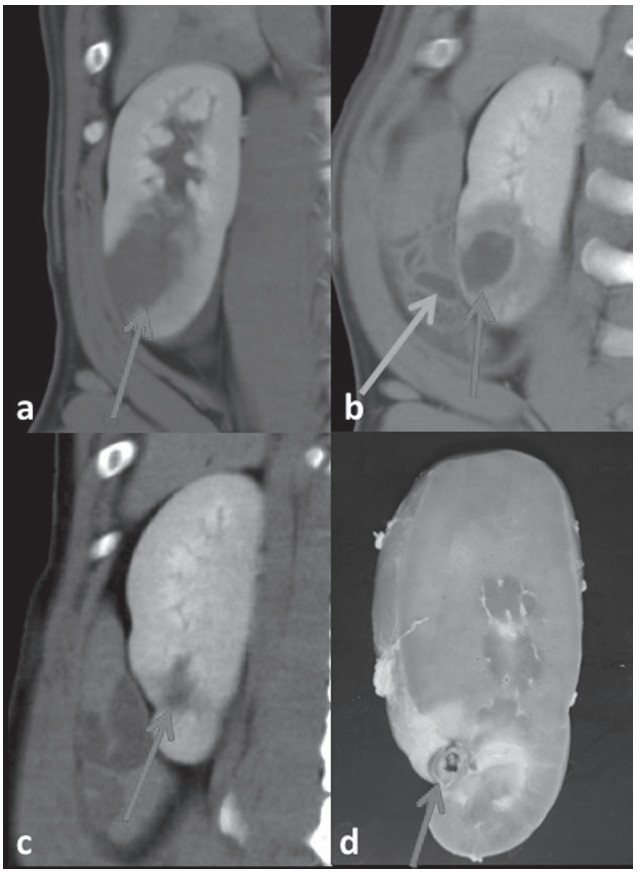

Chronic Treatment. a: Ablation zone (red arrow) immediately after treatment, b: Ablation after 1 week with uninjured bowel (green arrow) directly adjacent, c: At 4 weeks, zone has involuted to a small scar, d: Corresponding gross image with a small residual scar at site of ablation

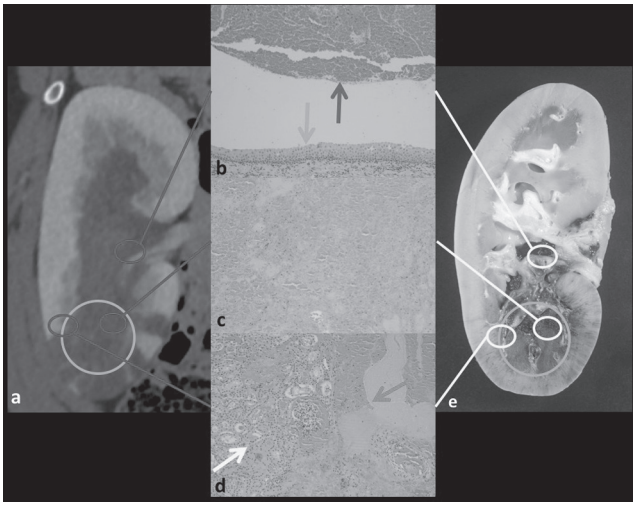

Acute Treatment. a: Coronal CT image of ablation (orange circle), b: Organized thrombus (blue arrow) within preserved collecting system (intact urothelium, orange arrow), c: Complete lysis of targeted parenchyma, d: Thin transition from ablation (green arrow) to normal parenchyma (yellow arrow), e: Corresponding gross kidney identifies extent of necrosis (orange circle)

Poster 5: Closure Devices: What Every Interventionalist Should Know

P. Moudgil, M.W. Warren, K. Singh, J.A. Ciacci; *Interventional Radiology, William Beaumont Hospital, Royal Oak, MI.*

Objectives: Vascular closure devices (VCDs) improve patient comfort, free medical staff resources, and shorten the time needed for hemostasis, ambulation, and discharge. There are two types of VCDs: active and passive. Passive VCDs enhance hemostasis with prothrombotic material or mechanical compression, but do not achieve prompt

hemostasis or shorten the time to ambulation. Active VCDs can be categorized as suture devices, collagen plug devices or clips. The goal of this exhibit is to familiarize the reader with current closure devices on the market and their proper clinical uses.

Methods: Seldinger invented his technique for arterial access in 1959. For 30 years arterial access sites were managed exclusively with manual compression (MC) and bed rest. Unfortunately, MC necessitates interruption of anticoagulation and requires considerable time and personnel resources to achieve hemostasis. MC also requires prolonged bed rest, associated with patient discomfort, back pain and urinary retention. Reducing the time, labor, bedrest, and patient discomfort associated with MC was the goal of Vascular closure devices (VCDs) which were introduced in the early 1990's.

Results: The Perclose device relies on percutaneous placement of sutures. Angio-Seal is based on the delivery of a collagen plug. The Duett VCD utilizes a balloon-positioning catheter to inject a procoagulant mixture of bovine microfibrillar collagen. StarClose uses a Nitinol circumferential clip. The femoral introducer sheath and hemostasis device, FISH, employs an extracellular matrix closure patch. The Mynx system deploys a self-expanding water-soluble sealant. The ExoSeal delivers a bioabsorbable plug atop the femoral artery. The FemStop is a mechanical compression device. The Axera device utilizes a controlled preprocedure arteriotomy results in an overlap of arterial tissue after sheath removal that is reinforced by hydrostatic arterial pressure that creates closure. The Catalyst II and III are passive closure devices which are adjunctive aids to MC.

Conclusions: There are many VCD's available. Knowing the proper clinical setting for their use and how the device works helps the Interventionalist to choose the right device in any situation.

Poster 6: LIRADS v2017: A Multimodality Review

M.A. Sultenfuss, N. Gupta; *Radiology, Houston Methodist Hospital, Houston, TX.*

Objectives: 1. Review recent updates to LIRADS v2017. 2. Review updated LIRADS categories with multimodality examples for each category. 3. Understand the Major and Ancillary feature definitions, with associated examples for each feature. 4. Implement suggested work-up options and follow-up diagnostic imaging for both treated and untreated observations. 5. Apply the new LIRADS treatment response categories to follow-up imaging from locoregional therapy.

Methods: LIRADS v2017 changes were reviewed. Imaging examples were obtained through review of Multidisciplinary Liver Tumor Board cases, Montage, Interventional Radiology case log, and interesting case files. The new LIRADS v2017 criteria were then retrospectively applied to the imaging and specific examples obtained for educational purposes. LIRADS Treatment Response categories were applied to imaging from patients who underwent locoregional therapy.

Results: Multimodality examples of the updated LIRADS v2017 criteria were obtained and organized for benefit of educating the physicians and residents involved in image interpretation and/or treatment/management of cirrhotic patients with liver lesions. Treatment response categories were applied to patients undergoing locoregional therapy.

Conclusions: LIRADS was designed to create consistent interpretation/management of liver lesions in cirrhotic patients. LIRADS criteria continues to expand, in an effort to improve the care of these patients. The 2017 version of LIRADS includes updates on previous categories, as well as new Treatment Response assessment categories and imaing work-up recommendations. Multimodality imaging examples of liver observations are provided, with application of the LIRADS v2017 criteria.

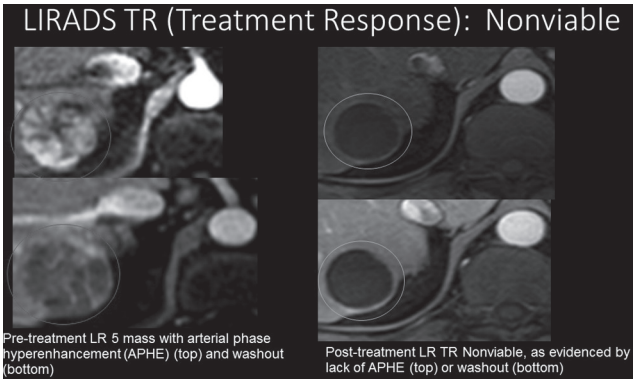

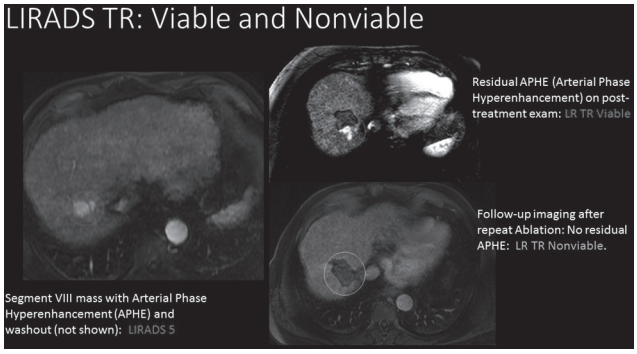

Poster 7: Retrospective Review of Falciform Artery Radiotracer Uptake Prior to Y90 Treatment: Consequences of Non-Reporting, Potential Need for Intervention and Risk of Complications

T. Bochnakova, L. Walker, P. Faulhaber, J. Giesler, S. Tavri, C. Sutter, E. McLoney, I. Patel; *Radiology, University Hospitals Cleveland Medical Center, University Heights, OH.*

Objectives: Potential complications of falciform artery (FA) nontarget embolization following transarterial hepatic chemoradiation therapies have been described. Injection of technetium-99m macroaggregated albumin (MAA) during pretreatment planning studies allow for identification of potential variant anatomy that may place a patient at risk for nontarget radioembolization prior to yttrium-90 (Y90) treatment. The purpose of this study is to identify all cases at our institution of FA radiotracer uptake during MAA pretreatment planning prior to Y90 administration utilizing SPECT/CT. Our goal is to describe the clinical consequences of reporting or failing to report FA uptake and the need for possible intervention prior to Y90 to avoid potential complications such as skin rash and necrosis.

Methods: A retrospective review was performed for pretreatment injection of MAA from 2014-2017 (n= 116). Of these cases, 103 patients underwent SPECT/CT at the time of MAA injection, which were reviewed for potential FA radiotracer uptake. The patient record was then reviewed for all cases of positive FA uptake to determine if intervention was performed at the time of the procedure and if there were postprocedure adverse effects.

Results: Of 103 patients reviewed, 9 showed FA uptake (11.4%) on initial MAA injection for pretreatment planning. The FA was visualized in 1/9 angiographic exams prior to treatment. Despite being visualized retrospectively, only 2/9 nuclear medicine MAA reports mentioned uptake in the FA. An ice pack at the anterior abdominal wall was used to minimize symptoms in 3/9 patients. Coil embolization of the FA prior to Y90 was performed in 1/9 cases. There were no documented immediate or latent postprocedure complications.

Conclusions: There is limited knowledge regarding the implications of nontarget radioembolization of the FA after Y90 or the need for preprocedure intervention. While MAA pretreatment planning is instrumental in identifying uptake in the FA, it is often underreported. Greater attention must be paid to this anatomic variant to limit complications such as peri-umbilical rash and necrosis. However, small amounts of radiotracer uptake in the FA are unlikely to result in such complications.

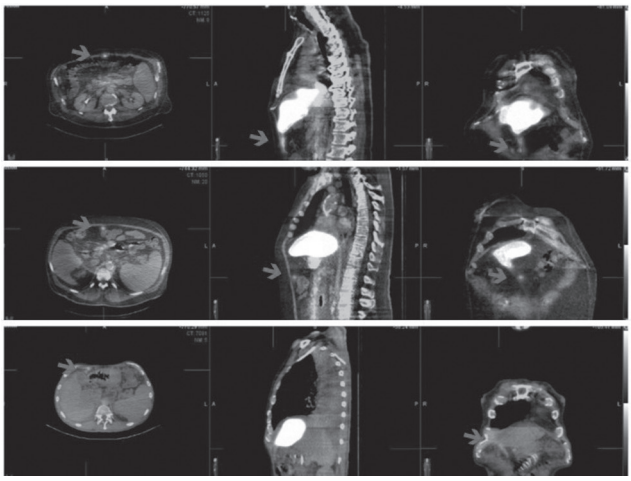

SPECT/CT fusion images are provided for three different patients after intra-arterial injection of MAA for preprocedure planning, which demonstrate radiotracer uptake within the falciform artery (green arrows).

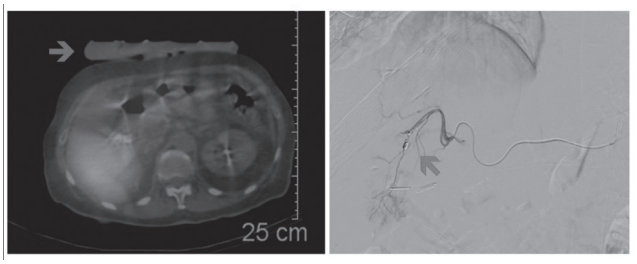

Left Image: Axial SPECT/CT image after Y90 treatment demonstrates radiotracer uptake within the liver. Note is also made of an ice pack on the anterior abdominal wall (blue arrow) that was placed prior to the procedure to minimize symptoms of falciform artery nontarget embolization.
Right Image: Angiographic image in a different patient shows coil embolization of the falciform artery after radiotracer uptake was identified on the preprocedural MAA examination.

Poster 8: Understanding Immune Checkpoint Inhibitors and the Potential Synergistic Role of Interventional Radiology Procedures

R.H. AlHalawani[1], A. Pillai[1], H. Wang[2]; [1]*Diagnostic and interventional imaging, UTHSC Houston, Houston, TX;* [2]*Institute of Molecular Medicine, UTHSC, Houston, TX.*

Objectives: Review the Cancer-Immunity cycle. Immune checkpoint inhibitors (ICI) definition and mechanism of action. Describe the different classes of ICI along with their different targets. Describe the effect of interventional radiological procedures on expression of immune checkpoint proteins with a review of literature. Discuss the prospects of ICI and its implications on the management of IR patients.
Methods: Background: Cancer immunotherapy is one of the new strategies to fight cancer. It acts by triggering patient's innate immune antitumor response. In cancer state, the interaction of PD-L1 on the tumor cells with PD-1 on a T-cell generates an immunosuppressive effect and allows the tumor to evade immune destruction. Recently the developments of immune checkpoint inhibitors that inhibit the interaction between PD-L1 and PD-1 have demonstrated clinical activities across a variety of tumor types. What is more impressive is that these immune checkpoint inhibitors can be augmented with interventional ablation or embolization treatments, creating synergistic effect and very promising results in patients with solid tumors.
Results: Content: The poster will cover the following topics: Illustrative Overview of the immune system and the check point proteins A review of the common check point proteins and mechanism of action of check point inhibitors Current status of immune checkpoint therapy in clinical studies. Potential synergistic role of interventional radiology procedures and immunotherapy
Conclusions: Summary and Implications: National Cancer Institute predicts that 39% of the American population will develop cancer at some point in their lifetime. Novel treatment options for cancers are being explored actively. Interventional radiologists with the ability to target treatments with image guidance are playing a greater role in cancer treatments. Understanding immunotherapy and the effect of interventional procedures on the immune system will enhance the field of interventional oncology. The reader will get a clear understanding of immunotherapy pertaining to check point inhibitors and the potential synergistic effect for interventional radiology procedures

Poster 9: Assessment of Cold Sink Effect in Renal Cryoablation by Analyzing Radiographic Ice Ball on Computed Tomography

S. Park; *Department of Radiology, Samsung Medical Center, Seoul, Korea (the Republic of).*

Objectives: We analyzed CT characteristics of radiographic ice ball according to anatomical location and ablation number in renal cryoablation.
Methods: Thirty patients who underwent percutaneous cryoablation for renal lesions (renal cell carcinoma, n= 29; carcinoid tumor, n= 1). Computed tomography (CT) was conducted at 9 minutes during every freezing time in order to evaluate a radiographic ice ball. Software was used to reconstruct CT images of the radiographic ice ball perpendicular to the cryoprobes. For each radiographic ice ball, two types of radius were measured: (a) lateral radius from epicenter to perirenal direction and (b) medial radius from epicenter to renal sinus direction. Lateral and medial radius or diameters (lateral radius plus medial radius) during the first and second freezing were compared using paired t-test, respectively.
Results: Medial radius of radiographic ice ball was significantly shorter than lateral radius (first freezing, 13.8mm versus 17.0mm, p< 0.001; second freezing, 16.0mm versus 19.3mm, p< 0.001). The diameter during the second freezing was significantly longer than that during the first freezing (35.3mm versus 30.8mm, p< 0.001).
Conclusions: In renal cryoablation, evaluating radiographic ice ball helps identify potential cold sink effect in the central portion of kidney. This information may help plan optimal placement of cryoprobes for securing sufficient safety margins.

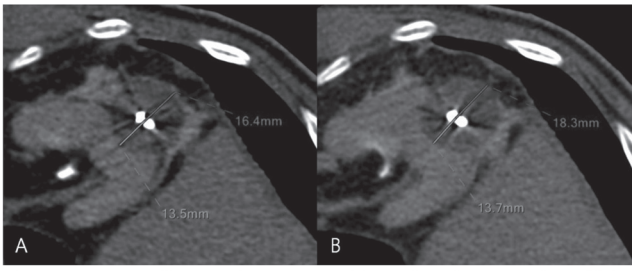

Figure. Reconstructed CT images from a 75 year-old man who underwent renal cryoablation using two cryoprobes. (A) The lateral radius (blue line) of a radiographic ice ball was longer than the medial radius (red line) during the first freezing (16.4 mm versus 13.5mm). (B) The lateral radius (blue line) of a radiographic ice ball was also longer than the medial radius (red line) during the second freezing (18.3 mm versus 13.7 mm).

Poster 10: Chyluria as a Consequence of Renal Tumor Percutaneous Microwave Ablation

D. Hillman, A. Heilala, S. Schwartz, D. Kastan; *Radiology, Henry Ford Hospital, Detroit, MI.*

Objectives: To review chyluria as a consequence of renal tumor invasive and minimally-invasive intervention and to present a case of chyluria after microwave ablation visualized on multiple imaging modalities.
Methods: Case report and literature review.
Results: A 79 year old male who presented with increasing dementia was found to have a solitary brain lesion on MRI. CT chest, abdomen, and pelvis with contrast was performed to assess for metastatic versus primary brain tumor and found a 3.6 cm upper pole enhancing mass in the left kidney. CT guided biopsy specimen was nondiagnostic. Given the concerning features on further dedicated kidney CT, the patient and family opted for image-guided percutaneous microwave ablation over partial nephrectomy given the patient's age and functional status. A single AMICA probe (HS Hospital Service SpA) was placed under CT guidance in the renal mass with subsequent successful ablation. Follow-up CT kidney at three and six months demonstrated post-ablative changes and a rim of peri-renal mixed fatty and soft tissue. Follow-up CT in one-year again showed stable post-ablation changes without disease recurrence. The patient later presented to the ED with chest pain. A CT chest, abdomen, pelvis aortic dissection protocol was performed demonstrating a fat-fluid level within the bladder compatible with a post-ablation chyluria. Subsequent lumbar spine radiographs and lumbar spine MRI also demonstrated a fat-fluid level within the bladder.
Conclusions: Chyluria, passing of lymphatic fluid into the urinary collecting system, has been long reported in tropical locations due to the parasite Wuchereria bancrofti as well as other etiologies such as tuberculosis. In recent years, incidental chyluria has been described as a consequence after partial nephrectomy and radiofrequency ablation (RFA) of renal tumors. While thought to be rare, Kaur et al. described up to 41% incidence of chyluria after renal RFA. Microwave ablation is becoming more popular in the interventional oncology field for a multitude of reasons. Microwave has advantages over RFA as it uses the inherent asymmetrical molecular orientation of water to create even heating of the tissue in the ablation zone rather than RFA which uses direct heat induction with radio waves. Microwave ablation avoids the phenomenon of RFA heat sink wherein vasculature contiguous with the tumor acts as an area of increased heat capacity leading to uneven heating and an incomplete ablation zone. This patient had four separate CT kidney examinations after the microwave ablation, including one after the chyluria was detected, which did not include the bladder or detect the chyluria. The patient did not report clinical urinary symptoms other than lower urinary tract symptoms from his known BPH. A standard urinalysis performed one year after his ablation was unremarkable, but the patient was lost to urology follow-up after the chyluria was found. The fat-fluid level from the chyluria was only seen on a CT dissection protocol performed for reasons unrelated to the ablated renal tumor. The chyluria was also visualized, through vaguely, on a lateral radiograph of the lumbar spine but was clearly visualized on both axial T1 and T2 sequences of a MRI of the lumbar spine several days after it was seen on the dissection CT. Incidental chyluria after percutaneous microwave ablation of renal tumors has not been previously described in the literature and to the best of our knowledge, this is the first description of chyluria after renal tumor intervention seen on MRI. As renal tumor ablations becomes more common the findings and imaging features of chyluria should be known to interventional and diagnostic radiologists alike.

Poster 11: Comparison of Magnetic Resonance Imaging/Ultrasound Fusion Prostate Biopsy Versus Systematic Biopsy for the Diagnosis of Clinically Significant Prostate Cancer in Patients with Negative Ultrasound Findings

Y. Zhu[1], Y. Chen[1], J. Xu[1], W. Guan[2]; [1]*Ultrasound in Medicine, Xinhua Hospital Affiliated to Shanghai Jiaotong University School of Medicine, Shanghai, China;* [2]*Pathology, Xinhua Hospital Affiliated to Shanghai Jiaotong University School of Medicine, Shanghai, China.*

Objectives: To assess magnetic resonance imaging (MRI)/ultrasound fusion prostate biopsy versus systematic biopsy (SB) for the diagnosis of clinically significant prostate cancer (PCa) in patients with negative transrectal ultrasound findings.
Methods: Prospective cohort study of 85 men undergoing prostate biopsy was conducted from January 2016 through October 2017. Patients were referred for abnormal multiparametric prostate MRI (PI-RADS category 3 or above) without suspicious lesion(s) on both grey-scale and power Doppler transrectal ultrasound. All patients underwent targeted MRI/ultrasound fusion biopsy followed by standard 12-core SB. The diagnostic performance for clinically significant PCa of targeted biopsy was evaluated in comparison with SB.
Results: In our series of patients with abnormal MRI and negative transrectal ultrasound, the overall PCa detection rate was 47.6% (40/84). PCa was detected by targeted MRI/ultrasound fusion biopsy in 37 patients (44.0%, 37/84) and SB in 29 patients (34.5%, 29/84, P=0.033). Among 40 PCa patients, 36 (90.0%, 36/40) were diagnosed as significant PCa. The significant PCa detection rate by MR/ultrasound fusion biopsy was 41.7% (35/84), which was statistically higher than SB (29.8%, 25/84, P=0.004). MR/ultrasound fusion biopsy resulted in an additional diagnosis of 11 patients with significant cancers, including 9 patients missed by SB and 2 patients under-graded by SB. Only one patient with clinical significant cancer would be missed if SB was omitted.
Conclusions: In patients with negative transrectal ultrasound findings, targeted MRI/ultrasound fusion biopsy was associated with a higher detection and more accurate grading of PCa compared with standard 12-core SB. Therefore, this approach is recommended in such patients for accurate diagnosis of clinically significant PCa.

Poster 12: Comparison of Pyeloperfusion Versus Non-Pyeloperfusion for Microwave Ablation of Renal Cell Carcinoma

K. Samadi, R. Arellano; *Radiology, Division of Interventional Radiology, Massachusetts General Hospital, Boston, MA.*

Objectives: To compare the clinical outcomes using pyeloperfusion versus non-pyeloperfusion for microwave ablation (MWA) of renal cell carcinoma (RCC).
Methods: A retrospective review of patients' records was undertaken to identify similar number of patients with RCC who were treated with MWA with and without adjunctive pyeloperfusion. A cohort of matched patients based on patient and tumor characteristics comprised the comparison group Patient demographics (age, gender) and tumor characteristics (size, distance from ureter, polarity); procedure time and complications were recorded. Pre-and post-ablation serum creatinine (Cr) was assessed. The decision to use pyeloperfusion was based on the presence of tumors in the medial lower pole of the kidney. Technical success was defined as completion of the planned ablation, primary efficacy was defined as no residual disease on the first follow-up imaging study and secondary efficacy was defined as lack of residual disease on the imaging following repeat treatment (Table 1). In cases of risk of thermal injury to the surrounding structures hydrodissection was performed. Surveillance imaging was done with CT or MRI with interval of 1, 6 and 12 months post-ablation, then annually thereafter.
Results: 18 biopsy proven RCC in 18 patients (M: F= 15/3) were treated with 19 sessions of MWA. Pyeloperfusion was performed in 9 patients. Mean tumor diameter was 31cm(±2.2cm). Average distance between ureter and the tumor in axial views was 20.8 (±2.9) mm. Technical success was achieved for all patients. Primary efficacy was achieved for 8/9 (89%) in the pyeloperfused group and 9/9 (100%) in the non-pyeloperfused group. One patient in the pyeloperfusion group required repeated ablation for residual disease at one month. Secondary efficacy was achieved in 100% of cases. There were two mild complications, including one patient with small retroperitoneal hematomas in the pyeloperfused group and another patient with a small hematoma and asymptomatic small pneumothorax in the non-pyeloperfused group. There were no statistically significant differences in pre-and post-ablation serum creatinine levels in either group. Pyeloperfusion was protective in 8 out of 9 pyeloperfused patients, one patient(11%) developed ureteral stricture followed by hydronephrosis.
Conclusions: CT-guided renal microwave ablation with pyeloperfusion is a safe and effective method in the treatment of tumors in the proximity of ureter and is not associated with significant major complication rate.

Clinical Outcomes of Pyeloperfusion versus Non-Pyeloperfusion

	Pyeloperfusion group	Non-pyeloperfusion group	p-value
Technical Success	9/9 (100%)	9/9 (100%)	1.00
Primary Efficacy	8/9 (88%)	9/9 (100%)	1.00
Secondary Efficacy	1/1 (100%)	0	
Procedure Time	144(+/- 35.34 min)	95.5 (+/- 35.04 min)	0.004
Serum creatinine (Cr)	1.44 (+/-0.49)	2.16 (+/-1.54)	0.33
Complications	2/9 (22%)	1/9 (11%)	1.00

Poster 13: Image-Guided Thermal Ablation for Non-Resectable Recurrence of Renal Cell Cancer Following Nephrectomy: Clinical Experience with Eleven Patients

W. Zhou[2], R. Uppot[1], R. Arellano[1]; [1]*Radiology, Division of Interventional Radiology, Massachusetts General Hospital, Boston, MA;* [2]*Tufts University School of Medicine, Boston, MA.*

Objectives: To assess the feasibility, safety, and clinical outcomes of image-guided percutaneous thermal ablation as salvage therapy for local recurrence of renal cell carcinoma (RCC) in patients initially treated surgically with curative intent.
Methods: A retrospective review of 11 consecutive patients (M:F = 8:3, mean age = 77yrs) who underwent computed tomography (CT) guided thermal ablation for locally recurrent RCC after partial (8/11,72%) or radical nephrectomy (3/11, 28%) with a mean time-to-recurrence of 48 months (range= 2-156 months). Assessment of technical success, complications, oncological outcome and survival analysis were performed. Patient baseline and follow-up renal function surrogates including creatinine level (Cr) and estimated glomerular filtration rate (eGFR) were statistically compared.
Results: 11 biopsy-proven recurrent RCC measuring 1.4 to 3.9 cm (mean =2.8 cm) were treated with CT-guided thermal ablation. Technical success was achieved in 100% (11/11) of the cases. There were no major complication except for one (9%) asymptomatic hemorrhage (Clavien-Dindo grade I complication). Complete response, disease free-, and overall survival rate were 91%, 100%, 82% during the mean follow-up time of 3 years (range = 1-7). Renal function was overall stable without significant change at 1 month and last follow up (p =0.09, 0.17, respectively).
Conclusions: Image-guided percutaneous thermal ablation is a feasible, safe and effective for local recurrence after nephrectomy, representing a non-surgical alternative for unresectable disease.

Poster 14: Impact of Body Mass Index (BMI) on Treatment Outcome in Thermal Ablation for Renal Cell Carcinoma: Does Obesity (or Weight) Matter?

W. Zhou[2], R. Uppot[1], R. Arellano[1]; [1]*Radiology, Division of Interventional Radiology, Massachusetts General Hospital, Boston, MA;* [2]*Tufts University School of Medicine, Boston, MA.*

Objectives: To evaluate whether the body mass index (BMI) affect the treatment response and oncological outcome for thermal ablation in renal cell carcinoma (RCC), given the global epidemic of obesity and its associated risk of cancer.
Methods: A retrospective analysis of 373 patients (M:F = 255:118, mean age = 72 yrs) was performed between October 2006 and December 2017. Patients were stratified according to BMI as normal (less than 25 kg/m^2), overweight (25 to 30 kg/m^2), or obese (more than 30 kg/m^2). Complication rate (peri- and post-procedural), residual disease rate and local recurrence rate were compared across the three groups.
Results: Of the 373 patient who underwent CT-guided thermal ablation for RCC, 82% of patients has greater than normal BMI with 140: 37% (overweight) and 169: 45% (obese). The major complication rate was not significant different among normal weight (1/64, 1.5%), overweight (3/140, 2.1%), and obese patients (4/169, 2.4%), respectively (p =0.14). Residual disease was observed in 9/139 (6 %) in overweight and 15/167 (9 %) in obese patients, when compared to 5/64 (8 %) in normal weight individuals. Although local recurrence was more prevalent in patients exceed the normal weight [normal weight (3/64, 5%), overweight, (11/140, 8%) and obese (17/169, 10%)], this finding is not statically significant (p = 0.32).
Conclusions: Thermal ablation can be safely performed for RCC irrespective to BMI. Obesity does not confer adverse oncological outcome compared to normal weight.

The effect of body mass index on complication, residual disease and local recurrence

		Normal weight	Overweight	Obese	p-values
Major Complication					
	Yes	1/64 (1.5%)	3/140 (2.1%)	4/169 (2.4%)	0.93
	No	63/64 (98.5%)	137/250 (97.9%)	165/169 (97.6%)	
Residual Disease					
	Yes	5/64 (8%)	9/139 (6%)	15/167 (9%)	0.71
	No	59/64 (92%)	130/139 (94%)	152/167 (91%)	
Recurrent Disease					
	Yes	3/64 (5%)	11/140 (8%)	17/169 (10%)	0.39
	No	61/64 (95%)	129/140 (92%)	152/169 (90%)	

Poster 15: Inadvertent Dislodgement of Percutaneous Nephrostomy Catheters in Patients with Malignant Urinary Obstruction

Y. Epelboym, K. Desai, S. O'Horo; *Radiology, Brigham & Women's Hospital, Chestnut Hill, MA.*

Objectives: To evaluate the prevalence of inadvertent nephrostomy tube dislodgement in native kidneys of adults with malignant urinary obstruction. In addition, this study evaluated the success rate of nephrostomy tract recannulation.
Methods: An IRB approved retrospective review between 2012 and 2017 of 268 consecutive nephrostomy tube cases was undertaken. Patients without malignant urinary obstruction were excluded. The remaining 227 patients were categorized based on size of nephrostomy tube placed. Age, gender, and BMI were recorded. The primary outcomes were total tube dislodgement and partial tube dislodgement. A total tube dislodgement was defined as the tube being completely extracorporeal. A partial tube dislodgement was defined as the tube partially retracted outside of the kidney but remaining within the soft tissues. Primary tract recannulation in total extracorporeal dislodgement was also calculated. A Chi square test for statistical significance was performed.
Results: A total of 227 patients underwent 346 nephrostomy tube placements. Nephrostomy catheter caliber ranged from 6 French (F) to 12F. A total of 290 8F tubes and 53 10F tubes were placed. Prevalence of total tube dislodgement across all tube sizes was 4.9%. 1.9% of 10F tubes became dislodged compared to 5.1% within the 8F group, a reduction of 63%. Prevalence of partial tube dislodgement across all tube sizes was 3.2%. Partial tube dislodgement in the 10F group was reduced by 39% compared to the 8F group with dislodgements at 1.9% for 10F tubes and 3.1% for 8F. These results were not statistically significant. Technical success was achieved in 12 of 16 tract recannulation attempts (75%). 4 patients (25%) required new percutaneous access in the setting of failed recannulation.
Conclusions: A higher prevalence of total and partial tube dislodgement amongst 8 French catheters as compared to 10 French catheters may suggest that smaller caliber catheters are more prone to dislodgement in this population. Although our results did not achieve statistical significance, this was likely attributable to the low number of dislodgements in the 10F group.

Poster 16: Percutaneous Microwave Ablation of cT1 Renal Masses: Safety and Oncologic Outcomes

S.M. Thompson[1], J. Schmitz[1], R.H. Thompson[2], A. Weisbrod[1], B.T. Welch[1], G. Schmit[1], T. Atwell[1], B.R. Viers[2], B.C. Leibovich[2], A.N. Kurup[1]; [1]*Radiology, Mayo Clinic, Rochester, MN;* [2]*Urology, Mayo Clinic, Rochester, MN.*

Objectives: To determine the safety and oncologic outcomes of percutaneous microwave ablation (MWA) for cT1 renal masses.
Methods: An IRB-approved retrospective review of a percutaneous renal ablation registry identified 26 patients with a total of 27 cT1 renal masses treated with microwave ablation (MWA) between 2012 and 2017. Mean patient age was 63.8 years and 16 (61.5%) patients were male. Mean renal mass size was 2.3±0.8 cm (range 1.1 to 4.7 cm) with exophytic (n=17; 63%), intraparenchymal (n=9; 33%) and central (n=1; 4%) tumor position. The main outcome parameters investigated were complications, local tumor progression, and survival rates. Complications were categorized using the Clavien–Dindo classification system. Local recurrence-free, overall (OS), and cancer-specific (CSS) survival rates were estimated using the Kaplan–Meier method.
Results: No technical failures were identified in any of the 26 patients on contrast-enhanced imaging performed immediately following renal MWA. Twenty-five tumors (93%) had follow-up imaging at 3 months or later, with no local recurrences observed (0%). Estimated 3-year local-recurrence-free, overall and cancer-specific survival were 100%, 96% and 94%, respectively. Two patients (7.7%) experienced minor complications (Grade I or II), and three patients (11.5%) experienced major bleeding or urinary-related complications (Grade III or higher).
Conclusions: The present data suggest that percutaneous microwave ablation is a promising and relatively safe minimally invasive treatment option for cT1 renal masses. Nonetheless, major bleeding and urinary-related complications can occur and further studies are needed to determine optimal patient and tumor selection for renal microwave ablation.

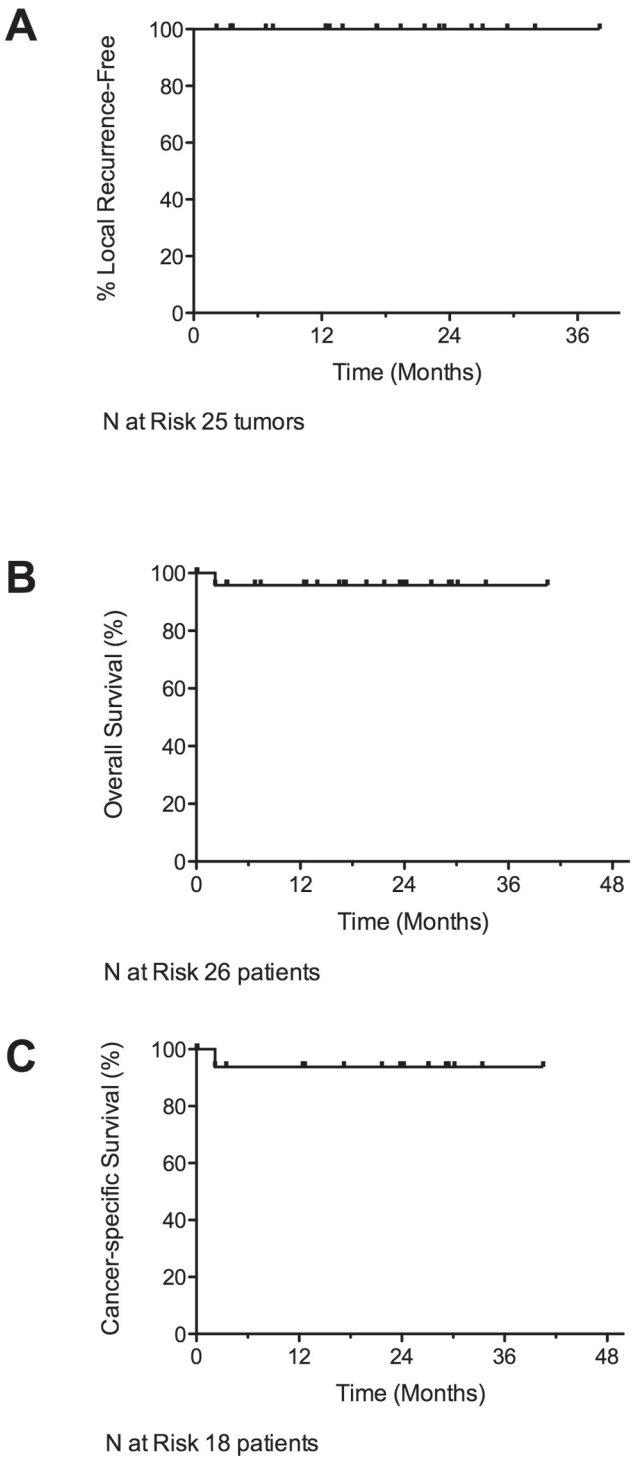

Figure 1: Kaplan-Meier curves show a) local progression-free survival for 27 cT1 renal masses treated with microwave ablation, b) overall survival for 26 patients with 27 cT1 renal masses treated microwave ablation and c) cancer-specific survival for 18 patients with biopsy-proven T1 RCCs treated with microwave ablation.

Poster 17: Percutaneous Radiofrequency Ablation vs. Cryoablation for Treatment of Renal Tumors: A Single-Center Experience

M.L. Roca[1], F. Galambo[1], a. jung[1], J. Choi[2], B. Kis[2], B. Biebel[2], J. Sweeney[2], N. Parikh[2], P. Spies[3], G.E. El-Haddad[2]; [1]*Radiology, University of South Florida, Tampa, FL;* [2]*Interventional Radiology, Moffitt Cancer Center, Tampa, FL;* [3]*Urology, Moffitt Cancer Center, Tampa, FL.*

Objectives: The purpose of this study is to compare the short term and long-term outcomes as well as complication rates in patients with small renal masses treated with percutaneous Radiofrequency Ablation (RFA) vs. Cryoablation.
Methods: A retrospective study was performed evaluating a total of 170 renal tumors treated with either ablative therapy between 2003 and 2017. Tumor size and anatomic characteristics were described using the RENAL nephrometry scoring system based on the most recent imaging study prior to the procedure. Short-term success was determined by follow-up MRI or CT imaging available, most commonly 1 to 3 months post-ablative therapy. Long-term success was determined based on the latest follow-up MRI or CT imaging available ranging from 6 months to 8 years post-ablative therapy.
Results: A total of 154 renal tumors were evaluated with 77 renal tumors treated with RFA and 77 treated with Cryoablation. Of the evaluated data, a total of 68 were biopsy proven RCC tumors and 24 biopsy proven Oncocytoma tumors. The remaining were either treated based on classical imaging characteristics or were attempted to be biopsied during ablative therapy but were unsuccessful. The average tumor size (cm) and nephrometry score for the RFA treated tumors was 2.4 and 5.9, respectively. The average tumor size and nephrometry score for the Cryoablation treated tumors was 2.1 and 6.3, respectively. There was a statistically significant difference in the short-term recurrence rate between the two groups with a recurrence rate of 19% in the RFA group and a recurrence rate of 3.9% in the Cryoablation group (p= 0.002, r= -0.254). There was also a statistically significant difference in long-term recurrence rate (which included tumors requiring re-ablation) with 10.8% in the RFA group and 4.3% in the Cryoablation group, (p= 0.012). There was a statistically significant difference in the rate of complications, with the RFA group having 2.6% complication rate and 14.2% in the Cryoablation group (p= 0.009, r= 0.163).
Conclusions: When evaluating renal tumors with an average size of 2.2 cm and nephrometry scores in the range of 6, percutaneous Cryoablation may have an overall superior short-term and long-term success rate when compared to RFA. Overall, complication rates from either procedures are low; although, Cryoablation did show a statistically significant increased rate when compared to RFA.

Poster 18: Risk Assessment of Chronic Kidney Disease Following Microwave Ablation for cT1 Renal Cell Carcinoma

W. Zhou[2], C. MccCarthy[1], R. Uppot[1], R. Arellano[1]; [1]*Radiology, Division of Interventional Radiology, Massachusetts General Hospital, Boston, MA;* [2]*Tufts University School of Medicine, Boston, MA.*

Objectives: To assess the safety and renal function outcomes after microwave ablation (MWA) for stage-cT1 renal cell carcinoma (RCC).
Methods: A retrospective analysis was performed of 38 patients (M:F = 28:10; mean age = 69 yrs [range = 51-88 yrs]) who underwent computed tomography (CT)-guided MWA for cT1N0M0 RCC. Baseline and follow-up renal function surrogates including creatinine level (Cr) and estimated glomerular filtration rate (eGFR) were statistically compared. Peri- and post-operative complication rates, technical success and treatment response were also assessed.
Results: A total of 44 cT1N0M0 biopsy-proven RCC measuring 1.2 to 6.9 cm (mean = 2.5cm) were treated and measured renal function 1 month after treatment. Mean pre-ablation GFR was 60 ml/min/1.73m^2 at baseline, and 59 ml/min/1.73m^2 at 1 month post-ablation. At the 1- year and last follow-ups, the mean difference were 3.3% (95% CI, -4.4 to 4.3, p= 0.99) and 3.0 % (95% CI, -4.3 to 4.8, p= 0.91), respectively. The 2-years freedom from GFR decline below 60 was 2% (p= 0.91). Among the 5 patients (13%) that had pre-existing stage 3b chronic kidney disease (CKD; eGFR <30 ml/min/1.73 m^2) before ablation, there was no significant post-ablative onset of decline or CKD upstaging (p= 0.001). There was no major complication, only 5/44 (13%) of patients developed small asymptomatic perinephric hematomas (SIR minor complication A-B) that were managed conservatively. There were no cases of local tumor progression in the 1-year follow-up imaging.
Conclusions: At intermediate two years follow-up, CT-guided percutaneous MWA is safe, well-tolerated and achieves nephron-preservation similar to existing ablative modalities.

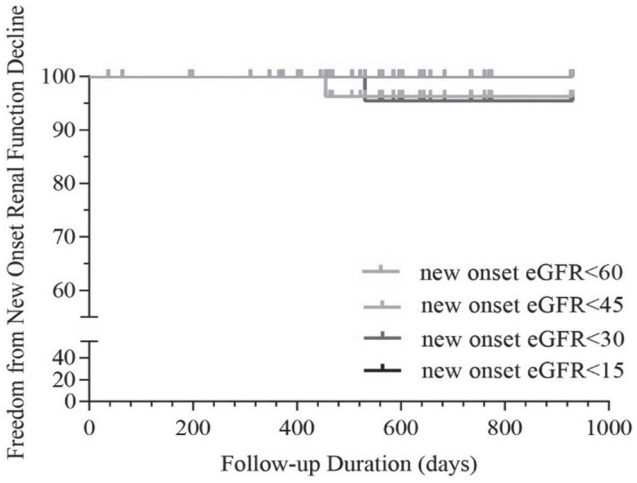

Poster 19: The Impact of Thermal Ablation on Renal Function Outcome: A Comparative Assessment of Radiofrequency, Cryo- and Microwave Ablation For T1a Renal Mass

W. Zhou[2], C. MccCarthy[1], R. Uppot[1], R. Arellano[1]; [1]*Radiology, Division of Interventional Radiology, Massachusetts General Hospital, Boston, MA;* [2]*Tufts University School of Medicine, Boston, MA.*

Objectives: To compare the renal function outcome and assess the relative risk of chronic kidney disease (CKD) following radiofrequency ablation (RFA), cryoablation (CA) and microwave ablation (MWA) for the treatment of T1a renal masses.
Methods: A retrospective study of 320 patients (mean age 71 yrs, range=22-90 yrs) was performed between October 2006 and December 2017. Patient baseline and follow-up renal function surrogates including creatinine level (Cr) and estimated glomerular filtration rate (eGFR) were statistically compared. Assessment of peri- and post-procedural complication rate were performed.
Results: 365 T1a biopsy proven RCC measuring 1.2 to 4.0 cm were treated with computed tomography (CT)-guided MWA (n=40, 11%), RFA (n=291, 80%), or CA (n=34, 9%). At 1-year and last follow-up, there were no significant differences in GFR change between the three cohorts (p=0.18, 0.09, respectively). The 2-years freedom from GFR decline below 60 was 99% (RFA), 96% (CA), and 100% (MWA). Among patients that had pre-existing CKD (CKD; GFR< 60 ml/min/1.73m^2) before ablation, there was no significant post-ablative onset of decline or CKD upstaging among the three groups (p=0.08). Complication rate and treatment response were similar between the three groups.
Conclusions: CT-guided percutaneous MWA is non-inferior to RFA or CA with regard to nephron-preservation with minimal predisposition to chronic kidney disease.

Comparison of Glomerular Filtration Rate (GFR) Change Following Thermal Ablation

	RFA	CA	MWA	p-values
Pre-ablation mean (IQR)	65 (46-90)	67 (47-90)	60 (36-90)	0.00
Last follow-up mean (IQR)	62 (42-90)	64 (46-90)	62 (36-90)	0.00
Mean difference	-3.06	-1.44	-.025	0.09

Poster 20: Therapeutic Outcome of Thermal Ablation for Peri-Hilar Versus Non Peri-Hilar Renal Cell Carcinoma: Assessment of the Heat-Sink Effect

W. Zhou[2], R. Uppot[3], R. Arellano[1]; [1]*Radiology, Division of Interventional Radiology, Massachusetts General Hospital, Boston, MA;* [2]*Tufts University School of Medicine, Boston, MA;* [3]*Radiology, Division of Interventional Radiology, Massachusetts General Hospital, Boston, MA.*

Objectives: To compare the treatment response and oncological outcome of computed tomography (CT)-guided thermal ablation in renal cell carcinoma (RCC) in peri-hilar versus non peri-hilar locations.
Methods: A retrospective analysis of 389 patients (M:F = 263:126, mean age = 72 yrs) was performed between October 2006 and December 2017. Tumor lesions located proximal (<5 mm diameter) to the ureter and renal sinus was used to stratify peri-hilar versus non peri-hilar RCC. Complication rate, residual disease rate and local recurrence rate were compared between the peri-hilar and non peri-hilar groups.
Results: Of the 442 biopsy proven cT1N0M0 RCC that were treated with percutaneous CT-guided thermal ablation, 65 (15 %) were peri-hilar and 377 (85 %) were non peri-hilar. Major complication rate was significantly higher in the peri-hilar (5/65, 8%) tumors, in comparison to non peri-hilar tumors (4/377, 1%) (p = 0.004). Residual disease was observed in 5/65 (8 %) in the peri-hilar tumors and 30/377 (8 %) in the

non peri-hilar tumors. There was no significant difference in local recurrence between peri-hilar tumors (3/65, 4%) when compared to the non peri-hilar tumors (34/377, 9%) (p = 0.33)

Conclusions: Contrary to the "heat-sink" phenomena, proximity to the renal sinus does not predispose patients to higher risk of residual or locally recurrent disease. However, careful planning may be require as thermal ablation at this location poses significantly more complication.

Effect of peri-hilar location on complication, residual and recurrent disease

		Peri-hilar	Non Peri-hilar	p-values
Major Complication				
	Yes	5/65 (8%)	4/377 (1%)	
	No	60/65 (92%)	373-377 (99%)	0.0047
Residual Disease				
	Yes	5/65 (8%)	30/377 (8%)	
	No	60/65 (92%)	347/377 (92%)	0.99
Recurrent Disease				
	Yes	3/65 (4%)	34/377 (9%)	
	No	62/35 (96%)	343/377 (91%)	0.33

Poster 21: A New Software for Immediate Volumetric Assessment of Tumor Ablation Completeness: Could It Allow to Spare Local Retreatments?

L. Solbiati, M. Solbiati, R. Muglia, K. Passera, A. Rotilio; *Department of Radiology, Humanitas University, Milano, Italy.*

Objectives: To retrospectively evaluate the accuracy of a new software (AblationFit®, R.A.W. Endosight, Milan, Italy) in assessing complete ablation of tumors with percutaneous thermal ablation.

Methods: Out of 320 HCCs treated with microwave ablation (AMICA, HS, Aprilia, Italy) from 2010 to 2016, 90 patients in which ablations were technically successful were at random technical selected. Imaging follow-up of at least one year was performed. With AblationFit® the ceCT volumes of the 90 HCCs before ablation and the corresponding achieved volumes of necrosis were segmented, co-registered and superimposed, to estimate complete target inclusion into the necrosis volume. Predictions of complete vs partial ablation provided by the software were verified analyzing presence or absence of local tumor progression (LTP) on 1-yr follow-up ceCT.

Results: Two experienced radiologists confirmed the technical success of ablation in 90/90 cases. With AblationFit® reconstructions, only 73/90 HCCs were entirely included into the volumes of necrosis, while 17/90 were partially included. At 1-yr follow-up, ceCT showed no-LTP in 69/90 and LTP in 21/90. With AblationFit® no-LTP and LTP were correctly predicted, respectively, in 65/73 and 13/17. In 8/73 cases of complete ablation and in 4/17 of partial ablation according to AblationFit® LTP did not develop. Sensitivity of AblationFit® was 62% and specificity 94%. In the 13 cases of correct prediction of LTP, tumor regrowth occurred in the location where AblationFit® showed residual tumor.

Conclusions: If AblationFit® had been used at the time of ablations, in 13/90 HCCs local re-treatment could have been spared thanks to the immediate detection of non-ablated tumor.

Poster 22: CT-Guided Radiofrequency Ablation of Lung Metastases

X. Zhang, Y. Xiao, Y. Wei; *Radiology, Chinese PLA General Hospital, Beijing, China.*

Objectives: To prospectively evaluate the safety and efficacy of radiofrequency ablation (RFA) of lung metastases with diameter of less than 30 mm.

Methods: Fifty patients (29 men and 21 women; age range, 15–79 years; mean age, 62 years) with lung metastases (93 lesions) which were confirmed by biopsy or diagnosed by image examination were enrolled in during 2015-2017. RFA was performed in tumors by CT-guided, each with a diameter of less than 30 mm (mean deviation, 18 mm). Written informed consent was obtained in this prospective study that was approved by the local ethics committee. Follow-up CT scans were obtained within 48 hours after treatment and at 1,3 and 6 months thereafter to evaluate treatment outcome and complications. Lung spirometry measurements were obtained before and 1 month after RFA.

Results: Ninety-three successful RFA treatments were performed. The complications occured in the periprocedural period were 18 cases of pneumothorax, 11 cases of pleural fluid, 5 cases of sputum cruentum, 3 cases of lung inflammation, 1 case of pulmonary abscess. There were 30 lesions of reduced size, 18 lesions of stabilized lesion size, and 10 lesions of increased size on the follow-up contrast-enhanced CT images at 6-month after RFA in 32 patients. There was no modification of respiratory function was found between the spirometry measurements before the treatment and 1 month after.

Conclusions: RFA is a safe and effective method to treat lung metastases with diameter of less than 30 mm. Larger studies are necessary to fully evaluate its potential combination with other treatment techniques.

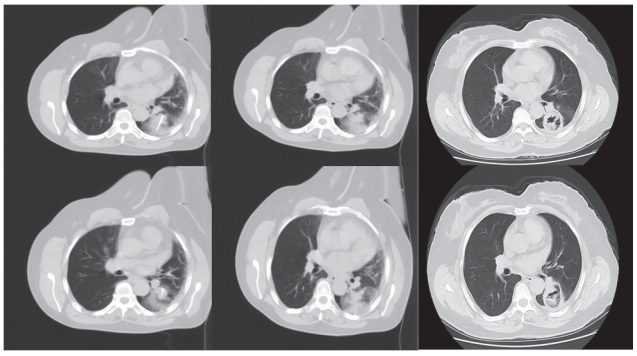

Poster 23: Lobar Versus Selective Conventional Transarterial Chemoembolization: An Interim Report of a Prospective Pharmacokinetic Study

L.J. Savic[1], J. Chapiro[1], T. White[1], E. Funai[1], E. Isufi[1], E. Chen[1], P. He[3], M.A. Rudek[3], H.S. Kim[1], R. Ayyagari[1], J. Pollak[1], J. Geschwind[2], T. Schlacter[1]; [1]*Department of Radiology and Biomedical Imaging, Yale School of Medicine, New Haven, CT;* [2]*PreScience Labs, Westport, CT;* [3]*Sidney Kimmel Comprehensive Cancer Center at Department of Oncology, Johns Hopkins University, Baltimore, MD.*

Objectives: To compare the pharmacokinetic (PK) drug profiles of doxorubicin (DOX) and its metabolite doxorubicinol (DOXOL) after conventional transarterial chemoembolization (cTACE) using a lobar or selective sub-segmental injection approach.

Methods: This interim report of an ongoing single-site, prospective trial included 22 patients who were treated with lobar (n=7) or selective (n=15) cTACE for liver malignancies including hepatocellular carcinoma (n=19), cholangiocellular carcinoma (n=1), and neuroendocrine tumor metastases (n=2) between May 2016 and October 2017. cTACE utilized 50 mg DOX and 10 mg mitomycin-C mixed 1:1 with Lipiodol followed by embospheres. Follow-up included non-contrast CT (1 day), blood chemistry, and clinical assessment of adverse events (3-4 weeks post-TACE). In addition, peripheral blood was sampled prior to and at multiple intervals after cTACE (5, 10, 20, 40 minutes, and 1, 2, 4, 24 hours, and 3-4 weeks) to measure PK of DOX and DOXOL utilizing standard non-compartmental analysis. Statistical analyses included the non-parametric Mann-Whitney and Chi-squared test.

Results: Doses of DOX during cTACE ranged from 12.5 to 50 mg with 17/22 patients receiving the full dose. For normalized doses (DN), the peak concentration (C_{max}) of DOX was 3.69 ± 3.34 ng/mL/mg measured at a median time (T_{max}) of 0.57 h (0.12-1.72 h) after injection. The DN area under the curve up to the last validated measurable DOX concentration (AUC_{last}) was 4.53 ± 3.94 ng*h/mL/mg. DOXOL was only detectable in 14 patients with a DN C_{max} of 0.25 ± 0.14 ng/mL/mg and a median T_{max} of 0.62 h (0.17-4.42 h). DOXOL DN AUC_{last} was 81.9 ± 96.1 ng*h/mL/mg. DOX and DOXOL were undetectable in samples obtained 3-4 weeks after cTACE. The mean DOX concentration at each of the various timepoints was lower after selective (150.76, 98.63, 56.66, 33.44, 18.89, 15.83, 12.00, 8.41 ng/mL) than lobar cTACE (201.47, 111.84, 60.85, 34.73, 22.66, 18.89, 15.29, 10.02 ng/mL) (Fig. 1 A). DOXOL concentrations were similar after selective (11.47, 10.33, 9.52, 8.78, 8.37, 6.67, 6.99, 8.27 ng/mL) and lobar cTACE (11.90, 9.56, 9.10, 8.01, 8.53, 7.91, 9.01, 9.74 ng/mL) (Fig. 1 B). However, comparative analysis did not reveal statistically significant differences between both groups. Clinical adverse events were generally rare and included diarrhea, fatigue, nausea, fever, abdominal pain, anorexia, and ascites of grade 1-3, which occurred more often after lobar than selective cTACE despite the smaller number of patients with statistical significance regarding the event of fever and abdominal pain (p=0.040 and p=0.030, respectively).

Conclusions: The preliminary results of this prospective trial show a throughout consistent trend suggesting higher systemic chemotherapy exposure and toxicity after lobar cTACE as compared to the selective delivery technique. If confirmed in the complete cohort, these findings may lead to a paradigm shift in intra-arterial therapy.

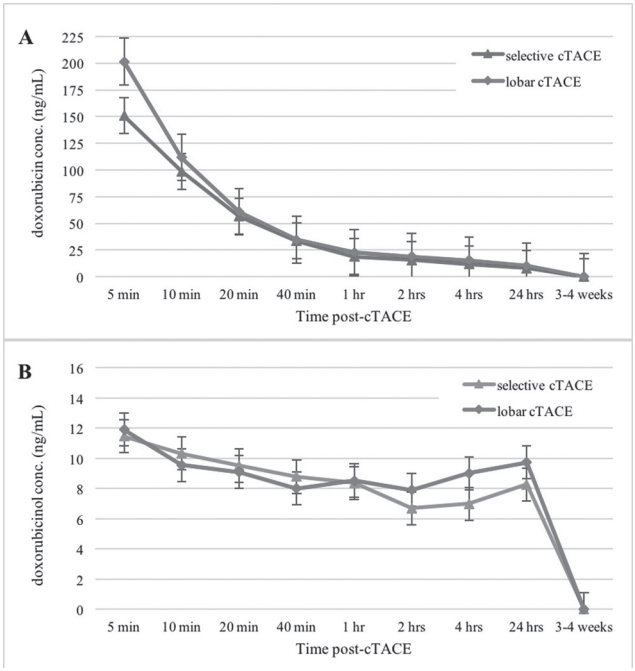

Figure 1: A) Doxorubicin and B) doxorubicinol plasma concentrations (mean; standard error) measured at different timepoints after selective and lobar cTACE.

Poster 24: MR Fluoroscopy with Free-Hand Techinique Guided Cryoablation of 37 HCC On Hepatic Dome Using 1.0-T Open High-Field Scanner

L. Chengli[1], H. Peilun[2], W. Ligang[3], L. Ming[1], X. Yujun[1], H. Xiangmeng[1]; [1]*Shandong Medical Imaging Research Institute, Jinan, China;* [2]*Jilin University, Changchun, China;* [3]*Yantai YuHuangDing Hospital, Yantai, China.*

Objectives: To prospectively evaluate the feasibility, safety and effectiveness of 1.0T open MR fluoroscopy with free-hand techinique guided percutaneous cryoablation of hepatic dome hepatocellular carcinomas.

Methods: 37 cases of HCC on hepatic dome underwent MR guided percutaneous cryoablations using 1.0 T open MR scanner. MR fluoroscopy with free-hand technique(T1-FFE, acquisition time 1.6s or Breath-hold THRIVE,acquisition time 4.8s) was applied to guidance in the puncture procedure. The lesions were 8 to 38 mm in the maximum diameter. Patients were followed for at least 12 months or until death. The supplementary cryoablation was performed if local tumor progression was found. Survival period, local tumor control and complications were recorded.

Results: MR-guided percutaneous cryoablation procedures were successfully performed in all the 37 lesions. The technical success rate was 100%. The median follow-up time was 21.0 months (from 10 to 26 months). Two patients with local tumor progression at the 4th and 11th month after the procedure were retreated with two supplementary cryoablations. One patient died from upper gastrointestinal hemorrhage at the 10th month postcryoablation. Local tumor progression and overall survival rates were 2.7% (1/37) and 100% (37/37) at 6 months, and 5.4% (2/37) and 97.3% (36/37) at 1 year, respectively. There were 2 patients with postoperative hydrothorax needing chest tube drainage, no other severe complications occurred.

Conclusions: Under 1.0T open MR fluoroscopy with free-hand techinique ,Cryoablation of hepatic dome hepatocellular carcinomas is a feasible, safe and effective therapy method.

Poster 25: Primary Endpoints In Interventional Oncology Clinical Trials: Towards A Consensus Paper

L. Fumi; *Wyfold Medical, READING, United Kingdom.*

Objectives: The growth of Interventional Oncology (IO) is negatively influenced by the limited number of referrals from medical oncologists; this is mainly due to the poor positioning of IO procedures in the guidelines, in turn due to the lack of solidity of clinical evidence. This is in turn due to the challenges in applying to IO clinical trials the standards established in the past 50 years by clinical trials of chemotherapy. The need for a consensus on primary endpoints, accepted by medical oncologists, is therefore key to the growth of IO.

Methods: A group of medics involved in different capacity in IO contacted the Oncology Department of the European Medicines Agency (EMA) in May 2015. The EMA was chosen as a key counterpart because, unlike the FDA, it is not institutionally involved in the approval of Medical Devices, and was therefore seen as super partes; its involvement, on the other hand, was seen as a seal of credibility in the world of medical oncology. A first meeting was held in London, UK, in September 2015, to share the issue with the Agency. A second meeting was held in April 2016, this time involving senior individuals of the Cardiovascular and Interventional Radiological Society of Europe (CIRSE - Oncology Subcommittee) and of the European Society of Surgical Oncology (ESSO). This resulted in the drafting of preliminary statements, which were circulated (the "Canary Wharf Statements"). The next step will be a formal workshop, involving also representatives from Patient Organisations, Oncology Organisations, Medical Device Companies, the FDA and European Medical Device Regulatory Organisations. The aim of the workshop is to lead to a consensus paper to be published in a relevant medical journal.

Results: Preliminary consensus statements: (1) outcomes of IO clinical trials depend on manual ability of the operator, number of cases done per year by a centre, difference in practice in different centres, dependency on sophisticated medical devices, which require a complex learning process, diversity of medical devices used in different centres, rapid technological evolution of techniques and devices, which makes it difficult to conduct studies of long duration. (2) Standards to generate good level clinical evidence should be similar in aims to those accepted for medical oncology but acknowledge the different regulations, challenges, specificities and flexibility needed for IO trials. Any standard must be proportionate, reasonable, pragmatic, and make the clinical studies possible and manageable to achieve realistic and clinically important objectives. (3) overall survival is still the gold standard as primary endpoint, but in practice it is often not the first choice in IO studies, for three reasons: average longer survival of the patients, compared to some decades ago; evolution of technology, making the comparator (standard of care) obsolete during the course of the study; diverse sequential treatments, making it impossible to associate overall survival with one specific treatment.

Conclusions: The choice of primary endpoints needs to consider reliable and readily measurable intermediate efficacy endpoints whilst ensuring no detriment on overall survival. Endpoints such as Overall Response Rate, Tumour Response, Depth of Response, Time to Progression, Organ-specific Progression-Free Survival, might be good candidates alongside Patient-reported Outcomes and Health Economics assessments.

Poster 26: Retrospective Review of Prophylactic Autologous Blood Clot Embolization Before Radioembolization/Chemoembolization

C. Chao; *Radiology, University of Maryland Medical Center, Baltimore, MD.*

Objectives: Radiation induced cholecystitis can be seen in 10% of radioembolization procedures by imaging and can be symptomatic requiring cholecystectomy in 0.6% to 2% of cases. Studies have described cystic artery embolization with coils or gel foam and a small risk of inducing right upper quadrant pain or injury requiring cholecystectomy. Autologous blood clot embolization may be effective and benign method of prophylactic embolization. In addition, autologous blood clot embolization may be an effective technique to spare radiation doses to parts of the liver that would otherwise require split dosing administered through more than 1 injection. We performed a retrospective review of all prior prophylactic embolization performed with autologous blood prior to radioembolization/chemoembolization.

Methods: Review of imaging and medical charts was performed for prophylactic embolizations by Interventional Radiology at a large academic institution. Patient demographics, diagnosis/indication, procedure, vessel embolized, reported pain, reported complication and post-embolization SPECT or PET/CT imaging findings and post-treatment cross-sectional imaging findings.

Results: A total of 6 prophylatic embolization procedures were performed (average age 63). Three procedures were for radioembolization, two for chemoembolization and one for mapping arteriogram. The cystic artery was embolized in 4 cases, the peripheral aspect of the left hepatic artery in one case and the anterior division of the right hepatic artery in another case. All cases had post-embolization arteriograms showing decreased flow, sluggish flow or stasis. Three patients had immediate post-embolization SPECT or PET/CT imaging showing no radiotracer in the gallbladder. Two patients had follow-up cross-sectional imaging confirming patency of the cystic or hepatic artery. One patient had a subsequent arteriogram showing patency of the cystic artery. No patient reported disproportionate right upper quadrant pain. There were no reported cases of imaging or clinical cholecystitis or hepatic abscess. For the patient with right hepatic artery anterior division embolization, there was qualitative decreased activity in the anterior aspect of the right hepatic lobe (which was without tumor) on post-radioembolization PET/CT.

Conclusions: Our small series of prophylactic autologous blood clot embolization performed prior to radioembolization or chemoembolization performed at a large academic center found no imaging of uptake of radiotracer in the gallbladder or clinical evidence of cholecystitis. For the patient with right hepatic artery anterior division embolization, there was qualitative decreased activity in the anterior aspect of the right hepatic lobe (which was without tumor) on post-radioembolization PET/CT. No complications were reported.

Poster 27: Safety of Yttrium-90 Radioembolization Using Resin Microspheres and the Medical Internal Radiation Dose Formula

A. Kudla, M. Ahmed, J. Weinstein, S. Faintuch, A. Sarwar; *Radiology, Beth Israel Deaconess Medical Center, Harvard Medical School, Boston, MA.*

Objectives: The purpose of our retrospective study was to review the safety of resin microsphere based yttrium-90 trans-arterial radioembolization (rTARE) using the medical internal radiation dose (MIRD) model for dosimetery instead of the routinely utilized body surface area (BSA) model.
Methods: All patients who underwent rTARE of hepatic malignancies at our institution between August 2015 and December 2017 were identified. Patients were included if they underwent rTARE using the MIRD formula for dosimetry. Data were obtained from clinical notes, procedure documentation, and imaging. Student's T-test was used to compare the dose administered based on MIRD and BSA models. Average follow-up was 10 months (range: 10 days to 25 months) after treatment.
Results: Overall, 28 rTARE administrations using MIRD dosimetry were performed in 26 patients (19M:7F, mean age 69 +/- 10 years). Treated malignancies included intra-hepatic cholangiocarcinoma (n= 14, 50%), hepatocellular carcinoma with portal vein invasion (n= 11, 39%), undifferentiated adenocarcinoma (n= 2, 7%), and metastatic colorectal cancer (n= 1, 4%). Most treated tumors were single lesions (n= 22, 79%) with a tumor size of 7.2 cm (1.8 - 14.0 cm). Treatment vessel was a segmental (15/28, 54%) or lobar (13/28, 46%) hepatic artery. For the MIRD model calculations, the average target absorbed dose was 147 Gy (120 - 200 Gy). Prescribed dose using the MIRD dosing model was 1.23 GBq (0.25 - 3.00 GBq), compared to 0.49 GBq (0.19 - 1.24 GBq) if a BSA model had been used for dosimetry ($p < 0.0001$). Average drawn dose was 1.28 GBq (0.24 - 3.02 GBq) and average delivered dose was 1.24 GBq (0.24 - 2.98 GBq). Successful delivery of the prescribed dose occurred in all cases (101.8%, range: 90.0 - 109.5%). No anti-reflux catheters were used. In 6/28 cases (21%), extra-hepatic arterial embolization was performed due to vessels arising close to the treatment position proximally (3/6) or vessels arising distal to the treatment position (3/6). No immediate post procedural complications occurred. Two Common Terminology Criteria for Adverse Events Grade 3 complications occurred: one patient developed radiation pneumonitis (resolved with steroids in 2 months) and one patient required hospital admission for pain control.
Conclusions: TARE with resin-based microspheres using the MIRD model for dosimetry results in a higher dose administration compared to the BSA model and is safe to perform without extra-hepatic vessel embolization in selected patients.

Poster 28: Software Assisted MRI-visible Grid for Transperineal MR-Guided Prostate Needle Interventions

I. Bakhutashvili[1], S. Xu[1], R. Li[2], Z. Tsz Ho Tse[3], I.B. Turkbey[4], P. Choyke[4], P. Pinto[5], B. Wood[1]; [1]*Center for Interventional Oncology, National Institutes of Health, Bethesda, MD;* [2]*College of Engineering, University of Georgia, Athens, GA;* [3]*3T Technologies, LLC, Marietta, GA;* [4]*Molecular Imaging Program, National Cancer Institute, Bethesda, MD;* [5]*Urologic Oncology Branch, National Cancer Institute, Bethesda, MD.*

Objectives: The aim of the study is to test the feasibility of a patient-specific, software-smart, targeted modality for biopsy and treatment of prostate cancer. In-bore direct magnetic resonance imaging (MRI)-targeted biopsy has many advantages, however, it comes at a higher cost and is time-consuming. A new modality is proposed based on a novel software which registers manually selected tumor locations on MRI images, and semi-automatically computes the optimal insertion points (on an MRI-visible grid) and depths allowing for accurate biopsy needle insertion into the selected tumor centers.
Methods: The MRI-visible grid was 3D printed using a Formlabs 3D printer (Form Inc., Watertown, MA). The size of the template is 80 mm x 80 mm. It has 144 MRI fiducial markers separated by 4 mm throughout the template, with each marker filled with a diluted gadolinium solution for MRI visualization. Each guide hole is centered in a square measuring 4 mm on each side with gadolinium fiducial markers arranged at the corners of each square. The grid was attached to a prostate phantom with three lesions (CIRS Inc., Norfolk, VA). An MR image of the grid and phantom was obtained, and both were registered to MRI coordinates. The spatial relationship between the tumor targets and the grid guide holes was registered by the software. Three lesions (with depths of 79 mm, 86 mm, and 69 mm) were manually selected within the software and designated as targets. The software then picked a single best guide hole for targeting a specific lesion and gave a suggested depth of needle insertion. The software outputs were used to perform needle insertions into the corresponding lesions and CT scan was used to assess the accuracy of the needle placement. This was validated by determining the distance of the needle from the center of each lesion, which was quantified by software.
Results: Targeting errors of needle insertion to the three lesions were measured to be 1.6 mm, 3.5 mm, and 4 mm.
Conclusions: It is feasible to use a software-assisted MRI-visible grid in transperineal MR-guided prostate needle interventions. Despite this being a feasibility study, the low magnitude of the needle placement errors justifies further translational studies. Furthermore, this technique has potentially wide-ranging applications beyond prostate biopsy, including non-prostate targeted needle interventions. Although somewhat speculative, patient-specific paradigms with semiautomatic targeting could potentially both facilitate and standardize needle-based interventions.

Poster 29: Technical Efficacy, Complications, Migration Rate, and Clinical Outcomes of Fiducial Marker Placement for Lung Tumors Prior to Stereotactic Ablative Radiotherapy: A Retrospective Analysis

A. Fang, R. Agarwal, A. Patel, A. Sharif, A. Sethupathi, M. Morel, K. Pereira, J. Kao, S. Gadani, K. Vaheesan; *Saint Louis University, Saint Louis, MO.*

Objectives: During stereotactic ablative radiotherapy (SABR), fiducial markers are implantable devices that help in localization of lung tumors in order to apply highly concentrated radiation doses to a small target area while sparing surrounding healthy tissue. The purpose of this study is to evaluate the technical efficacy, complications, migration rate, and clinical outcomes of fiducial marker placement in lung cancer patients undergoing SABR.
Methods: From 2009 to 2017, we retrospectively reviewed a total of 57 patients who underwent computed tomographic (CT) fluoroscopy-guided fiducial marker implantation with and without concurrent lung biopsy for pulmonary lesions prior to SBRT. Technical, demographic, and clinical outcomes of fiducial marker implantation were reviewed using the electronic medical records. Complications and fiducial marker migration were assessed based on intra-procedural and post-procedural follow-up computed tomography (CT) and positron emission tomography (PET)/ CT studies.
Results: Fifty-seven patients (24 men and 33 women, age, 70.2 ± 7.9 y) underwent CT-fluoroscopy-guided percutaneous placement of 140 lung fiducial markers (mean per tumor, 2.4 ± 1.0; range, 1-5) in 56 non-small cell lung cancer and 1 metastasis in the thorax (mean tumor size, 1.8 ± 1.1 cm). Forty-three patients (75%) had simultaneous biopsy performed prior to fiducial marker implantation. Gold seed (n=134) and twin line (n=6) fiducial markers were implanted intratumoral in 23 (16%), at tumor margin in 76 (54%), and outside in 41 (29%) cases. Lung fiducial marker placement was technically successful in all procedures. A total of 39 patients (68%) developed self-limited post-biopsy pulmonary hemorrhage. Thirty patients (52%) developed a pneumothorax and eight patients (14%) required a chest tube. A total of 16 gold seed fiducial markers (12%) migrated after insertion in a variety of locations including the abdomen (n=2), within the same lung (n=5), pleural space (n=5), right ventricle (n=1), right coronary artery (n=1) or undetermined location (n=2). None of the twin line fiducial markers migrated. Only 1 (0.7%) gold seed fiducial marker, which migrated into the right coronary artery 1 day after implantation, resulted in complication with myocardial infarction. Fifty-five patients (96%), including patients with migrated fiducial markers (n=11), completed SABR with an average of 3.9 ± 1.1 fractions and received a total average of 50 ± 8 Gy.
Conclusions: Lung fiducial marker placement and concurrent lung biopsy can be performed with high technical success. While self-limited pulmonary hemorrhage and pneumothorax are frequently observed, chest tube placement is less frequently required. Fiducial marker migration rarely resulted in significant complication or prevented completion of SABR.

Poster 30: Value of Superb Microvascular Imaging Guided Biopsy for Diagnosis of Solid Tumors in Children

Y. Chen[1], Y. Zhu[1], W. Guan[2], J. Fang[1]; [1]*ultrasound in medicine, Xinhua Hospital Affiliated to Shanghai jiaotong university school of medicine, Shanghai, China;* [2]*Pathology, Xinhua Hospital Affiliated to Shanghai jiaotong university school of medicine, Shanghai, China.*

Objectives: To investigate the value of superb microvascular imaging (SMI) in imaging vascularity and guiding biopsy of solid tumor in children.
Methods: A total of 65 children with solid tumor scheduled for biopsy were recruited in this study during March 2016 and June 2017. Eight children were excluded due to contradiction to anesthesia and unsafety puncture path. And another 9 children were excluded because color Doppler flow imaging/ color Doppler energy (CDFI/ CDE) was not performed. Finally, 48 patients with 48 solid tumors were enrolled in this retrospective study with mean age 4.58±3.62y (0.08-15y). All patients underwent CDFI/ CDE and SMI for tumor vascularity imaging before biopsy and Adler criteria was adopted for the evaluation the blood flow of the tumor. Biopsy was then performed targeting the hyper-vascularity region of the tumor within 3 days after ultrasound examination. Another 35 patients with mean age 5.6±3.2y (1.6-15y) underwent CDFI/ CDE guided biopsy between July 2012 and March 2015 were served as control group. The sample adequacy of these two groups was compared retrospectively.

Results: The Adler grade of 48 solid tumor was as follows: 2 tumors with grade 0 (4.2%, 2/48); 16 with grade I (33.3%, 16/48); 16 with grade II (33.3%, 16/48) and 14 with grade III(29.2%,14/48). By applying SMI technology, no tumor was scored with grade 0, 1 patient with grade I (2.1%, 1/48), 8 with grade II (16.7%, 8/48) and 39 with grade III (81.3%, 39/48). SMI was more sensitive in imaging tumor vascularity than CDFI/ CDE (P<0.001). The pathologic diagnosis was confirmed in all 48 tumors evaluated with SMI technology with sample adequacy of 100% (48/48). In the control groups, the biopsy was sampled in necrosis regions in 4 tumors and the pathologic diagnosis was then confirmed by open biopsy. The pathologic diagnosis was confirmed in 31 tumors with sample adequacy of 88.6% (31/35). The sample adequacy was significantly higher in SMI group than the control group (P=0.025).
Conclusions: SMI technology can improve tumor vascularity imaging by increasing micro vessel display. The solid tumor biopsy guided by SMI can avoid sampling necrosis or fibrotic regions and thus improve sample adequacy.

Poster 31: A Clinic Efficacy Study of CT Guided ^{125}I Seeds Implantation in the Treatment of Vertebral Metastasis of Hepatocellular Carcinoma (HCC)

Y. Chen; *The First Affiliated Hospital of the Army Medical University, Chongqing, China.*

Objectives: To explore the clinical efficacy of CT guided ^{125}I seeds implantation in the treatment of vertebral metastasis of hepatocellular carcinoma.
Methods: the clinical and imaging data of 16 cases with 23 metastatic tumors were collected. The prognosis was evaluated by Tokuhashi revised scale, the efficacy was evaluated by Karnofsky Performance Status (KPS) Numerical Rating Scale (NRS) and ASIA damage classification before and after surgery.
Results: All of 23 targets were implanted with ^{125}I seeds. The prescribed dose was 12000cGy, the gross tumor volume (GTV) was(22.9±21.4)cc, the median number of seeds was 24(5,50), the radioactive activity of seed was 0.8mCi, the D90 were (12399.7±837.4)cGy and (10506.2±427.1)cGybefore and aftersurgery. The KPS and NRS were both improved significantly 1 month later(P=0.000,P=0.000), the median survival time were 8 months while the survival rate of 3,6,12 months was 100%,56.2%,12.5%. All patients had no serious complications during follow-up.
Conclusions: CT guided ^{125}I seeds implantation is an effective and safe palliative treatment in vertebral metastasis of hepatocellular carcinoma, which can effectively relive the pain and improve the function of spine.

Poster 32: Application of Three-Dimensional Visualization Operative Treatment Planning System in Ultrasound-Guided Percutaneous Microwave Ablation for Liver Malignancies: A Randomized Controlled Trial

P. Liang, X. Li, M. Zhang, X. Yu, Z. Cheng, F. Liu; *Chinese PLA General Hospital, Beijing, China.*

Objectives: To assess the clinical efficiency of US-guided percutaneous microwave ablation (US-PMWA) assisted by three-dimensional (3D) visualization operative treatment planning system in liver malignancies.
Methods: Between July 2012 and Dec 2015, a single-center, randomized controlled trial was conducted on 120 patients with liver malignancies who received US-PMWA. Patients were randomly assigned to 3D visualization operative treatment planning system group (3D group) and the 2D preoperative planning group (2D group). The major outcome for assessment was local tumor progression (LTP) and complications.
Results: The 3D group (3.0±1.1cm) needed more the insertion number (2.4±1.3 vs. 2.0±1.0, P=0.035) and more treatment time (971±800s, vs. 736±437s, P=0.031) than the 2D group (2.9±1.2cm). At a mean follow-up period of 14.3 months, the LTP rates in the 3D group and the 2D group were 12.2% and 21.1%, respectively (P=0.147). According to the tumors size, the tumors were divided into smaller (D≤3cm) and larger (D>3cm) groups. For smaller tumors, there were no significant difference between two groups in all clinical varies. For larger tumors, the insertion number (3.2±1.4 vs 2.5±1.1, P=0.034) and treatment time (1394±945s vs. 993±457s, P=0.030) in the 3D group were more than those in the 2D group, and the LTP rate in the 3D group was lower than that in the 2D group (13.5% vs. 33.3%, P=0.049). No severe complications related to ablation occurred between the groups.
Conclusions: 3D visualization operation treatment planning system provides spatial structure of the tumor and the surrounding structures. US-PMWA assisted by 3D visualization operation treatment planning system appears to be a feasible, safe and effective technique for the management for larger liver malignance (D>3cm). The combination treatment would enlarge indications of US-PMWA and improve the clinical efficiency. Therefore, some selected patients beyond of guideline may be benefit from this therapy.

Poster 33: Case Report: Interventional Treatment for a Ruptured Large-Sized Hepatocellular Carcinoma

Z. Wang[1], Z. Lai[2], X. Hou[1], S. Fu[3], Z. Fang[4]; [1]*Radiology Department, Fujian Provincial Hospital, Fuzhou, China;* [2]*Hepatobiliary Surgery, Fujian Provincial Hospital, Fuzhou, China;* [3]*Anesthesiology Department, Fujian Provincial Hospital, Fuzhou, China;* [4]*Vascular Intervention Department, Fujian Provincial Hospital, Fuzhou, China.*

Objectives: Description The 64-year-old male patient with a left lobe hepatocellular carcinoma (5.8 / 9.3 cm) was treated with transcatheter arterial embolization (TAE) in another hospital. Three days later after the treatment, the patient was transferred to our hospital due to acute abdominal pain on Sep. 5th, 2017 and the lesion was found rupture hemorrhage with sub-capsular hematocele. And it was demonstrated that there was no portal vein tumor thrombus (Figure 1 A and B).
Methods: Treatment Two drainage tubes were inserted into the hematomas percutaneously two weeks after the hospitalization to drain away the hydrops (Figure 1 C and D). Two weeks later, MRI demonstrated a recurrence of hepatic carcinoma and transcatheter arterial chemoembolization (TACE) was performed immediately (Figure 1 E and F). One week after the TACE treatment, microwave ablation (MWA) for lesion in segment IV was performed (Figure 1 G and H) combined with ethanol ablation for lesion adjacent to porta hepatis (Figure 1 I and J) under CT guidance with intravenous anesthesia. And two weeks later after the combination treatment, MRI indicated tumor residual at segment IV and there was a metastasis at right hepatic lobe (Figure 2 A, B, C and D), which was treated with ethanol ablation (Figure 2 F, G, H and I) and MWA (Figure 2 E), respectively. After that, two drainage tubes were inserted to treat the liver abscess caused by ablation treatment (Figure 2 J and K).
Results: At present, MRI indicates no local tumor progression or metastasis (Figure 2 L). And the liver function and blood routine examination remained normal. The patient is in a quite good condition with regular follow up.
Conclusions: For large-size ruptured HCC adjacent to porta hepatis, combination of TACE, MWA and ethanol ablation may be a good method for treatment.

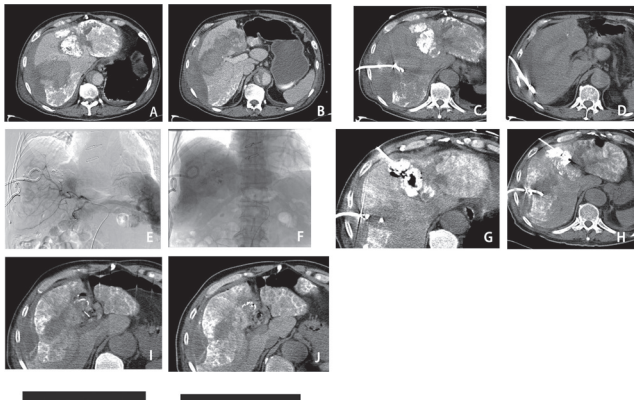

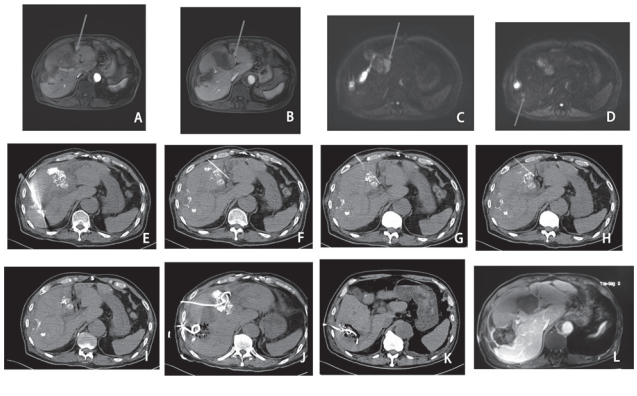

Poster 34: Clinical Safety and Efficacy of Radioembolization for Hepatocellular Carcinoma in Patients with Elevated Lung Shunt Fraction

A. Das, A. Gabr, R. Ali, R. Mora, S. Mouli, A. Riaz, R.J. Lewandowski, R. Salem; *Vascular Interventional Radiology, Northwestern University - Feinberg School of Medicine, Chicago, IL.*

Objectives: Technetium-99m macroaggregated albumin (Tc99m-MAA) administration is used to estimate lung shunt fraction (LSF) prior to yttrium-90 radioembolization (Y90). Recent studies have debated the safety and efficacy of Y90 in patients with LSF >15%. This study aims to demonstrate the role of Y90 in hepatocellular carcinoma (HCC) patients with LSF >15%.

Methods: With IRB approval, we searched our prospectively acquired database of all patients with HCC treated with Y90 between 2004 and 2017. Inclusion criteria were: patients with LSF >15% and imaging follow-up ≥1 month after Y90. Median LSF, dose to the liver, and dose to the lung were calculated. Follow-up laboratory values, imaging, and clinical encounters were reviewed from the electronic medical records for up to 1 year after Y90 to evaluate for toxicity. Response was assessed using the RECIST guidelines. Overall survival (OS) was calculated form date of first Y90 treatment.

Results: 103 HCC patients with LSF >15% underwent Y90 since 2004. Median baseline LSF was 24.4% (IQR: 18.1–28.8). Patients most commonly presented with multifocal disease (59/103, 60%) with median tumor size of 7.85 cm (IQR: 5.2, 10.57). BCLC Class A, B, C, and D were present in 7 (7%), 5 (5%), 85 (83%), and 6 (6%) patients. LSF reduction was attempted in 30 patients (29%) via coil embolization (21, 13%), bland embolization (6, 4%), and transarterial chemoembolization (TACE) (3, 2%). Median dose delivered to the liver was 84.6 Gy (IQR: 57.4, 107.55). The median lung dose per session was 22.9 Gy (IQR: 15-28) and median cumulative lung dose was 29.5 Gy (IQR: 20.5-44.3). Using the RECIST criteria, 33 patients (32%) demonstrated partial response of the index lesion, 57 patients (55%) demonstrated stable disease and 13 patients (13%) had progressive disease. Median OS in the entire cohort was 7.3 months (95%CI 5.3,11.47). 20 patients (19%) had non-specific pulmonary symptoms (cough, shortness of breath, wheezing, or difficulty breathing) at any time in the 1 year post-Y90. Median time to appearance of non-specific pulmonary symptoms was 63 days post-Y90 (range: 7-224). Analysis of thoracic imaging in these patients demonstrated that none had evidence of pulmonary fibrosis following treatment. 3 patients (3%) had non-specific pleural effusions. Median OS in patients with non-specific pulmonary symptoms was 6.67 months (95%CI: 5.2,20.6) compared to 7.33 months (95%CI: 5.27,12.8) in patients without symptoms (Log-Rank, p = 0.90).

Conclusions: Our data shows that Y90 can be performed in patients with LSF >15% with a 0% incidence of radiation pneumonitis. Response using RECIST guidelines was identified in 32% of the patients. In isolation, LSF >15% should not deter from treatment with Y90.

Poster 35: Combined Laparoscopic Hepatectomy and Microwave Ablation for Multifocal Liver Neoplasms

Y. Ge, J. Ma; *The First Affiliated Hospital Of USTC(Anhui Provincial Hospital), Hefei, China.*

Objectives: The aim of this study was to evaluate the effect,safety and feasibility of laparoscopic hepatectomy combined with microwave ablation in the treatment of multifocal liver Neoplasms.

Methods: Clinical data of 9 patients with Liver Neoplasms treated in Anhui Provincial Hospita between January 2014 to May 2017 were retrospectively studied. There were 6 males and 3 females, aged 42~77 years, with average age of (56.7±11.4) years old. The informed consents of all patients were obtained and the local ethical committee approval had been received.9 patients were all treated with Laparoscopic hepatic resection of partial liver and Other lesions with microwave ablation. The intraoperative and postoperative blood loss, operation time, postoperative hospital stay, postoperative complications and curative effect were observed.

Results: In all 9 patients,7 patients completed laparoscopic hepatectomy combined with microwave ablation,and 2 patients transfered to the laparotomy due to high risk of bleeding. There are 2 cases of cholecystectomy. The operation time was (191.6 ±42.2)min, blood loss was(85.5 ±63.2)ml, and hospital stay time after operation was(6.0 ±1.8)d. All patients did not use Hepatic vascular exclusion and no patients received blood transfusion during and after operation. All patients recovered well after the operation and no complications such as abdominal bleeding and bile leakage were observed.

Conclusions: Laparoscopic hepatectomy combined with microwave ablation is a safe, feasible and effective method for the treatment of multifocal liver Neoplasms.

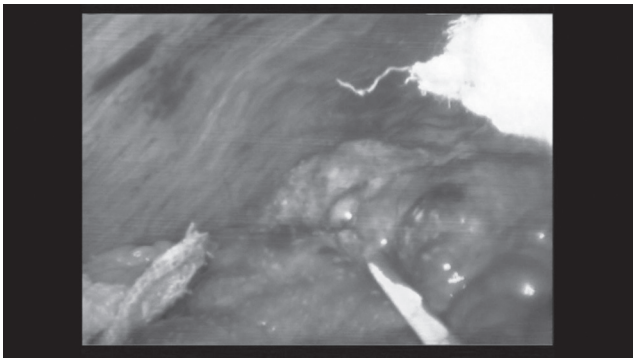

microwave ablation

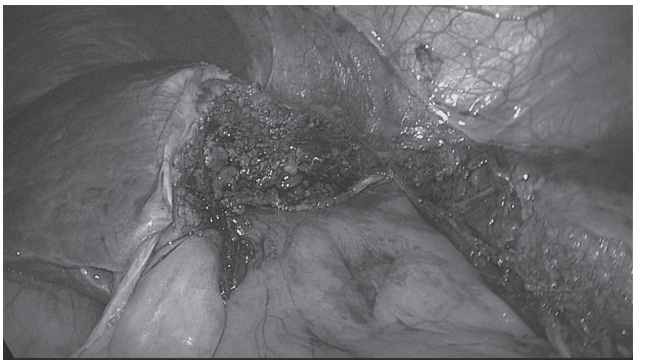

laparoscopic hepatectomy

Poster 36: Comparative Outcomes of Combined Hepatocellular-Cholangiocarcinoma and Hepatocellular Carcinoma After Locoregional Therapy: A Propensity Score Analysis

Y. Huang[1], B.V. Park[1], Y. Chen[2], R.C. Gaba[1], R. Lokken[1]; [1]*Radiology, University of Illinois, Chicago, IL;* [2]*Center for Clinical and Translational Science, University of Illinois at Chicago, Chicago, IL.*

Objectives: Combined hepatocellular-cholangiocarcinoma (HCC-CC) is a rare tumor with higher rate of recurrence and lower survival after resection or transplant compared to HCC. The purpose of this study was to determine tumor response and time-to-progression (TTP) of HCC-CC after locoregional therapy (LRT) compared to HCC.

Methods: Records of 9 patients (7 men, 2 women; median age 59 y) with 10 biopsy-proven HCC-CC (mean diameter, 4.4±2.1 cm; mean number, 3.4±2.5) treated with LRT between 2007-2017 were retrospectively reviewed. Patients were treated with transarterial chemoembolization (TACE) (n=5, 56%), yttrium-90 radioembolization (Y90) (n=2, 22%), radiofrequency ablation (RFA) (n=1, 11%), and combination TACE/RFA (n=1, 11%). A control cohort comprised 124 patients (92 men, 32 women; median age 59 y) with 134 biopsy-proven HCC (mean diameter, 4.8±4.0 cm; mean number, 2.6±2.2) treated with TACE (n=51, 41%), Y90 (n=17, 14%), ablation (n=41, 33%), and TACE/ablation (n=15, 12%). Propensity score matching (1:4) was conducted using a nearest-neighbor algorithm with caliper range of 0.20 to match for age, gender, LRT modality, infiltrative phenotype, macrovascular invasion, tumor diameter, tumor burden within Milan criteria, and Child-Pugh classification. Radiologic response and TTP were assessed by mRECIST. Objective response rates were compared by the Chi-Square test, and TTP by Kaplan-Meier method and univariate Cox proportional hazard model.

Results: Median follow-up was 129 (interquartile range (IQR), 102-239) d for HCC-CC and 329 (IQR, 184-660) d for HCC. On univariate analysis of all patients, initial LRT achieved complete response in 1 of 8 (12.5%) HCC-CC and 53 of 107 (49.5%) HCC; partial response in 1 of 8 (12.5%) HCC-CC and 23 of 107 (21.5%) HCC; stable disease in 2 of 8 (25.0%) HCC-CC and 26 of 107 (24.3%) HCC; and progressive disease in 4 of 8 (50.0%) HCC-CC and 5 of 107 (4.7%) HCC. Objective response rate after LRT was significantly lower for HCC-CC vs. HCC (25.0% vs 71.0%; P = 0.01). On follow-up, progression was observed in all 9 (100%) HCC-CC patients and 64 (60%) HCC patients, with median TTP of 66 d (IQR 30-120 d) in the HCC-CC cohort and 178 d (IQR 81-311 d) in HCC controls (HR: 4.3, 95% CI 2.1-8.8, P < 0.0001). Propensity score matched analysis demonstrated significantly shorter TTP (median 72 d vs. 177 d, P = 0.04), and trends toward greater progression within 100 d (63% vs. 23%, P = 0.06), and poorer objective response (38% vs. 73%, P = 0.09) after LRT for HCC-CC vs. HCC patients.

Conclusions: Patients with HCC-CC demonstrated worse radiologic response, a higher rate of progression after LRT, and significantly shorter TTP compared with HCC controls. These findings suggest a need for adjunctive treatment strategies to improve clinical outcomes.

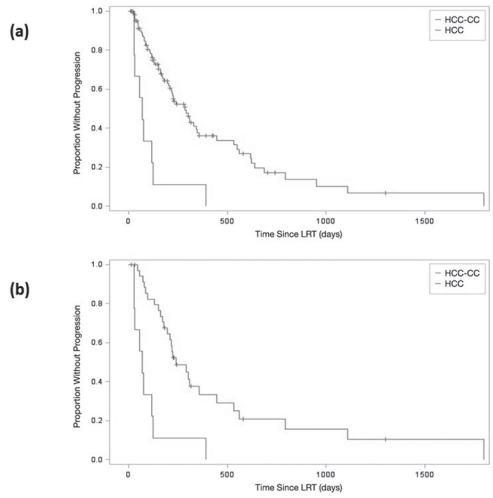

Figure. Kaplan-Meier curves of TTP for all patients **(a)** and for propensity-matched patients **(b)**. Median overall TTP **(a)** was 66 d in the HCC-CC cohort and 178 d in the HCC controls with a higher hazard of progression (HR, 4.30; 95% CI 2.10, 8.82; $P < 0.0001$). For propensity-score matched patients **(b)** the overall median TTP was 72 d in the HCC-CC group and 177 d in the HCC controls with a propensity score-adjusted hazard ratio of 4.02 (95% CI: 1.79, 9.02; $P = 0.0007$).

Poster 37: Direct Radioembolization of the Cystic Artery for Hepatic Malignancy

C.T. Stuart, D. Kies, R. Ermentrout; *Interventional Radiology, Emory University, Atlanta, GA.*

Objectives: Yttrium-90 (Y90) transarterial radioembolization (TARE) is used to treat primary and metastatic liver cancers. Prior to treatment, a detailed map of the visceral arteries is crucial to avoid non-target embolization to abdominal viscera, particularly bowel and gallbladder (GB). Embolization may be used to occlude visceral arteries prior to therapy. For the cystic artery, embolization can itself cause ischemic cholecystitis, and Y90 delivery to the cystic artery may cause radiation-induced cholecystitis. But in some cases the cystic artery can be parasitized by hepatic malignancies in such a way that treatment demands TARE of this vessel.
Methods: From 2015-2016 two patients were treated with direct cystic artery TARE. The first patient (A) was 59 years old with a 2 cm HCC in segment IV. He underwent TARE as bridge to orthotopic liver transplantation (OLT). The second patient (B) was 71 years with a 4.0 cm GB mass and synchronous 4.1 cm metastasis to segment VIII. The patient did not want systemic chemotherapy. Both patients were treated with Y90 glass microspheres (Therasphere, BTG). All treatments were performed as outpatients.
Results: Patient A was initially treated with radiation segmentectomy (RS) via segment IV hepatic artery. He recurred locally after 15 months with a 3.2 cm mass and a new 1.0 cm HCC in segment II. His recurrent HCC was being supplied exclusively by the cystic artery. RS was utilized with segment IV as the treatment volume. The segment II lesion was not treated. 2 month MRI demonstrated partial treatment response and importantly he was again within Milan criteria. He underwent OLT the day after his MRI. For patient B the metastasis was treated first with RS, and 4 weeks later the GB mass was treated via the cystic artery. Again, segment IV was utilized as the treatment volume. At 25 months follow-up the patient shows continued complete response. No complications occurred in either patient and there were no readmissions for post-embolization syndrome.
Conclusions: Direct TARE of the cystic artery with glass microspheres is safe and in this small series there was no clinical evidence of cholecystitis.

Poster 38: Does Conventional TACE (C-TACE) vs. Drug-Eluting Bead TACE (DEB-TACE) for Intermediate Stage Hepatocellular Carcinoma (HCC) Affect Patient Survival and Disease Progression?

J.L. Martin, J. Kachura; *Joint Department of Medical Imaging, University of Toronto, Toronto, ON, Canada.*

Objectives: The objective of this study was to determine differences in overall survival (OS) between patients receiving C-TACE and DEB-TACE for HCC, and the effects on local and distant disease progression.
Methods: Consecutive patients treated for intermediate stage HCC from Jan. 1, 2011 to July 1, 2017 were retrospectively reviewed, totalling 291 patients. Demographic, clinical, and radiologic information was collected, including OS. Patients surviving longer than 3 years after initial TACE were labelled "super survivors" (SS). Statistical analyses were performed using MedCalc for Windows, version 15.0 (MedCalc Software, Ostend, Belgium).
Results: The C-TACE group had 181 patients, and the DEB-TACE group 110. The C-TACE group was significantly younger (median age 64.0 vs. 67.3 years, P=0.0069). There were no differences in gender, weight, BMI, Child-Pugh, MELD score, multifocal disease, INR, bilirubin, creatinine and albumin between the C-TACE and DEB-TACE groups (P>0.05). Doxorubicin dose was higher in the C-TACE group (103.2 vs. 83.4 mg, P<0.0001). Time to local progression was significantly higher in the C-TACE group (253 vs. 167 days, P=0.0054) and there was no difference in time to distant progression (P=0.0678). Downstaging as per Milan criteria was not significantly affected by TACE type (OR=0.8051, CI 0.544-1.4265). There was no significant difference in disease progression beyond Milan criteria between TACE types (OR=0.3889, CI 0.1292-1.1705). OS was significantly higher in the C-TACE group (892 vs. 417 days, P<0.0001). ANOVA demonstrated significant differences in OS (P<0.001). However, Kaplan-Meier survival analysis demonstrated no significant differences in survival curves (1259 vs. 1039 days, Logrank test, P=0.230). SS status was more common in the C-TACE group (35% vs. 29%, P<0.0001). Logistic regression demonstrated TACE type was a significant predictor of SS status (P<0.0001). Multiple regression demonstrated TACE type was a significant predictor of days to local progression (P=0.0054), but was not a predictor of days to distant progression (P=0.0678).
Conclusions: Overall survival is not significantly different between C-TACE vs. DEB-TACE for intermediate stage HCC. However, C-TACE is a significant predictor of obtaining super survivor status and longer time to local disease progression. Doxorubicin dose was significantly higher in patients undergoing C-TACE.

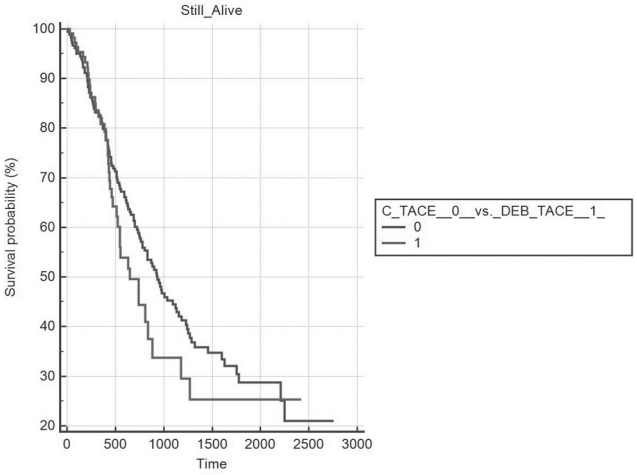

Poster 39: Efficacy of Percutaneous Thermal Ablation for Patients with Recurrent Hepatocellular Carcinoma After Hepatectomy and A Nomogram to Predict the Survival Possiibility

Z. Yuan, Y. Wang, C. Hu, J. Zheng, W. Li; *Center of Interventional Oncology and Liver Diseases, Beijing You'an Hospital, Capital Medical University, Beijing, China.*

Objectives: This study aimed to evaluate the efficacy of percutaneous thermal ablation for recurrent hepatocellular carcinoma (rHCC) after hepatectomy and establish an effective prognostic nomogram to predict the survival possibility.
Methods: This study consisted of 168 patients with rHCC after hepatectomy who were treated with thermal ablation. Overall survival (OS) was the primary endpoint. The primary cohort (117 patients) which received ablation was used to establish a prognostic nomogram. And 51 rHCC patients were enrolled in the validation cohort to validate the predictive accuracy of the proposed nomogram. The performance of the nomogram was assessed by concordance index (C-index) and compared with 5 conventional HCC staging systems.
Results: The 1-, 3-, and 5-year OS of primary cohort (PC) were 88.4%, 70.7% and 64.1%, respectively. The 1-, 3- and 5-year PFS rates of PC were 44%, 14% and 8.7%, respectively. In multiple analysis of prognostic factors for PC, tumor size (P=0.0469; HR,1.020; 95%CI, 1.0004-1.040), preoperative extrahepatic disease (P=0.0675; HR,2.604; 95%CI, 0.933-7.264) and close to hepatic hilum < 2 cm (P=0.0053; HR,3.691; 95%CI, 1.474-9.240) were classified as independent predictive factors for OS. These variables were used to develop a nomogram able to predict survival (C-index, 0.752; 95% CI, 0.656 - 0.849). According to the predicted OS, rHCC patients were divided into 3 risk classes (P<0.05): low risk (total score < 55; predicted OS, 82.9%), intermediate risk (55 ≤ total score < 99; predicted OS, 52.8%) and high risk (HR, total score ≥ 99; predicted OS, NA). The C-indices of contemporary staging systems were ranging from 0.511 to 0.653, while the proposed nomogram demonstrated a C-index exceeding 0.7, indicating that conventional systems to predict survival of rHCC were no better than the proposed nomogram.

Conclusions: Percutaneous thermal ablation appears to be an effective procedure for treating rHCC after hepatectomy. The proposed nomogram provided a mechanism to accurately predict survival and stratify risk among rHCC patients treated by locoregional ablation therapy.

Table 1. Multivariate analysis of prognostic factors for primary cohort

Variables	HR	95%CI	P value
Close to hepatic hilum < 2 cm	3.691	1.474-9.240	0.0053
Size of tumor (mm)	1.020	1.0004-1.040	0.0469
Preoperative extrahepatic disease	2.604	0.933-7.264	0.0675

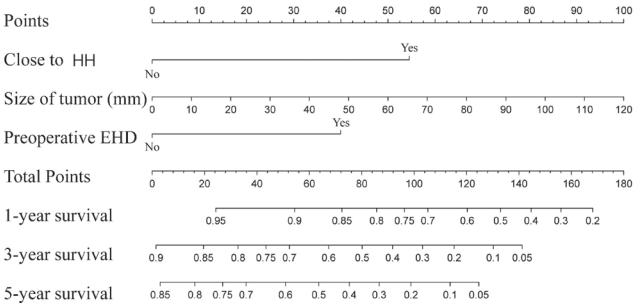

Fig 1. Recurrent hepatocellular carcinoma prognostic nomogram.

Poster 40: Hepatic Arterial Infusion Chemotherapy with Oxaliplatin and 5-fluorouracil with or without Sorafenib for Hepatocellular Carcinoma with Major Portal Vein Tumor Thrombosis

J. Hu[1], G. Cao[2], X. Zhu[2], R. Yang[2], X. Wang[2], X. Wang[3], B. Xing[4]; [1]*Department of Interventional Radiology, Peking University Cancer Hospital & Institute, Beijing, China;* [2]*Peking University Cancer Hospital & Institute, Beijing, China;* [3]*Peking University Sixth Hospital, Beijing, China;* [4]*Department of Hepatic, Biliary & Pancreatic Surgery, Beijing, China.*

Objectives: To evaluate the efficacy of hepatic arterial infusion chemotherapy (HAIC) with oxaliplatin (OXA) and 5-fluorouracil (5-FU) with or without sorafenib in hepatocellular carcinoma (HCC) patients with major portal vein tumor thrombosis (PVTT).

Methods: This single institutional retrospective study included 14 HCC patients with major PVTT in Child-Pugh class A. HAIC consisted of infusion of OXA 35-40 mg/m^2 for 2 h, followed by 5-FU 600-800 mg/m^2 for 22 h on days 1–3, every four weeks. Nine patients also received sorafenib 400 mg/m^2 twice daily. Tumor response, overall survival (OS), and adverse events were investigated.

Results: The median number of HAIC cycles was 5 (range, 2–6). Overall response rate of the patients was 64.3% (9/14). Median progression-free survival (PFS) and OS were 10.6 and 20.3 months, respectively. Median OS of 22.8 months for nine patients treated with HAIC + sorafenib was significantly longer than patients treated with HAIC alone (14.8 months) (P = 0.02). Adverse events were mild and well tolerated. The only grade 3 toxicities were gastrointestinal (1/14) and liver (2/14) recoverable disorders.

Conclusions: HAIC with OXA and 5-FU may be a feasible and safe treatment for selected HCC patients with major PVTT in Child-Pugh class A. Patients may benefit more from combination of HAIC and sorafenib.

Poster 41: Importance of Interventional Oncology in Bridging/Downstaging of Patients with Hepatocellular Carcinoma to Liver Transplantation

E. Meram[1], A. Hinshaw[2], O. Ozkan[1], P.F. Laeseke[1]; [1]*Radiology, University of Wisconsin-Madison, Madison, WI;* [2]*University of Wisconsin-Madison, Madison, WI.*

Objectives: Interventional oncology (IO) treatments are vital in the management of patients with hepatocellular carcinoma (HCC), including in bridging/downstaging patients to liver transplantation. This study aims to characterize the role of IO therapies in bridging/downstaging of HCC patients to liver transplantation in a single center setting based on the decisions of multidisciplinary tumor board on treatment allocations.

Methods: This study was approved by our institutional review board and was compliant with HIPAA guidelines. A total of 516 patients that have presented to the primary liver tumor board of our institution from 2012 to 2017 were reviewed retrospectively. Among them, 288 patients (56%) with a definitive diagnosis of HCC were identified. Patient demographics, tumor characteristics and liver function at the time of tumor board were recorded to calculate Barcelona Clinic Liver Cancer stage. After reviewing patients' medical records, the patients with prior treatments or inadequate medical information were excluded, resulting in 176 patients with HCC that were included in the study. Descriptive statistics were used for analysis.

Results: Of 176 patients with a definitive diagnosis of HCC, 37 patients were found to undergo liver transplantation. Of 37 patients, 2 were BCLC stage 0, 24 were stage A, 2 were stage B, 7 were stage C, and 2 were stage D. Of all transplantations, only two were first-line treatments with no other prior therapies, while 35 patients were treated with at least one type of IO therapy as a bridge to their transplantation. Of the 35 patients, 26 underwent one treatment prior to transplant while 9 patients had more than one treatment. For bridging/downstaging of 35 patients, a total of 46 procedures were performed with a median of one (range, 1-5) procedure per person. Among the 46 procedures, ablative therapies were the most common (32/46, 71.1%) followed by TACE (8/46, 17.8%), radioembolization (4/46, 8.9%), and resection (1/46, 2.2%). Median time to liver transplantation was 11.3 months (range, 0.6-28.4 mo).

Conclusions: The majority of patients with HCC who underwent liver transplantation at our institution were bridged or downstaged with IO therapies including ablation, chemoembolization and radioembolization. IO therapies are vital in increasing the number of patients that can receive a transplant or in maintaining their transplant candidacy.

Poster 42: Incidence, Predictors, and Survival Effects of Portal Vein Thrombus Post-TACE for Hepatocellular Carcinoma (HCC)

J.L. Martin, J. Kachura; *Joint Department of Medical Imaging, University of Toronto, Toronto, ON, Canada.*

Objectives: The objective of this investigation was to determine the incidence, distribution, and impact on overall survival (OS) of portal vein thrombus (PVT), post-transarterial chemoembolization (TACE) for intermediate stage HCC. Factors affecting the development of PVT and the time to PVT formation were also investigated.

Methods: Consecutive patients treated from Jan. 1, 2011 to July 1, 2017 were retrospectively reviewed, totalling 291 patients. Of these, 74 patients developed PVT post-TACE. Demographic, clinical, and radiologic information was collected, including OS. Cross-sectional imaging and angiography was reviewed. Statistical analyses were performed using MedCalc for Windows, version 15.0 (MedCalc Software, Ostend, Belgium).

Results: From patients undergoing TACE, 25.4% developed PVT. The average time to PVT formation was 298 days (range 7-1393, SD 329). PVT most commonly occurred in a segmental branch (67.6%), followed by right PV (33.8%), main PV (32.4%) and left PV (24.3%). Bland thrombus comprised 63.5%, and tumor thrombus 36.5%. PVT formed acutely (within 60 days) in 24.32% and remotely (>60 days) in 75.68%. Logistic regression demonstrated age, sex, weight, BMI, interval between TACE procedures, TACE type, MELD score and multifocal disease were not predictors of PVT formation (P>0.05). Kaplan-Meier survival analysis demonstrated the formation of PVT post-TACE significantly decreased OS (P<0.05). The presence of tumor thrombus significantly decreased OS (599 vs. 1144 days, P=0.0019, HR 2.25 (95% CI 1.23-4.12)). Cox proportional-hazards regression demonstrated PVT development, time to PVT development, and formation of tumor thrombus significantly affected OS (P=0.0168, 0.0364, and 0.0020, respectively). PVT formed acutely vs. remotely did not have a significant effect on overall survival (P=0.6604). The vascular distribution of PVT did not affect OS (P>0.05). TACE type (conventional vs. drug-eluting beads) was not significantly related to PVT formation (P=0.2023) or time to PVT formation (314 vs. 263 days, P=0.513). Patients with PVT formation post-TACE were 60% less likely to be downstaged as per Milan criteria (OR 0.40, CI 0.2059-0.7811).

Conclusions: PVT formation commonly occurs post-TACE, usually presenting as bland thrombus affecting segmental branches. The formation of PVT post-TACE, time to PVT formation, and the presence of tumor thrombus significantly decrease overall survival. Patients with PVT formation post-TACE have significantly lower odds of being downstaged by Milan criteria.

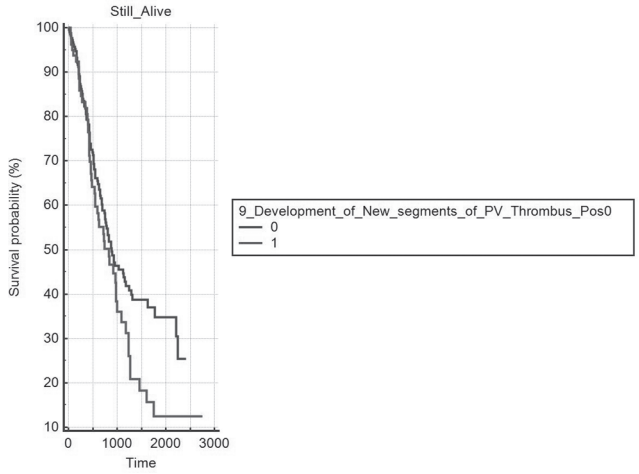

Figure 1. Kaplan-Meier curve comparing differences in overall survival between patients with (green) and without (blue) formation of PVT post-TACE.

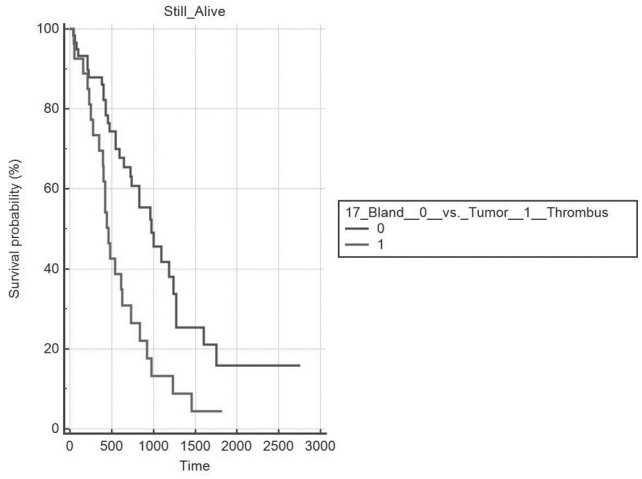

Figure 2. Kaplan-Meier curve comparing differences in overall survival between patients with formation of tumor thrombus (green) or bland thrombus (blue) post-TACE.

Poster 43: Increased Incidence of Significant Bleeding Associated with Percutaneous Biopsy of Hepatocellular Carcinoma: A Single Institution Experience

I. Talati, A. Miller, D. Buckley, T. Caridi, J. Cardella, E. Cohen, D. Field, G.E. Lynskey, J. Spies, A. Kim; *Medstar Georgetown University Hospital, Washington, DC.*

Objectives: To evaluate if percutaneous biopsy of hepatocellular carcinoma (HCC) results in increased procedure-related complications when compared with percutaneous biopsy of non-HCC liver lesions.

Methods: A retrospective review of patients was performed to identify patients who underwent percutaneous liver biopsy at Medstar Georgetown University Medical Center between 2012 and 2017 (HCC) or 2015 and 2017 (non-HCC). Percutaneous biopsies were obtained using a coaxial biopsy system. Post-procedure imaging, either with focused CT or US, were routinely performed by the operator to evaluate for immediate post-operative complication (e.g. bleeding).

Results: 95 liver biopsies were performed for non-HCC diagnoses. Average INR, platelet count and bilirubin were 1.1, 232,000/uL and 0.7mg/dl respectively. There were no biopsy-related complications in the non-HCC group. 61 biopsies were performed for hepatocellular cancer. Of these, 13 were negative for malignancy and 48 were positive for HCC. Average INR, platelet count and bilirubin were 1.2, 208,000/uL and 1.4mg/dl. A 20-gauge core biopsy needle was used in 92% of HCC biopsies (44/48; 19 gauge coaxial) while the remaining 4 were performed with an 18-gauge core biopsy needle (17 gauge coaxial). An average of 3.4 cores were obtained per patient/lesion (n = 39; range 1 – 9; median = 3). There were 6 biopsy-related complications in the HCC group. Three patients (6.3%) developed post-procedural hemorrhage requiring intervention (angiogram and embolization); one of these patients later developed multi-organ system failure and died. Two of these three patients had greater than the average number of cores removed (4 and 9 cores); the third patient did not have the number of cores recorded. All 3 patients were biopsied with a 20/19 gauge coaxial system. Minor complications not requiring intervention (n=3) included abdominal pain requiring ER evaluation, incidental small subcutaneous hematoma, and a tiny pneumothorax.

Conclusions: There were a total of 6 adverse events related to percutaneous biopsy of HCC (12.5%), including 3 cases of hemorrhage requiring intervention. There were no complications in the non-HCC patient group. The increased bleeding risk seen in our HCC group is likely related to intrinsic liver dysfunction (cirrhosis) as well as hypervascularity of HCC lesions. Due to increasing requests for molecular tumor profiling (and biopsy) to guide therapy, patients with HCC should be counseled appropriately on the increased risk of bleeding associated with percutaneous biopsy.

Poster 44: Liver Tumor Embolic Practices (LITE) Survey

V. Chandra[1], E. Wajswol[1], H. Wei[1], J.L. Leibowitz[1], B.C. Liu[1], S. Contractor[2]; [1]*Medicine, Rutgers New Jersey Medical School, Newark, NJ;* [2]*Interventional Radiology, Rutgers New Jersey Medical School-University Hospital, Newark, NJ.*

Objectives: To determine the usage of embolic agents in transcatheter directed locoregional therapy for liver tumor treatment.

Methods: A survey of Interventional Radiologists (IRs) was done utilizing Research Electronic Data Capture. A link to the survey was posted on the Society of Interventional Radiology's interventional oncology and general forums and all practicing IRs with experience treating liver tumors were invited to complete the survey. A direct email was also sent to IR program directors at multiple institutions. Questions in the survey included experience embolizing liver tumors, embolic agent (Lipiodol, drug-eluting bead (DEB), or Yttrium-90 (Y90)), and follow-up imaging modality after embolization amongst others (see http://j.mp/2CXU3iQ for sample survey). A usage pattern score was devised using a weighted average system for each type of embolic agent. Chi-square analysis was used to compare discharge and follow-up imaging modality preference among the different embolic regimens.

Results: To date, 69 participants have completed the survey since posting on Dec 2017. 36 participants specified their location, including numerous US states, Taiwan, and Seoul. Of the 69 participants, 29.4%, 42.6%, and 27.9% performed <25, 25-50, and >50 liver tumor embolizations per year respectively. 47.8% of participants practice in academic centers compared to 52.1% in private settings. 69.5%, 91.3%, and 84.1% of participants use a Lipiodol, a DEB, and a Y90 based regimen respectively. Usage pattern scores (described in methods) for the three regimens were as follows: Lipiodol 1.75, DEB regimen 1.94, and Y90 2.21. 68.1%, 26.9%, and 12.1% of Lipiodol, DEB, and Y90 users respectively use an additional embolic agent, with microspheres (43.5%) being the most common one. 23.4%, 26.7%, and 98.2% of participants discharge patients on the same day after Lipiodol, DEB, and Y90 based treatment respectively. A chi-square test of embolic technique (Lipiodol, DEB, Y90) vs. same-day discharge yielded a chi-square statistic of 80.044 and a p-value <0.00001 (significant at $p<0.05$). A chi-square test of embolic technique vs. post-embolization imaging modality (CT, MRI) yielded a chi-square statistic of 0.5548 and a p-value of 0.758 (not significant at $p<0.05$). Only 23.6% noted uniform practice for Lipiodol based embolization. 30.4% and 33.8% of respondents think that cost and training, respectively, are factors in deciding embolic regimen. In the end, 47.8% of the participants answered Yes to "do you believe profession societies should advocate a uniform embolization protocol?"

Conclusions: The conducted LITE survey provides insight into the heterogeneity of practice patterns between IRs for transcatheter directed locoregional therapies for liver tumors. Based on the results of the survey, Y90's relative popularity may be secondary to preliminary data from the PREMIERE trial showing superiority over TACE. Y90 treatment also lacks many of the systemic side effects of chemoembolics, often times allowing for same day discharge. Aside from Y90, which showed consistency in same day discharge and lack of use of additional embolic agent, there were no discernible differences in practice patterns between Lipiodol and DEB in follow-up imaging study, discharge pattern, or use of an additional embolic agent. Only 23.6% of participants noted a uniform practice for Lipiodol based embolization. No current societal or national guideline exists for type of embolic agent, most practice is based on local training factors. Further study is needed to examine the potential benefit of consolidating practice patterns among IRs for liver tumor treatment.

Poster 45: Pre-Existing Portal Vein Thrombosis Effect on Clinical Response and Outcomes After Microwave Ablation for Hepatocellular Carcinoma

A. Fang[1], E. Pang[1], J. Kao[1], M. Morel[2], S. Gadani[3], K. Pereira[4], K. Vaheesan[5]; [1]*SAINT LOUIS UNIVERSITY, SAINT LOUIS, MO;* [2]*SAINT LOUIS UNIVERSITY, SAINT LOUIS, MO;* [3]*SAINT LOUIS UNIVERSITY, SAINT LOUIS, MO;* [4]*SAINT LOUIS UNIVERSITY, SAINT LOUIS, MO;* [5]*SAINT LOUIS UNIVERSITY, SAINT LOUIS, MO.*

Objectives: To evaluate the clinical response and outcomes of patients with pre-existing portal vein thrombosis (PVT) undergoing microwave ablation (MVA) for hepatocellular carcinoma (HCC).
Methods: This retrospective study included 51 patients with HCC who underwent MVA between 2013 and 2017. Patients were followed with CT or MR imaging for at least 18 months to identify tumor progression. Clinical responses and outcomes were reviewed. New or worsening portal vein thrombosis, progression free survival (PFS), and overall survival (OS) were assessed.
Results: Out of 51 patients who underwent MVA for HCC, 8 patients (15.7%) had pre-existing PVT (5 M, 3 F; mean age, 67.6 y ± 6) and 43 patients (84.3%) had no pre-existing PVT (31 M, 12 F; mean age, 63.1 y ± 8.7). Prior to MVA, there were no significant differences between patients with and without PVT in terms of tumor etiology, MELD, ECOG, Child-Pugh, BCLC scores, and median tumor size. During MVA, there were no significant differences between groups for ablation time, wattage, number of overlapping sessions, antennae, and ablations per patient. Post-MVA, new or worsening PVT developed in 50% of patients with pre-existing PVT and only 7% of patients without PVT ($p<0.01$). Among the cohort with pre-existing PVT, patients with progressive thrombosis showed decreased OS at 18 months post-ablation (median: 9 vs. 17 mo, respectively, $p<0.05$), with no significant change in PFS compared with patients that did not have worsening thrombosis.
Conclusions: MVA of HCC in patients with pre-existing PVT is associated with worsening thrombosis and poorer clinical response. Caution should be used before proceeding with MVA in patients with pre-existing PVT and alternative treatment options should be explored.

Poster 46: Safety of Hepatic Transarterial Chemoembolization for Patients with Hyperbilirubinemia

T. Donovan, M. Albertson, W. Blair, S. Williams, S. Kunnathil, C. Vargo; *Interventional Radiology, University of Nebraska Medical Center, Omaha, NE.*

Objectives: To evaluate the safety of hepatic transarterial chemoembolization (TACE) for patients with and without preexisting hyperbilirubinemia. Hyperbilirubinemia can be a marker of poor liver function and inadequate hepatic reserve and is frequently encountered in patients with hepatocellular carcinoma (HCC) due to sequela of chronic underlying liver disease and tumoral related biliary ductal obstruction, especially in cases of advanced multifocal disease. Our specific objective was to determine if patients with preoperative total serum bilirubin levels >2 mg/dL have a statistically significant higher mortality compared to patients with normal bilirubin levels undergoing TACE.
Methods: Retrospective analysis performed on 235 patients undergoing hepatic TACE from 3/2012 - 9/2016 at the University of Nebraska Medical Center. Relevant perioperative laboratory and survivability data was obtained. Mortality was determined by using both hospital and governmental records. Chi-squared test was used to determine association in bilirubin levels and mortality rates between the two groups at 1, 6, and 12 months.
Results: 42/224 (18.8%) patients undergoing TACE had preoperative hyperbilirubinemia. 3/42 (7.1%) patients with hyperbilirubinemia were deceased at 1 month, 8/39 (20.51%) at 6 months, and 20/38 (52.63%) at 12 months. Comparatively, 4/182 (2.20%) patients with normal bilirubin levels were deceased at 1 month, 29/172 (16.86%) at 6 months, and 62/167 (37.13%) at 12 months. 11 patients were excluded from analysis at 1 month, 24 patients at 6 months, and 25 patients at 12 months as they were lost to follow-up after the procedure, despite review of mortality from hospital and government records. There was no significant association between bilirubin levels and mortality at 1 month (p-value, 0.0620) or 6 months (p-value, 0.3407). There was a statistically significant difference between bilirubin levels and mortality at 12 months (p-value, 0.0483).
Conclusions: We found a significantly higher mortality rate for patients undergoing TACE with hyperbilirubinemia at 1 year, although mortality rates were similar at 1 and 6 months. Given these findings, careful consideration and clinical expertise should be applied when selecting patients with hyperbilirubinemia for TACE.

Poster 47: Single Center and Exploratory Investigator-Initiated Trial to Evaluate the Safety and Efficacy of Needle Guiding Robot System for Radiofrequency Ablation in Hepatocellular Carcinoma Patients

S. Lee; *Asan Medical Center, Seoul, Korea (the Republic of).*

Objectives: This study evaluates the safety and efficacy of CT guided robotic needle targeting on patients with HCC.
Methods: The robot system including 5-axis robot arm, a mobile platform with motor controllers, dedicated workstation for planning of needle path, and the navigation system (Polaris Spectra®; NDI, Canada) was developed. It provides useful functions including such as needle path planning, respiration monitoring, laser guidance, automatic needle positioning and guiding. To evaluate the feasibility and accuracy of the system in needle placement, patient with HCC requiring retheraphy were included. CT scan was performed to localize the target lesion and the CT data was transferred to the system. The spatial relation between patient and the robot system was registered with navigation system. After planning the needle path on workstation, the spatial information was translated to the robotic system. The robot system automatically angulates the needle to the target and depth of insertion is determined. Total of 10 needle insertion trials were performed. Using the CT images after the insertion, distance between the target and actual needle tip and angle between preplanned route and actual needle pathway were measured.
Results: The distances between the target and the needle tip for robot assisted was 9.5±8.2mm. Angular deviation was 6.8 ±3.5°. Procedure was 55m ± 10m. Since additional CT scanning was performed.
Conclusions: CT guided robot assisted needle insertion appears to have high accuracy, safety and technically easier than the non-robotic assisted procedure.

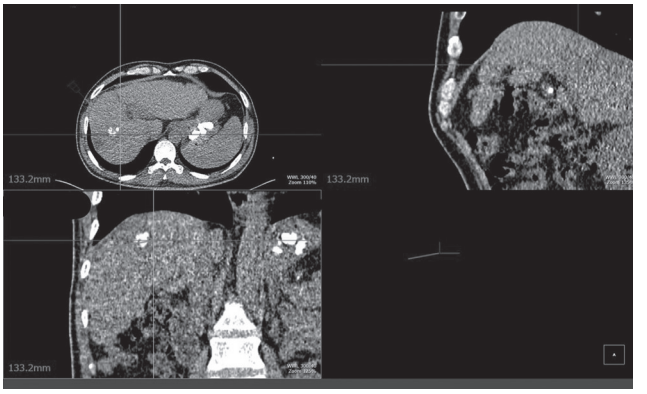

Screenshot of the path-planning user interface of CT-guided needle placement robot.

Poster 48: Stratification and Prognosis for Portal Vein Invaded Hepatocellular Carcinoma Treated with Transarterial Chemoembolization Monotherapy

B. Zhong[1], G. Teng[1], C. Ni[2], S. Chen[3]; [1]*Center of Interventional Radiology & Vascular Surgery, Department of Radiology, Zhongda Hospital, Southeast University, Nanjing, China;* [2]*Department of Interventional Radiology, First Affiliated Hospital of Soochow University, Suzhou, China;* [3]*Department of Interventional Radiology, Cancer Hospital of Jiangsu Province, Cancer Institution of Jiangsu Province, Nanjing, China.*

Objectives: Due to patient heterogeneity, who would benefit from transarterial chemoembolization (TACE) monotherapy for portal vein invaded hepatocellular carcinoma (HCC) is still uncertain. We aim to establish a prediction model to determine and select the beneficial patients.
Methods: HCC patients with portal vein invasion and treated with TACE monotherapy at three hospitals between January 2008 and December 2016 were included. In the training cohort, independent risk factors associated with overall survival (OS) were identified by univariate and multivariate Cox proportional hazards analyses. Then, a prognostic model was established to find out who will benefit most from TACE monotherapy. The accuracy of the model was validated externally in the validation cohort.
Results: A total of 180 patients (training cohort: n=126; validation cohort: n=54) were included. In the training cohort, the median OS was 6.4 months. The prognostic prediction (PP) model was established based on the following three independent risk factors: Cheng's classification (0 if type I, 1.5 if type II, 11 if type III), number of HCC nodules (0 if 1, 6.5 if >1), and Child-Pugh stage (0 if A, 5.5 if B7). PP score of 9.5 was identified as cut-off point and patients were divided into two groups by PP score of <9.5 and >9.5 in survival benefit and prognostication (8.5 vs. 4.2 months). The PP model received high accuracy with C-index of 0.742 when validated in the validation cohort.
Conclusions: Portal vein invaded HCC patients with PP score <9.5 may benefit most from TACE monotherapy.

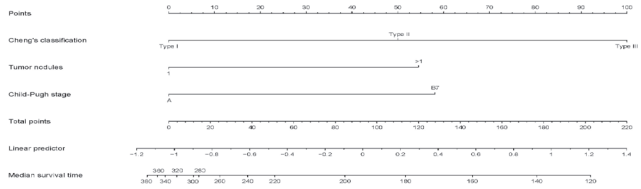

Prognostic nomogram for patients with portal vein invaded HCC after TACE monotherapy. To use the nomogram, an individual patient's value is located on each variable axis, and a line is drawn upward to determine the number of points received for each variable value. The sum of these numbers is located on the total points axis, and a line is drawn downward to the survival axes to determine the likelihood of median survival time.

Poster 49: Summarize the Nursing Highlights of CT-Guided Percutaneous Microwave Ablation of Primary Liver Cancer

x. xing; *Center of Interventional Oncology and Liver Disease, Beijing YouAn Hospital, Capital Medical University, Beijing, China.*

Objectives: To summarize the nursing highlights of CT guided percutaneous microwave ablation of primary liver cancer
Methods: 126 patients with primary liver cancer treated with TACE and CT guided percutaneous microwave ablation were applied of high quality perioperative nursing care, perioperative adverse reactions were analyzed and summarized.
Results: 126 patients received TACE and CT guided percutaneous microwave ablation successfully, 89 patients had mild complications, 4 patients had severe complications, all recovered after active treatment and care, no death occurred.
Conclusions: adequate preoperative preparation, intraoperative nursing cooperation, and postoperative effective treatment and care is beneficial to disease recovery, and it is important for complication prevention and improvement of life quality.

Poster 50: Transarterial Chemoembolization with Apatinib for Hepatocellular Carcinoma with Main Portal Venous Tumor Thrombus: A Retrospective Study

T. Si; *Interventional treatment, Tianjin medical university cancer hospital and institute, Tianjin, China.*

Objectives: To investigate the effcacy and safety of combined therapy with transarterial chemoembolization (TACE) and Apatinib for hepatocellular carcinoma with main portal venous tumor thrombus (mPVTT).
Methods: The medical records of consecutive patients with HCC and mPVTT who underwent TACE-Apatinib or TACE alone from January 2015 to January 2017 were retrospectively evaluated. Apatinib (250 mg) was administered once daily. Clinical information on the patients was collected. Adverse events, overall survival, objective response rate based on mRECIST criteria (American Association for the Study of Liver Diseases, 2008) were reviewed and evaluated. Outcomes of patients who underwent TACE-Apatinib were compared with outcomes of patients who underwent TACE alone by using the Kaplan-Meier method.
Results: All patients had complete follow-up records and the median follow-up time was 13 months (1–24 months). 60 patients were included in the analysis; 25 patients underwent TACE-Apatinib and 35 underwent TACE. The objective response rates for the tumor were 60% and 42.9%, respectively, and the objective response rates for PVTT were 68% and 34.3%, respectively. TACE-Apatinib showed signifcant survival benefits compared with TACE (median survival, 15 months vs 10 months; P = .003). The most common apatinib-related adverse events were hand-foot-skin reaction, fatigue, dyspepsia, diarrhea, and hypertension, and the most common TACE-related adverse event was fever. No procedure-related mortality or grade 4 adverse events were observed, but grade 3 adverse events were observed in two patients.
Conclusions: This exploratory study suggested that apatinib combined with TACE treatment was safe and might improve overall and progression-free survival in patients with hepatocellular carcinoma with mPVTT. Further randomized controlled trials are warranted.

Poster 51: Utilization of Radioembolization by a Liver Tumor Board for the Treatment of Hepatocellular Carcinoma at a Single Tertiary Care and Liver Transplant Center

E. Meram[1], A. Hinshaw[2], O. Ozkan[1], P.F. Laeseke[1]; [1]*Radiology, University of Wisconsin-Madison, Madison, WI;* [2]*University of Wisconsin-Madison, Madison, WI.*

Objectives: Hepatocellular carcinoma (HCC) is a complex disease with multiple treatment options. Radioembolization (RE) is a relatively recent addition to the HCC treatment arsenal and has not yet found a place in treatment guidelines. This study aims to characterize the utilization of radioembolization in the treatment of patients with HCC discussed at a multidisciplinary primary liver tumor board of a single tertiary care and liver transplant center.
Methods: This IRB approved study was compliant with HIPAA guidelines. A total of 516 patients who were discussed by the primary liver tumor board of our institution from 2012 to 2017 were reviewed retrospectively. Among them, 288 patients (56%) with a definitive diagnosis of HCC were identified. Patient demographics, tumor characteristics, and liver function at the time of the initial tumor board were recorded to calculate Barcelona Clinic Liver Cancer (BCLC) stage. Timing and type of therapies (transarterial chemoembolization [TACE], etc.) were also documented. Patients treated previously or with inadequate data were excluded, resulting in a final cohort of 176 patients with HCC. Descriptive statistics were used for analysis.
Results: The 176 patients with HCC received a total of 348 treatments, of which 143(41.1%) were ablation, 90(25.9%) were TACE, and 52(14.9%) were RE. The 52 RE procedures were performed in 42 patients. RE was the 3rd most common first-line treatment (19.3% of 176 patients) behind ablative therapies(51.7%) and TACE(20.1%). RE was most commonly performed as first-line treatment in patients with BCLC stage C disease (73.5%) followed by patients with BCLC B disease(20.5%). More than half (25/48) of patients with BCLC C disease underwent RE as first-line therapy. In contrast, none received sorafenib, the recommended therapy according to BCLC algorithm. RE was performed as first-line therapy in 7 of 19 patients(36.8%) with BCLC B disease compared to 36.8% receiving the BCLC recommended TACE. Of 91 patients with stage A disease, only 1 patient was treated with RE as first-line and most (61 patients) underwent ablation as recommended by BCLC. Eight patients, most of whom(87.5%) underwent ablation as the first-line therapy, underwent RE as second- (6 patients) or third-line therapy (2 patients). Median time to RE for those 6 patients receiving RE as the second-line therapy was 3.5 months (range, 1.0-47.6 mo). Fifteen (44.1%) of the patients who underwent RE as the first-line therapy subsequently underwent additional non-RE treatments. Median time to the additional treatments was 6.9 months (range, 0.9-21.4 mo).
Conclusions: Radioembolization, which has yet to find its place in treatment guidelines, is frequently recommended by our multidisciplinary liver tumor board for the treatment of patients with HCC. As first-line therapy, ablative therapies are preferred at our institution for treatment of very early and early stage HCC while radioembolization is used more commonly for patients with more advanced disease.

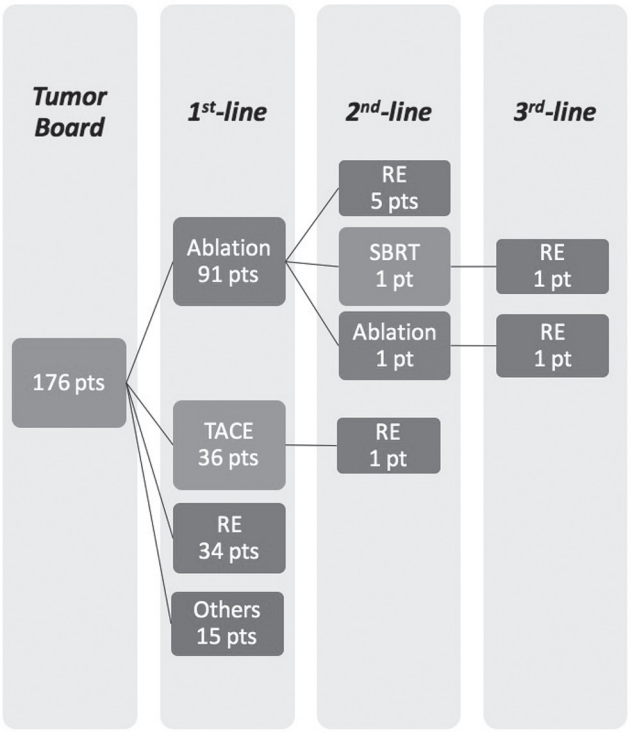

Type and order of treatments of patients with HCC.

Poster 52: Assessment of Liver Perfusion Before and After Transarterial Embolization Based on 2D-Digital Subtraction Angiography: A Feasibility Study

E. Meram[1], S. Schafer[2], J.R. Baumgart[3], O. Ozkan[1], P.F. Laeseke[1]; [1]*Radiology, University of Wisconsin-Madison, Madison, WI;* [2]*AT, Siemens Healthineers, Madison, WI;* [3]*Siemens Healthineers, Hoffman Estates, IL.*

Objectives: Intra-arterial therapies used in the treatment of primary and secondary liver cancer mostly rely on inducing tissue ischemia via interruption of blood flow in addition to delivering chemotherapeutics or radiation particles. However, assessment of the success of the procedures is based on subjective angiographic endpoints relying on the flow of contrast-mixed blood. This study aimed to evaluate the feasibility of quantifying changes in blood flow and tissue perfusion in liver before and after trans-arterial embolization (TAE) using a novel reconstruction algorithm based on 2D digital subtraction angiography (DSA).
Methods: Hepatic arteriography and left lobar TAE were performed in five female domestic swine using bland microspheres (100-300µm and 300-500µm Embosphere Microsphere; Merit Medical Systems, South Jordan, UT). Conventional 2D-DSAs were performed before and after each embolization. 2D-DSA images were reconstructed using a post-processing tool based on time of arrival and density of the contrast media to quantify perfusion and construct a color-coded perfusion map. Pre- and post-embolization images were compared visually and using paired t-tests of signal-to-noise ratio (SNR) of embolized and non-embolized regions of interest.
Results: Color-coded post-processed images clearly depicted changes in perfusion after TAE. When the regions of interest were analyzed before and after embolization, there was a significant decrease in SNR of embolized lobes (-21.4±4.7, $p<0.05$) while a significant SNR increase (15.4±3.7, $p<0.05$) was observed in the non-embolized lobes. The increase in SNR of non-embolized liver lobes might be related to the same volume contrast being redistributed to a smaller liver volume. There were artifacts visible around the diaphragm, mostly related to the impact of motion on subtraction imaging.
Conclusions: Processing of 2D-DSA images to construct perfusion maps can be used to demonstrate the change in blood flow and tissue perfusion before and after transarterial embolization. Future development of real-time perfusion mapping can aid in interventional procedures with easy to detect, color-coded images.

	Left Lobe Before	Left Lobe After	Change in Left Lobe	Right Lobe Before	Right Lobe After	Change in Right Lobe
Mean of Peak SNR	35.4±5.8	4.5±1.4	-30.9±4.6	22.8 ±5.6	36.2±6.2	13.4±4.2
Mean of AUC SNR	25.0±5.4	3.6±0.7	-21.4±4.7	18.3±5.8	33.7±8.8	15.4±3.7

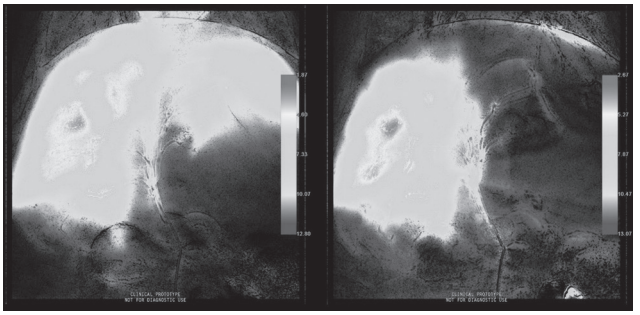

Color-coded perfusion maps of a swine liver before (left) and after (right) particle embolization of left liver lobe.

Poster 53: Automated Assessment of Lipiodol Deposition: An Early Predictor of Treatment Response After Conventional Transarterial Chemoembolization (cTACE)

N. Murali[1], C. Wang[1], A. Windham-Herman[1], M. Lin[1], E. Chen[1], T. Schlacter[1], J. Geschwind[2], J. Chapiro[1]; [1]*Department of Radiology & Biomedical Imaging, Yale School of Medicine, New Haven, CT;* [2]*Prescience Labs LLC, Westport, CT.*

Objectives: Conventional TACE (cTACE) involves transarterial and intra-tumoral injection of a water-in-oil chemotherapy cocktail, which is emulsified in Lipiodol as a micro-embolic agent visible on imaging. Lipiodol deposition within tumor tissue is known to correlate with tumor necrosis and treatment response; however, it is primarily estimated qualitatively rather than precisely quantified on intra- or post-procedural imaging. Hypothetically, a quantitative and geographic assessment of Lipiodol deposits may be used to identify under-treated tumor tissue immediately after delivery. This retrospective study aimed to develop an automated method to quantify the volume of Lipiodol within a target tumor after cTACE and evaluate this volume as a potential early marker of treatment response.
Methods: A retrospective cohort of 63 patients with metastatic liver tumors of neuroendocrine origin treated with cTACE were analyzed. Target tumor boundaries were segmented using semi-automated segmentation software as 3D masks. These masks were applied to semi-automated software to create masks of enhancing tumor voxels on arterial phase magnetic resonance imaging. Volumetric masks of total Lipiodol coverage were generated from post-embolization non-contrast Computed Tomography (CT) by an algorithm that classified tumor voxels as Lipiodol if they exceeded the reported upper limit of normal liver parenchyma, statistically identified as 67 Hounsfield Units (HU). Additional volumetric masks of "high density" Lipiodol deposits were similarly calculated by applying a higher HU threshold (>200 HU). By overlaying 3D masks, the volumes of Lipiodol (high density and total) within target tumor tissue (enhancing tissue and all tissue) were compared after cTACE between treatment response groups as determined by quantitative European Association for the Study of Liver (qEASL) volumetric response criteria.
Results: The percent of target tumor volume covered by Lipiodol was higher in patients that responded to cTACE compared to non-responders (76.8% vs. 26.8%; $p=0.008$). The percentage of enhancing tumor volume covered by Lipiodol was also higher in cTACE responders compared to non-responders (65.7% vs. 54.2%; $p= 0.019$). The percent of enhancing tumor tissue covered by "high density" Lipiodol deposits differed between treatment responders and non-responders (47.9% vs. 4.5%; $p<0.001$) with the largest effect size of all comparisons made (Cohen's term $d=2.02$). An ROC curve identified 12.57% of enhancing tumor tissue covered by high density Lipiodol as the cutoff value best differentiating treatment responders from non-responders (AUC=0.77, sensitivity 76.92%, specificity 83.33%). Tumors with "high density" Lipiodol deposition above and below this cutoff differed significantly in treatment response (Chi square $p<0.001$). The reduction in enhancing tumor tissue observed after cTACE plateaus even as the proportion of high density Lipiodol covering enhancing tumor tissue increases.
Conclusions: An automated method of quantifying volumetric Lipiodol in a target region may serve a precise early imaging biomarker of treatment response to cTACE, quantifiable within 24 hours of treatment. Specifically, measuring the density of Lipiodol deposited and distribution of Lipiodol to enhancing tissue within the tumor increases the accuracy of the Lipiodol biomarker in predicting treatment responders. This method should be applied to a larger cohort of hepatic tumors to validate a cutoff value for ideal Lipiodol deposition, which could contribute to the identification of reliable embolization endpoints.

Poster 54: Contrast-Enhanced Ultrasound for Early Local Efficacy Assessment After Irreversible Electroporation Ablation of Locally Advanced Pancreatic Cancer

M. Lin[1], X. Xie[2], M. Kuang[1]; [1]*Department of Medical Ultrasound, Institute of Diagnostic and Interventional Ultrasound, Guangzhou, China;* [2]*Interventional Ultrasound, The First Affiliated Hospital, Sun Yat-sen University, Guangzhou, China.*

Objectives: To evaluate the diagnostic value of contrast-enhanced ultrasound (CEUS) in early assessing local efficacy after irreversible electroporation (IRE) ablation of locally advanced pancreatic cancer (LAPC).
Methods: Fifteen LAPC patients treated with IRE and received CEUS examination one month after ablation were recruited. Technical efficacy was classified as technical efficiency (TE) and technical inefficiency (TIE). Diagnostic performance was analyzed using receiver operating characteristic (ROC) curve.
Results: Ten patients was considered as TE and five as TIE. Complete non-enhancement was displayed in 7 ablation zones (70.0%) in TE group, remaining enhancement was displayed in all 5 ablation zones (100.0%) in TIE group. Non-enhanced pattern was significantly different between TE and TIE group (P=0.026), and had significant correlation with the technical efficacy (P=0.007). The area under ROC curve was 0.85 (95%CI: 0.65 to 1.05).
Conclusions: Non-enhanced pattern on CEUS might be useful in early assessing local efficacy after IRE ablation of LAPC.

Patient characteristics for 15 locally advanced pancreatic cancer patients treated with IRE

Characteristics	Value
No. of patients	15
Gender (M/F)	10/5
Mean age (y)	57.7± 10.7 (34-75)
Tumor location (head/body)	7/8
Tumor size (cm)	3.9±1.4 (2.1-7.5)
Tumor TNM stage	
T (T3/T4)	1/14
N (N0/N1)	7/8
CA-199(normal/elevated)	3/12
CEA (normal/elevated)	10/5
CA125(normal/elevated)	11/4
Chemo-therapy before ablation (Y/N)	3/12

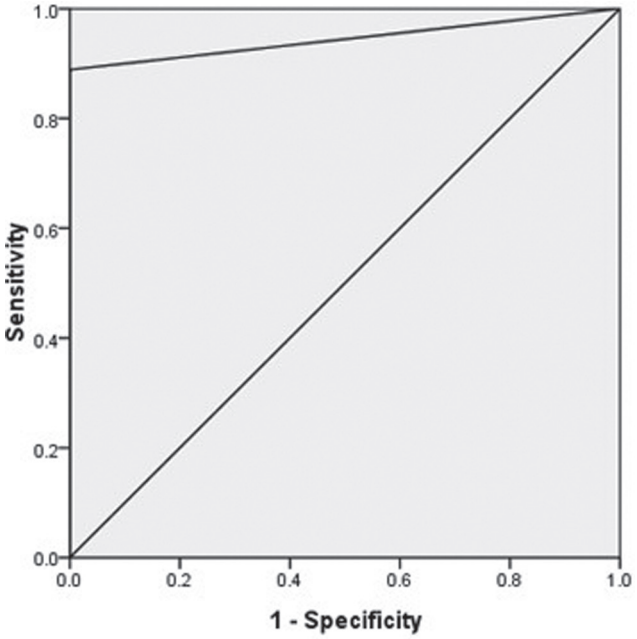

ROC curves for diagnostic performance of complete non-enhancement pattern on CEUS in regard to discrimination of technical efficacy between technical efficiency group and technical inefficiency group

Poster 55: Evaluating Parenchymal Enhancement Characteristics Utilizing a Novel Imaging Software

M.A. Welnick[1], S. Schafer[2], M.A. Back[1], A. Fairchild[1], w. lea[1], P.J. Patel[1], R.A. Hieb[1], J.R. Baumgart[3], S.B. White[1], S.M. Tutton[1], W.S. Rilling[1], E.J. Hohenwalter[1]; [1]*Interventional Radiology, Medical College of Wisconsin, Milwaukee, WI;* [2]*AT, Siemens Healthineers, Madison, WI;* [3]*Siemens Healthineers, Hoffman Estates, IL.*

Objectives: Final catheter position for therapeutic agent delivery in Liver Directed Therapy (LDT) relies heavily on 2D digital subtraction angiography (DSA) and is subjective. This feasablity study utilizes a prototype Siemens software package to evaluate parenchymal enhancement characteristics on 2D DSA by subtracting vasculature and evaluating the underlying contrast time curve information.

Methods: Retrospective analysis of DSA was performed on 19 patients previously enrolled in an IRB approved study. Angiograms of patients who underwent DEB-TACE were reviewed. Images were acquired at a standard frame rate of 3 frames per second. The prototype software package was installed on a standalone research workstation with de-identified images. The software algorithm used a band pass filter to suppress vascular structures and a gain multiplier to enhance the underlying parenchyma enhancement in each image. The resulting contrast time curves for each pixel in a 2D DSA series were evaluated for: Time to peak (TTP), time to half peak (THP), time to half washout (THW), time of arrival (TOA), area under the curve (AUC) and wash-in rate (WIR). Resulting images displayed the values in a color wash, compressing the underlying functional information of the complete 2D DSA run into a single color image. The color images were evaluated by a group of board certified interventional radiologists.

Results: Of the 19 enrolled patients, six datasets were excluded due to breathing motion image quality degradation. The remaining thirteen datasets were evaluated for information gain for the six processing modes. TTP, THP showed to be to affected by contrast density fluctuation between systole and diastole resulting in noisy color images which yielded limited additional information. Evaluation of THW was limited in the available datasets. Evaluation showed that for reliable results additional frames until near complete wash-out of the contrast need to be acquired. TOA was robust and allowed assessment of contrast blockages or stenotic areas. AUC demonstrates the final distribution of contrast and the potential distribution of treatment agent. WIR highlighted further differences in contrast uptake, with regions of increased vascular supply filling faster than those with less tumor and/or less tumor vascularity.

Conclusions: Using this post-processing software, additional information can be derived that cannot easily be gained by simple review of 2D DSA data alone. Initial evaluation showed considerable potential for area under the curve and wash-in rate showing the most information gain to the reviewer panel on potential distribution of treatment agent. Next efforts will focus on optimizing the 2D DSA acquisition sequence and contrast injection, evaluating further functional parameters and patient motion compensation.

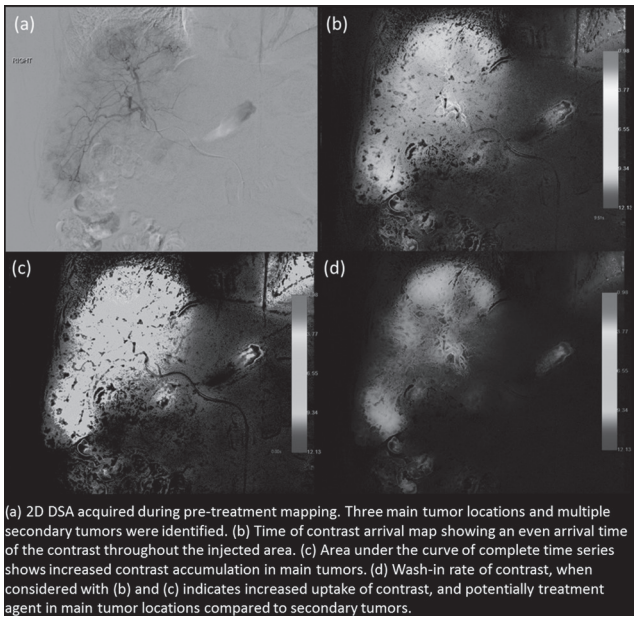

(a) 2D DSA acquired during pre-treatment mapping. Three main tumor locations and multiple secondary tumors were identified. (b) Time of contrast arrival map showing an even arrival time of the contrast throughout the injected area. (c) Area under the curve of complete time series shows increased contrast accumulation in main tumors. (d) Wash-in rate of contrast, when considered with (b) and (c) indicates increased uptake of contrast, and potentially treatment agent in main tumor locations compared to secondary tumors.

Poster 56: Comparing the Costs of Metastatic Neuroendocrine Tumor Treatments

A. Sadek[1], S. Dybul[1], E. Smith[1], W.S. Rilling[1], E.J. Hohenwalter[1], B. George[2], S.B. White[1]; [1]*Vascular and Interventional radiology, Medical College of Wisconsin, Milwaukee, WI;* [2]*Medicine, Medical College of Wisconsin, Milwaukee, WI.*

Objectives: To understand typical multi-modality treatment regimens for metastatic neuroendocrine tumors (mNETs) and their relative associated costs.

Methods: This is an IRB approved single center retrospective study evaluating adult patients treated for mNETs between 5/1994-6/2016. Demographics, date of diagnosis, location of primary tumor, date of liver metastasis, pathological grade, and surgical history were extracted. Liver directed therapy (LDT) dates and types were collected. Treatment duration, cycles, and reason for discontinuation was collected for all systemic therapies. Treatment related toxicities were recorded using the CTCAE v4.0. The hospital billing system was queried to identify standard costs of LDTs, hormonal, and intravenous (IV) therapies. Oral drug costs were obtained from the hospital pharmacy order acquisition system.

Results: A total of 161 hepatic mNET patients were identified; 83 males and 78 females with mean age of 57. 91 patients underwent a total of 264 LDTs (mean LDTs per patient 2.9±2.1), which included: cTACE (n=148), DEB-TACE (n=15), TARE (n=84), and TAE (n=7). Patients in the LDT group also received adjuvant systemic therapies. The following were the most common hormonal, IV, and oral agents, respectively: octreotide (n=77) and lanreotide (n=8); etoposide (n=10), carboplatin (n=7), and cisplatin (n=5); and capecitabine (cape) (n=28), temozolomide (tem) (n=27), everolimus (n=24) and sunitinib (n=17). LDT patients' systemic therapy durations were: octreotide 38.6 (SEM=3.3), lanreotide 5.7 (SEM=0.5), cisplatin/etoposide 4.7 (SEM=0.7), carboplatin/etoposide 3.4 (SEM=1.3), cape/tem 8.2 (SEM=2.2), everolimus 5.2 (SEM=1.3), and sunitinib 5.1 (SEM=1.6) months. 71 patients received systemic therapy only. The following were the most common hormonal, IV, and oral therapies, respectively: octreotide (n=56) and lanreotide (n=5); etoposide (n=18), carboplatin (n=12), and cisplatin (n=6); and cape (n=18), tem (n=19), everolimus (n=11), and sunitinib (n=7). These patients' systemic therapy durations were: octreotide 30.7 (SEM=3.5), lanreotide 4.6 (SEM=1.6), carboplatin/etoposide 2.9 (SEM=0.8), cisplatin/etoposide 2.1 (SEM=0.7), cape/tem 4.3 (SEM=0.9), everolimus 10.7 (SEM=2.0), and sunitinib 3.9 (SEM=1.3) months. Octreotide was the most common therapy and used as a baseline. Compared to 6 months of octreotide, each LDT, and 6 months of IV and oral chemotherapy was 0.8x ± 0.5, 1.63x ± 0.11, and 1.48x ± 1.95 the cost respectively.

Conclusions: Although a single session of LDT may incur higher costs, prolonged systemic regimens surpass LDT costs.

Costs

	(n=)	Relative Cost
LDT		
cTACE	148	0.53
Unilobar TARE*	84	1.32
DEB-TACE	15	0.54
Average		0.8 (SD=0.45)
Systemic Therapy (6 Months)		
Hormonal Regimens		
Octreotide	132	1.00
Lanreotide	13	1.15
Average		1.07 (SD=0.10)
IV Chemotherapy Regimens		
Cisplatin/Etoposide	10	1.71
Carboplatin/Etoposide	18	1.51
Average		1.63 (SD=0.11)
Oral Chemotherapy Regimens**		
Capecitabine/Temozolomide	37	0.07
Everolimus	34	0.68
Sunitinib	24	3.70
Average		1.48 (SD=1.95)

*Includes pre-Y90 MAA shunt study
**Oral regimen costs reflect only the direct pharmaceutical cost of the drug with no associated hospital costs

Poster 57: Intraprocedural Minimum Ablation Margin Assessment of FDG-Avid Liver Tumors During PET/CT-Guided Thermal Ablation: Feasibility and Utility for Predicting Local Tumor Progression

L. CASADABAN, K. Tuncali, P.B. Shyn; *Radiology, Brigham and Women's Hospital, Boston, MA.*

Objectives: The purpose of this study was to compare intraprocedural PET/CT measurements of the minimum liver tumor ablation margin during FDG PET/CT-guided microwave or cryoablation procedures with local tumor progression outcomes.
Methods: In this single-institution IRB approved retrospective study, 61 patients (28 men, 33 women; mean age 62, range 36-85) underwent FDG-PET/CT guided microwave ablation (n= 34) or cryoablation (n= 27) under general anesthesia to treat 79 FDG-avid liver tumors from 2012 to 2017. FDG was administered once approximately 60 minutes before the procedure. Fused breath-hold PET/CT images provided intraprocedural assessment of the minimum liver ablation margin. The PET and CT acquisitions were both obtained during a single < 80 second breath-hold to optimize image co-registration. Microwave ablation zones were visible on post-procedure CT performed with IV contrast; Cryoablation zones were visible on CT due to iceball hypodensity. The FDG-avid tumors were visible on PET even after ablation (FDG is not dissipated by thermal ablation). One attending and one resident radiologist reading in consensus measured the minimum ablation margin (shortest distance from FDG-avid tumor to ablation zone perimeter) on intraprocedural post-ablation PET/CT images of each tumor. Local tumor recurrence for each ablated tumor was assessed using CT, MRI or PET/CT imaging with follow-up ranging from 1-50 months (mean 13 months). Time-to-progression was compared for a minimum margin <5mm and ≥5mm using Kaplan-Meier analysis. ROC analysis was applied to the 42 ablated tumors with recurrence or at least 12-months follow-up.
Results: Intraprocedural PET/CT demonstrated a minimum ablation margin <5mm in 37/79 (47%) tumors and ≥5mm in 42/79 (53%) tumors. Local progression occurred in 14/79 (18%) of ablated tumors including 12/37 (32%) of tumors with a minimum margin <5mm and 2/42(5%) with a minimum margin ≥5mm. Median time-to-progression by Kaplan-Meier analysis was 13 months with minimum margin <5mm and 37 months with minimum margin ≥5mm (p<0.001)(Fig 1). ROC analysis showed a significant association between lower minimum margin and recurrence yielding an AUC = .831, SE .079 (P=0.001). The sensitivity and specificity for local progression with a minimum margin <5 mm were 68% and 82%, respectively, while that for <4 mm were 81% and 82%; positive and negative predictive values were 60% and 93%.
Conclusions: Intraprocedural breath-hold PET/CT, using PET to depict the persistently FDG-avid tumor and CT to depict the ablation zone, enables immediate assessment of the minimum ablation margin which is highly predictive of local tumor progression outcomes.

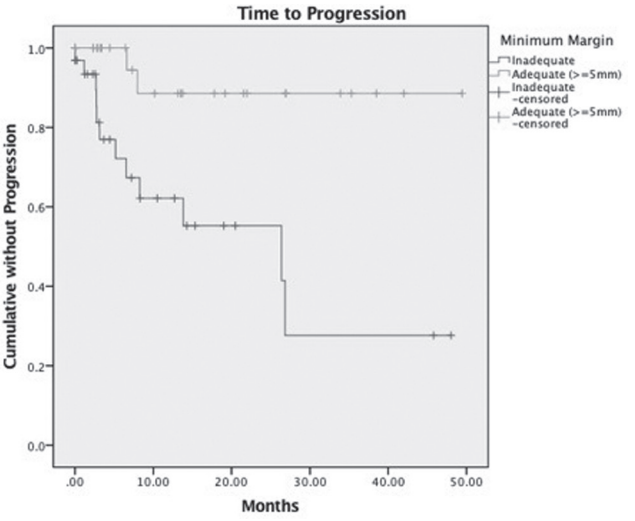

Poster 58: Long-Term Outcomes and Prognostic Analysis of Percutaneous Radiofrequency Ablation in Liver Metastasis from Breast Cancer

X. Bai, W. Yang, Z. Zhang, A. Jiang, W. Wu, H. Wu, M. Chen, K. Yan; *Ultrasound, Peking University Cancer Hospital, Beijing, China.*

Objectives: To evaluate the long-term efficacy and prognostic factors of ultrasound-guided percutaneous radiofrequency ablation (RFA) for breast cancer liver metastasis (BCLM)
Methods: Between 2000 and 2015, 69 patients who underwent ultrasound-guided percutaneous RFA for BCLM and had regular follow-up were included. The primary breast cancer had been removed by surgery in all patients and all patients had previous chemotherapy, endocrine therapy, or both after operation. There were 2 males and 67 females with an average age of 50.3±10.0 years (31-76 years). The mean maximum diameter of liver metastasis was 2.9±1.4 cm (1.0-6.0 cm). Thirty-five patients had a single metastasis, and 34 patients had multiple liver metastases (2-5 lesions). Survival results were generated using Kaplan-Meier estimates, and a multivariate analysis was performed using the Cox regression model.
Results: In total, 92 RFA sessions were performed, and 135 BCLM lesions were treated. Major complications occurred in 1 of 92 sessions (1.1%). The technique success was achieved in 92.6% of lesions (125/135 lesions). Local tumor progression occurred in 11.6% (9/69) of patients, and new intrahepatic metastasis presented in 55.1% (38/69) of patients. From the time of liver metastasis diagnosis, the median overall survival was 36 months, and the 1-, 2-, 3-, and 5-year survival rates were 92.6%, 75.2%, 48.7%, and 20.7%, respectively. From the time of initial RFA, the median overall survival was 26 months and 1-, 2-, 3-, and 5-year survival rates were 81.8%, 50.1%, 25.3%, and 11.0%, respectively. The median progression free survival and 1-, 2-, 3-, and 5-year survival rates after RFA were 24 months and 77.4%, 47.0%, 23.7%, and 8.5%, respectively. Based on the multivariate analysis, the following three factors were identified as independent prognostic factors for the overall survival after RFA: tumor size (P= 0.017), estrogen receptor positive (P = 0.009) and extrahepatic metastatic disease (P = 0.001).
Conclusions: This study showed that RFA was a safe and locally effective method for the treatment of BCLM, especially in patients who had lesions measuring less than 3 cm in diameter, single liver metastasis, estrogen receptor positive and without extrahepatic metastasis.

Poster 59: Operator Hand Exposure During Administration of Yttrium-90 Resin Microspheres: A Single Institution, Single Operator Experience

A. Miller, A. Kim; *Medstar Georgetown University Hospital, Washington, DC.*

Objectives: The purpose of this study was to measure radiation exposure to the primary operator's right hand during administration of Yttrium-90 resin microspheres.
Methods: Radiation exposure levels were monitored on a weekly basis using our institution's standard ring badge dosimeter. This was worn on the right hand of the operator only during radioembolization cases. The delivered patient dose (in mCi) was recorded and compared with dosimeter readings (mrem). Measurements were obtained for a total of 10 weeks prior to analysis.
Results: A total of 22 radioembolization procedures were performed over a 10 week treatment period (average 2.2 cases per week). The average delivered dose of Yttrium-90 resin microspheres per treatment was 25.5mCi (range 11.0 - 49.3). The average weekly delivered dose was 56.1mCi (range 13.9 - 92.8). Ring badge dosimeter readings ranged from 24 - 132 mrem with an average of 47.7mrem

per week. The highest 4 week exposure reading was 257 mrem (range 67 - 257). There was no correlation between measured ring badge dosimeter dose and delivered patient dose.

Conclusions: In this short study of operator hand radiation exposure during administration of Yttium-90 resin microspheres, there was no clinically significant hand dose received over a 10 week study period. The highest monthly exposure reached only 257mrem, well below the ALARA I threshold of 2000mrem/month for extremities. The findings of this study show that hand radiation exposure during administration of Yttrium-90 resin microspheres does not reach clinically significant levels when radioembolization is performed by a skilled operator.

Poster 60: Outcomes After Locoregional Therapy of Pancreatic Adenocarcinoma Liver Metastases

H. Yoon, J. Mandel, R. Zener, H. Yarmohammadi, S.B. Solomon, C.T. Sofocleous, F. Boas; *Interventional Radiology, Memorial Sloan Kettering Cancer Center, New York, NY.*

Objectives: To access response, progression - free survival, and overall survival of patients with pancreatic adenocarcinoma liver metastases after bland embolization, radioembolization, or ablation.

Methods: An IRB - approved retrospective review was performed of 14 patients with biopsy - proven pancreatic adenocarcinoma liver metastases who underwent 17 procedures: 5 bland embolization (29%), 5 radioembolization (29%), and 7 microwave or radiofrequency ablation procedures (41%). Radiologic response to treatment was evaluated using Response Evaluation Criteria in Solid Tumors 1.1 criteria with a mean initial follow-up period of 2.3 ± 1.5 months. Response rates were compared using a chi-squared test. Median progression - free survival and overall survival after initial locoregional therapy were calculated using the Kaplan-Meier method, and compared using log-rank tests.

Results: Complete or partial response was seen in 3 tumors (60%) after bland embolization, 1 tumor (20%) after radioembolization, and 6 tumors (86%) after ablation. No significant difference in response was detected between treatment arms. Overall median progression - free survival was 5.8 months and medial overall survival was 8.9 months. No significant difference was detected between bland embolization, radioembolization, or ablation based on progression - free survival (5.6 vs 6.1 vs 7.3 months) or overall survival (5.7 vs 8.6 vs 8.9 months)

Conclusions: Locoregional therapy of pancreatic adenocarcinoma liver metastases can produce complete or partial radiologic response, but survival remains poor.

Initial response following locoregional therapy and survival

Procedure	Number (%)	Progression-free survival (Months)	Overall survival (Months)
Bland Embolization		5.6	5.7
PR	3 (60%)		
PD	2 (40%)		
Radioembolization		6.1	8.6
PR	1 (20%)		
SD	4 (80%)		
Ablation		7.3	8.9
CR	5 (72%)		
PR	1 (14%)		
SD	1 (14%)		
CR-Complete Response PR-Partial Response PD-Progressive Disease SD-Stable Disease			

Poster 61: Percutaneous Thermal Ablation for the Treatment of Colorectal Liver Metastases and Hepatocellular Carcinoma: A Comparison of Local Therapeutic Efficacy

X. Xie; *Interventional Ultrasound, The First Affiliated Hospital, Sun Yat-sen University, Guangzhou, China.*

Objectives: This study aimed to compare the local therapeutic efficacy of percutaneous thermal ablation for colorectal liver metastases (CRLM) and hepatocellular carcinoma (HCC).

Methods: One hundred sixty-one CRLM nodules in 101 patients and 122 HCC nodules in 97 patients were treated with thermal ablation. Complications and local efficacy were retrospectively compared.

Results: Major complications were observed in two (2.0%) patients in the CRLM group and one (1.0%) in the HCC group (p=1.000). The complete ablation (CA) rate of lesions ≤3cm was lower in the CRLM group than in the HCC group (p=0.018). After a mean follow-up period of 21.1±20.7 months in the CRLM group and 22.1±17.6 months in the HCC group, the local tumour progression (LTP) rate of lesions >3cm was higher in the CRLM group than in the HCC group (p=0.036). The multivariate analysis revealed that only safety margin (≤0.5cm/>0.5cm) was a significant predictor of LTP in both CRLM and HCC.

Conclusions: To achieve better local tumour control, thermal ablation should be more aggressive for CRLM than for HCC, especially for large tumours in clinical.

Poster 62: Pre-Treatment 99mTc-Mebrofenin Hepatobiliary Scintigraphy, an Adjuvant Predictor of Post-Radioembolization Clinical Status

M. Ertreo[1], S. Chowdhury[2], J.Y. An[3], G. Esposito[4], T. Caridi[1], G.E. Lynskey[1], D. Buckley[1], E. Cohen[1], J. Cardella[1], D. Field[1], J. Spies[1], A. Kim[1]; [1]*Interventional Radiology, Georgetown University Hospital, Washington, DC;* [2]*Georgetown University Medical School, Washington, DC;* [3]*National Institutes of Health, Bethesda, MD;* [4]*Nuclear Medicine, Georgetown University Hospital, Washington, DC.*

Objectives: To correlate scintigraphic hepatobiliary 99mTc-mebrofenin uptake ratio prior to Y90-radioembolization (RE) with post-RE clinical status and liver function.

Methods: A single center retrospective review was performed of patients who underwent hepatobiliary 99mTc-mebrofenin scan in preparation for RE for primary or secondary liver malignancy from July 2015 to December 2017. Regions of interest for mebrofenin uptake were drawn over the entire image, heart and liver. Corrected mebrofenin uptake ratio (cMUR) was calculated as %uptake/min/BSA (body surface area). Pre-RE and 2-month post-RE albumin, total bilirubin, ECOG, MELD, ALBI, and Child-Pugh score (CP) were compared using Wilcoxon rank sum test for continuous variables and Fisher's exact test for categorical variables. Pre-RE cMUR was correlated with the 2-month post-RE measures of liver function using the Spearman's rank correlation test. Significance was considered at $p<0.05$. Results are presented as median and interquartile range.

Results: Thirty-two patients were included. Eleven (34%) patients had hepatocellular carcinoma and 6 (55%) of these had cirrosis. The remaining 21 (65%) patients had metastatic disease, of which 10 (48%) from primary colonic malignancy. Pre-RE cMUR was 6.69 %uptake/min/m2 (5.04-8.33). Four (13%) patients did not undergo RE. Total delivered activity and dose were 36.87 mCi (17.11-46.29) and 53.82 Gy (34.82-81.63), respectively. Two month follow up was available for a total of 23 (72%) patients, demonstrating albumin decrease (3.1 vs. 3.55 g/dL, p=0.03), CP (6.5 vs. 6, p=0.028) and ALBI scores (-1.79 vs. -2.375, p=0.009) worsening from pre-RE values, all statistically significant. Pre-RE cMUR demonstrated significant negative correlation with post-RE CP (r=-0.7408, p=0.0091) and ALBI scores (r=-0.633, p=0.0365). Total delivered activity and dose did not significantly correlate with post-RE status.

Conclusions: Pre-RE cMUR strongly correlated with post-RE CP and ALBI scores, suggesting possible use of cMUR as a surrogate marker for selecting ideal RE candidates. Although the results may have been limited by sample size, this study provides preliminary evidence to support further exploration of this relationship in future studies.

Poster 63: Y90 and Everolimus in Combination for Neuroendocrine Liver Metastases: Single-Center Experience

C. Raybon, C.N. Taylor, J. Watchmaker, J. Baker, F. Banovac, T. Borgmann, A. Ahmad, D.B. Brown; *Radiology and Imaging Sciences, Vanderbilt University, Nashville, TN.*

Objectives: Both everolimus and intra-arterial Yttrium-90 are used separately to treat neuroendocrine tumor (NET) liver metastases. The purpose of the current work is to review and evaluate both efficacy and safety of Y-90 combined with everolimus versus Y-90 alone in NET patients with hepatic metastases.

Methods: A retrospective chart review was performed after IRB approval. All patients were treated with Y90 resin microspheres. Fourteen were on everolimus at the time of Y90 referral. The decision to continue everolimus in addition to Y90 was made at our NET board. Primary tumor location, grade, presence of extrahepatic disease and delivered Y90 activity was tracked. Y90 activity was calculated using the body surface area model. Imaging response was assessed using mRECIST using the deepest response at 12 months. Common Terminology Criteria for Adverse Events version 4 (CTCAEv4) was used to evaluate toxicities and complications.

Results: 39 patients were treated with demographics in the table. The groups were similar in respect to age, tumor grade, presence of extrahepatic disease and administered Y-90 activity. 14/39 patients received everolimus. The Y90/everolimus group had 1 complete response (CR) (7%), 10 partial responses (PR) (72%), 1 stable disease (SD) (7%) and 2 progressive disease (PD) (14%). Overall response rate (ORR) was 79% and disease control rate (DCR) was 86%. Y90 monotherapy responses were 0 CR, 14 PR (56%), 6 SD (24%), and 5 PD (20%). The Odds Ratio for PR/CR with the addition of everolimus was 2.88, albeit with a p-value of 0.19. DCR was similar between groups. There were no CTACAEv4 grade 3 or greater toxicities in the Y90/everolimus group while there was 1 in the Y90 monotherapy group (grade 3 hyperbilirubinemia). Everolimus specific toxicities included grade 2 stomatitis in 1 patient (7%) and grade 1 rash in 2 patients (14%).

Conclusions: In this limited review, the addition of everolimus to Y90 for NET resulted in a nearly 3 times greater likelihood of an objective response without a notable increase in toxicity. Although the ORR did not reach statistical significance, a larger sample size could demonstrate clinical benefit. Prospective evaluation of Y90/everolimus in combination for NET may improve response to therapy.

Demographics

	Y90 + Everolimus	Y90 Monotherapy	p-value
n Patients	14	25	
Median Age (years)	60 (49-77)	59 (33-85)	0.96
WHO Grade			0.3
I	2 (14%)	9 (36%)	
II	8 (57%)	9 (36%)	
III	2 (14%)	3 (12%)	
Not Available	3 (21%)	4 (16%)	
Extrahepatic Disease	11/14 (79%)	18/25 (72%)	0.72
Median Y90 Dose (GBq)	1.7 (0.82-3.6)	1.9 (0.7-3.2)	0.83

Poster 64: Complications of CT-guided Percutaneous Irreversible Electroporation of Locally Advanced Pancreatic Cancer : A Preliminary Experience

Y. Wei; *Radiology, Chinese PLA General Hospital, Beijing, China.*

Objectives: Reviewing and evaluating the complications related to CT-guided percutaneous irreversible electroporation ablation,as well as to investigate optimal approaches to adequate prevention and resolution
Methods: Retrospectively collected data regarding to 17 patients who were evident with Locally advanced pancreatic carcinoma(LAPC)that have underwent CT-guided percutaneous IRE ablation procedures. There were 17 lesions in total with maximum diameter of(3.9±1.53)cm,range 2.0cm-6.9cm. Complications were documented and reviewed within 7- and 90-day follow up as well reexaminations were compared with pretreatment workup,predominantly CT/MRI scans. Complications were graded according to the Clavien–Dindo classification scheme
Results: 2 patients have suffered a transient tachycardia. A total of 11 complications were noted within 7-day follow up,whereas 5 have normalized within 3 days postoperatively,of which abdominal pain and slight nausea were most common. 90-day follow up records have demonstrated totally 5 complications (including 2 Clavien–Dindo grade II,1 grade IIIa and 2 grade V),except 2 deaths there were no evidence for other new complication occurrence.
Conclusions: CT-guided percutaneous IRE is kind of feasible ablation modality of considerable safety and with minimal invasion. Apprehension of mechanism of IRE,optimal patient screening,prudent operation as well immediate treatments and preventive measures allow minimal incidence of complications, by which it can raise the safety and feasibility of IRE.

Poster 65: Iatrogenic Celiac Axis and Hepatic Artery Dissections During Intra-Arterial Regional Tumor Therapies: A 16-Year Retrospective Review

E. Alexander[1], G. Nadolski[1], M.C. Soulen[2], W. Stavropoulos[2], S. Hunt[2], T. Gade[2], M. Itkin[1], S. Shamimi-Noori[1]; [1]*Radiology, Hospital of the University of Pennsylvania, Philadelphia, PA;* [2]*Radiology, University of Pennsylvania, Philadelphia, PA.*

Objectives: Retrospectively identify the incidence and outcome of iatrogenic celiac axis and hepatic artery dissections during transarterial embolization of liver tumors, including chemoembolization, radioembolization (TARE), and pre-TARE scintigraphic mapping.
Methods: Included were 2214 patients with 3729 treatment encounters from January 2001 to July 2017. The institution's QA database, EMR, and PACS were reviewed to identify incidence of dissection during trans-arterial oncology procedures, to evaluate immediate management of dissections, assess patency of the arteries after dissection, and ability to administer therapy.
Results: Among the 3729 arteriograms performed, iatrogenic dissections of celiac axis or hepatic arteries occurred in 39 procedures (1.0%), affecting 38 patients. The incidence of flow limiting dissections was 0.3% (12/3729) and non-flow limiting dissections was 0.7% (27/3729). Ten of the 39 dissections (6 flow limiting, 4 non-flow limiting) were treated intraprocedurally with: nitroglycerin (n=3), heparin (n=3), heparin and nitroglycerin (n=2), heparin and PTA (n=1), and heparin, nitroglycerin and PTA (n=1). Of the treated cases, 40% (4/10) of therapies were completed on the same day. Overall, 69% (27/39) of procedures were completed the same day as the dissection; either the dissection was non-flow limiting (n= 23), treatment was delivered via alternate artery (n=3), or the true lumen was traversed (n=1). In the remaining 12 cases, 7 patients subsequently underwent successful embolic treatment at a median of 67 days after the dissection (range, 37-83 days). Follow-up imaging was obtained in 25 of the 39 cases at a median time of 56 days; complete resolution was seen in 14 cases, near complete resolution (<30% luminal narrowing) in 3, unchanged appearance of a non-flow limiting dissection in 4, progressive luminal narrowing in 3, and complete occlusion in 1 case.
Conclusions: Iatrogenic celiac axis or hepatic artery dissections occur rarely during tumor embolization. Even after dissection, 69% of cases were still completed on the same date and another 18% were completed during follow up procedure. Thus, these rare injuries have little impact on the overall treatment of patients.

Poster 66: Large Gage Fenestrated Needle Allows Uniform and Penetrative Percutaneous Injection of Drug Eluting Beads

A.K. Dev[2], R. Abrol[3], M. Fujimori[1], G. Srimathveeravalli[1]; [1]*Radiology, Memorial Sloan-Kettering Cancer Center, New York, NY;* [2]*Staten Island Technical High School, Staten Island, NY;* [3]*High School for Health Professions and Human Services, New York, NY.*

Objectives: Percutaneous intratumoral injection of Drug Eluting Beads (DEBs) has shown anti-tumor efficacy in animal models. The objective of this study was to identify injection parameters for maximizing distribution of percutaneously injected DEBs in a repeatable fashion.
Methods: Tissue mimicking gelatin phantoms were used to test the effect of injection parameters on the distribution of Evans blue in solution (1 mg/ml) or loaded on DEBs (DC Beads, BTG). Constant volume (0.3 ml) of dye solution or DEBs was injected into phantoms with varying needle gauge size (19 or 25 G), injection time (1, 3 and 5 second infusion) and perforations (single end hole vs. perforated needle). Perforated needles were prepared by drilling six 0.5 mm holes at equal spacing along the length of the 19G needle. Following injections the gelatin sample was bisected and photographs along the needle insertion path were taken for measuring depth (from needle tip) and width (from needle axis) of sample distribution. Student's t-test was used to assess statistical significance of measurements.
Results: In needles with end holes, larger bore size resulted in significantly deeper (19G: 22.11±1.6 mm vs. 25G: 13.5±2.41 mm, $p<0.01$) and wider (19G: 2.53±1.04 vs. 25G: 1.16±0.26 mm, $p<0.01$) deposition of microparticles. Infusion time was not a determinant of microparticle distribution, and resulted in similar outcomes independent of needle gage or perforations. Perforated 19G needle further increased the depth (26.11±2.2 mm) and width (3.25±0.62 mm) of microparticle distribution ($p<0.01$). Conversely, smaller gage size provided deeper (19G: 20.54±2.52 mm vs. 25G: 25.49.5±2.75 mm, $p<0.01$) deposition of free dye in solution. When compared to a needle with end hole, additional perforations did not provide added benefit in the delivery of free in solution (depth: 26.04±2.57 and width: 2.4±0.68 mm).
Conclusions: Needle gage size and number of perforations impact distribution of percutaneously injected microparticles and free dye differently. Large gage perforated needles can allow deep and uniform deposition of microparticles for percutaneous intratumoral injections.

Poster 67: Microwave Ablation in the Management of Colorectal Cancer Pulmonary Metastases

I. Kurilova[1], A. Gonzalez-Aguirre[2], J. Erinjeri[2], E.N. Petre[2], M. Gonen[3], M. Bains[4], N. Kemeny[5], S.B. Solomon[2], R.G. Beets-Tan[6], C.T. Sofocleous[2]; [1]*Radiology, Memorial Sloan Kettering Cancer Center; The Netherlands Cancer Institute, New York, NY;* [2]*Radiology, Interventional Radiology Service, Memorial Sloan Kettering Cancer Center, New York, NY;* [3]*Department of Epidemiology and Biostatistics, Memorial Sloan Kettering Cancer Center, New York, NY;* [4]*Thoracic Service, Department of Surgery, Memorial Sloan Kettering Cancer Center, New York, NY;* [5]*Department of Gastrointestinal Oncology, Memorial Sloan Kettering Cancer Center, New York, NY;* [6]*Department of Radiology, Netherlands Cancer Institute, Amsterdam, Netherlands.*

Objectives: To review outcomes following microwave ablation (MWA) of colorectal cancer pulmonary metastases (CRCPM) and assess predictors of oncologic outcomes.
Methods: Technical success (TSR), primary and secondary technique efficacy rates (PTER and STER) were evaluated for 50 patients with 90 CRCPM at immediate, 4-8 weeks post-MWA and subsequent follow-up CT and/or PET/CT. Local Tumor Progression (LTP) rate, LTP-free, cancer specific (CSS) and overall survival (OS) were assessed. Modified Clinical risk score (mCRS) with tumor size (TS) decreased to 2cm and CEA level to 10 ng/ml was assessed as oncologic outcomes predictor. Complications were recorded.
Results: Median follow-up was 25.6 months. Median tumor size was 1 cm (0.3-3.2cm). TSR, PTER and STER were 99%, 90% and 92%, respectively. LTP rate was 10%. One-, 2- and 3-year LTPFS were: 93%, 86% and 86%, respectively with median LTPFS not reached. Median OS was 58.6 months, median CSS was not reached. One-, 2- and 3 year OS and CSS were 94% and 98%, 82% and 90%, 61% and 70%, respectively. On univariate analysis minimal ablation margin (MM) ($p<0.001$) and TS ($p=0.001$) predicted LTPFS, with no LTP for MM ≥ 5mm or TS <1cm. Cumulative 3-year LTP in low vs. high mCRS groups was 5% vs. 39%, $p=0.1$. Elevated pre-MWA CEA level ($p=0.046$) and ≥3 prior chemotherapy lines predicted decreased CSS ($p=0.02$). There was no death within 90 days and major complication rate was 3%.
Conclusions: MWA with MM ≥ 5 mm is essential for local control of CRCPM. CEA level and pre-MWA chemotherapy impacted CSS.

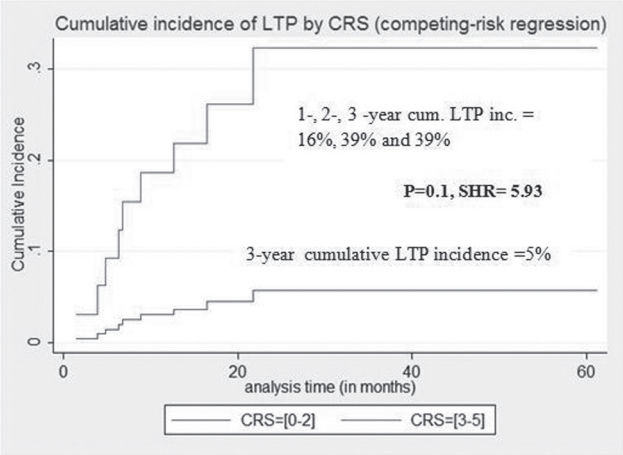

Modified CRS for CRC Lung metastases MWA One point for each risk factor Patients with 0-2 points: low risk Patients with 3-4 points: high risk	1	Node positive primary tumor
	2	Disease-free interval (DFI) from primary resection to metastatic disease <12 months
	3	Number of lung metastases >1
	4	Size of biggest lung metastasis > 2 cm
	5	CEA before MWA > 10 ng/ml

Modified clinical risk score (CRS) association with cumulative incidence of local tumor progression (LTP; patient-based competing risk analysis)

Nr.	Factor	P-value	Sub-hazard ratio (SHR)	95% CI
Univariate analysis: predictors of LTPFS				
1.	Minimal ablation margin size (0mm, 1-4mm, 5-9 mm, ≥10 mm)	<0.001	0.2	0.08-0.52
2.	Lesion size (cm)	0.001	5.38	1.9-15.1
Univariate analysis: predictors of cancer specific survival				
1.	≥ 3 prior chemotherapy ± target therapy lines	0.019	3.93	1.3-12.3
2.	Pre-MWA CEA level (≥10 ng/ml)	0.046	3.53	1.02-12.2

*Small number of events (local tumor progressions and cancer-related deaths) precluded from performing multivariate analysis

Predictors of local tumor progression-free survival (LTPFS; evaluated using competing risk analysis, adjusted for clustering) and cancer specific survival (evaluated using Cox regression analysis)

Poster 68: Percutaneous Management of Iatrogenic Abdominal Lymphatic Leaks: Preliminary Results After Therapeutic Intranodal Lymphangiography with and without Percutaneous Glue Injection

F. Kayali[1], H. Yoon[1], F. Gelambo[2], M. Maybody[1], G. George[1], E. Santos Martin[1]; [1]*Interventional Radiology, Memorial Sloan Kettering Cancer Center, New York, NY;* [2]*University of South Florida, Tampa, FL.*

Objectives: To analyze the safety and efficacy of intranodal lymphangiography (IL) +/- glue embolization as a treatment option for refractory abdominal iatrogenic lymphatic leakage.
Methods: Nine patients who experienced refractory iatrogenic lymphatic leakage (2 with lymphatic ascites, 5 with lymphoceles, and 2 with both) between October 2010 and September 2017 were retrospectively evaluated after failing conservative treatment. All patients underwent IL for diagnostic and therapeutic purposes. Adjunctive glue embolization was performed in 5 patients at the site of the leak or to the adjacent lymph node feeding the leak. Iatrogenic lymphatic injury were all due to complications from a surgical procedure. Clinical success was defined as discontinuation of the drainage catheter after the output dropped to < 10 cc/day.
Results: The mean time between iatrogenic lymphatic injury and percutaneous intervention was 58 days. The mean pre-intervention drain output was 928 cc/day (IL 950 cc/day, IL with glue injection 910 cc/day). One patient underwent two therapeutic ILs and one patient had two delayed glue injections under CT guidance. Clinical success was achieved in all 9 patients (100%). The mean time from the last IL procedure to achieving clinical success was 12 days (IL with glue injection 10 days, IL alone 15 days). No major complications were observed.
Conclusions: Therapeutic intranodal lymphangiography +/- adjunctive percutaneous glue embolization is safe with a high success rate in treating refractory iatrogenic lymphatic leakage. Glue embolization at the site of the lymphatic injury may shorten the time to achieve clinical success

Poster 69: Peri-Catheter Bleeding After Biliary Drainage in Combination with Hemobilia is Associated with Hepatic Arterial Injury

F. Kayali, R. Perez-Johnston, K.T. Brown, L. Brody, A. Covey, S.B. Solomon, F. Boas, G. George, M. Maybody; *Interventional Radiology, Memorial Sloan Kettering Cancer Center, New York, NY.*

Objectives: Determine if peri-catheter bleeding concomitant with hemobilia after percutaneous biliary drainage is a predictor of hepatic arterial injury.
Methods: All biliary drainage procedures excluding primary stenting performed between 01/2014 and 06/2016 were reviewed. Patients with hemobilia were identified and their records were reviewed. Hepatic arterial injury was identified with angiography. Absence of angiographic findings or resolution of hemobilia +/- pericatheter bleeding with catheter upsizing was defined as lack of arterial injury.
Results: Hemobilia occurred in 22 patients after 135 biliary drainage procedures. Peri-catheter bleeding was seen in 12 of 22 patients (4 female, 8 male, mean age 56 years, 11 malignant, 6 left, 6 right). Bleeding occurred at a median of 9.5 days (1-150 days) following biliary drainage. Hepatic angiography was performed on 11 patients with peri-catheter bleeding; arterial injury findings were seen in 10 (3 pseudoaneurysm [PSA], 2 arterio biliary fistula, 3 extravasation, and 2 abrupt caliber change of an artery crossing the catheter). Nine of these arterial injury findings were treated with embolization (n=7) and stent placement (n=2). One patient with a PSA was not amenable to treatment without sacrificing the entire hepatic artery. Catheter/sheath cholangiography (n=6) and contrast enhanced CT (n=5) performed prior to angiography each demonstrated arterial injury in one patient. One patient with peri-catheter bleeding who did not undergo angiography as well as all 10 patients with hemobilia without peri-catheter bleeding had resolution of hemobilia after exchange or upsizing of the biliary catheter. The positive predictive value (PPV) of hemobilia with peri-catheter bleeding for hepatic arterial injury was 83% (95% confidence interval [CI]: 52%-98%). The negative predictive vale (NPV) of hemobilia without peri-catheter bleeding for hepatic arterial injury was 100% (95% CI: 69%-100%).
Conclusions: Catheter angiography is indicated in patients after percutaneous biliary drainage if presenting with a combination of peri-catheter bleeding and hemobilia.

Biliary Drainage 01/2014 - 06/2016	n = 135				
Hemobilia	n = 22				
Peri-catheter bleed	Yes n = 12				No n=10
Angiography	Yes n = 11			*No n=1	*No n=10
Relevant angiographic findings	Yes n = 10		**No n=1	N/A	N/A
Intervention	Embolization (n=7) Stent (n=2)	*** No Intervention (n=1)	No Intervention	Catheter upsized	Catheter upsized

* Clinical suspicion for hepatic venous source as the source of Hemobilia
** Clinical suspicion for a GI bleed as the source of Hemobilia
*** Not amenable to safe endovascular treatment

Poster 70: Prevention of Hepatobiliary Infection Following Hepatic Embolization in Patients with Prior Biliary Manipulation

J.H. Wang[1], E.A. Addo[1], R.A. Patel[1], J.S. Smith[2], B. Biebel[2], G. El-Haddad[2]; [1]*University of South Florida, Tampa, FL;* [2]*Radiology, Moffitt Cancer Center and Research Institute, Tampa, FL.*

Objectives: Antibiotic prophylaxis is essential in reducing the risk of hepatobiliary infection in patients with prior biliary manipulation undergoing hepatic embolization; however, industry standardization and scientific evidence supporting effectiveness of various regimens are limited. Our study examines the effectiveness of Moxifloxacin 400 mg PO daily administered one week prior and two weeks post-embolization, without bowel preparation, in these high-risk patients.
Methods: Systematic retrospective review was performed on 376 patients during a seven year period (2009-2016). A total of 25 patients with prior biliary manipulation had undergone 36 embolic interventions that included yttrium-90 glass microsphere radioembolization (n=20), bland embolization (n=10), chemoembolization (n=5) and portal vein embolization (n=1). Prior biliary manipulations included pancreaticoduodenectomy (n=18), sphincterotomy (n=6), internal/external biliary catheter placement (n=3), ERCP with stent placement (n=3) and choledochojejunostomy (n=2). Moxifloxacin 400 mg PO daily for one week prior and two weeks post-embolization was administered in 10 embolizations as antibiotic prophylaxis. There were 26 embolizations utilizing alternative antibiotic prophylactic regimens which included lone administration or varying combinations of Metronidazole, Cephalexin, Cefazolin, Levofloxacin, Ciprofloxacin, SMZ-TMP and Moxifloxacin at varying doses/durations. Clinical and laboratory follow-up assessments were performed on all patients for the development of hepatobiliary infection for a median of 194 days.
Results: There were no hepatobiliary infection in patients who received Moxifloxacin 400 mg PO daily for one week prior and two weeks post-embolization (0/10). There were 4 hepatobiliary infections associated with alternative antibiotic prophylactic regimens (4/26 or 15.4%). Overall, 11% infection rate was observed (4/36) which is lower than the expected incidence of 20% with aggressive prophylactic

regimens (1). Our findings are in line with a pilot study which found no incidence of hepatic abscess when Moxifloxacin 400 mg was administered 3 days before and continuing for 17 days post-embolization in 10 high-risk patients whom underwent 25 embolizations (2).

Conclusions: Moxifloxacin, with its high degree of biliary excretion even in the setting of obstructive cholangitis (3), is an effective and promising prophylactic antibiotic for prevention of hepatobiliary infection in patients with previous biliary manipulation. Although this single institution study is limited by sample size, there is growing evidence to warrant further trials and investigations for global adaptation. 1. Patel S, Tuite CM, Mondschein JI, et al. Effectiveness of an Aggressive Antibiotic Regimen for Chemoembolization in Patients with Previous Biliary Intervention. Journal of Vascular and Interventional Radiology. 2006;12:965-968. 2. Khan W, Sullivan KL, McCann JW, et al. Moxifloxacin Prophylaxis for Chemoembolization or Embolization in Patients With Previous Biliary Interventions: A Pilot Study. American Journal of Roentgenology. 2011;197:2, W343-W345. 3. Schwab D, Grauer M, Hahn EG, Muhldorfer S. Biliary Secretion of Moxifloxacin in Obstructive Cholangitis and the Non-obstructed Biliary Tract. Alimentary Pharmacology and Therapeutics 2005; 22:417-422.

Poster 71: Radioembolization Time to Treatment: Retrospective Review

C. Chao[1], B. Tolaymat[2]; [1]*Radiology, University of Maryland Medical Center, Baltimore, MD;* [2]*University of Maryland Medical School, Baltimore, MD.*

Objectives: No published literature could be found identifying the average time to treatment for radioembolization procedures. The procedure currently necessitates a mapping arteriogram and SPECT imaging for identification of lung shunts. The time to treatment could potentially impact the disease process and outcomes. One manufacturer offers Ship Treat Access Program to decrease the time from mapping to treatment by offering a method to perform the mapping and treatment in the same week. For the other manufacturer, a prominent researcher is evaluating the need for mapping arteriograms before treating certain patient populations. To evaluate the potential benefit of these programs, we performed a retrospective review of all radioembolizations performed at our institution from 2013 to 2017.

Methods: Review of medical charts and imaging was performed for all radioembolization and related procedures performed at our institution from 2013 to 2017. Patient diagnosis, procedure, Tumor Board notes, Interventional Radiology clinic notes and Radiation Oncology clinic notes were reviewed.

Results: A total of 237 patients charts were reviewed. There were 212 patients treated with SIR-Spheres and 25 patients treated with Theraspheres. For all radioembolizations, the mean time from mapping arteriogram to first treatment and the overall mean time from consult (or tumor board meeting) to first treatment was 16.8 days and 49.4 days, respectively. The average time from consult to mapping arteriogram, time from mapping arteriogram to first radioembolization and time from first treatment to second treatment was 27.3, 16.8 and 36.5 days for all radioembolizations; 26.8, 15.6 and 36.4 days for SIR-Spheres; and was 31.0, 26.2 and 39.2 days for Theraspheres ($p = 0.03$, $p < 0.01$, $p = 0.5$), respectively.

Conclusions: In our series performed at a large academic center, the average time from consult to mapping arteriogram and time from mapping arteriogram to first radioembolization were significant on average 27 days and 17 days respectively. Valuable time can potentially be saved by eliminating the mapping arteriogram or decreasing the time from mapping arteriogram to first treatment.

Poster 72: Safety of Percutaneous Microwave Tumor Ablation in Patients with Implanted Cardiac Devices: A Single Center Retrospective Review

J. Swietlik, K. Longo, E.A. Knott, F.T. Lee, J.L. Hinshaw, S. Wells, M. Lubner, C. Brace, T. Ziemlewicz; *Radiology, University of Wisconsin-Madison, Grafton, WI.*

Objectives: When utilizing radiofrequency ablation in a patient with an implanted cardiac device, programming mitigation is recommended to minimize interaction of the radiofrequency energy with the device. Microwave (MW) ablation theoretically does not carry this same risk given the difference in energy delivery; however, this has not been studied in the clinical environment. The purpose of this study was to retrospectively evaluate patients with implanted cardiac devices who were treated with microwave ablation without programming mitigation.

Methods: An institutional database was queried for all percutaneous ablations performed from January 2011 through July 2017. A total of 13 MW ablations were performed on 12 patients with an implanted cardiac device (one patient underwent 2 procedures). No programming mitigation was performed for any of the procedures. A chart review was performed to assess for any changes in EKG activity or device complications during or immediately after the procedure. Additionally, CT imaging obtained prior to and during the procedure was reviewed to measure tumor size, tumor to implanted cardiac device distance, tumor to device leads distance, and ablation zone dimensions.

Results: MW ablations consisted of: 7 kidney, 5 liver, and 1 lung tumor. The tumors ranged in size from 1.3 - 4 cm in largest dimension. The mean tumor-to-pacemaker distance was 25 cm (range: 9-30 cm), and the mean tumor-to-leads distance was 12 cm (range 3.5 - 20 cm). No device based complications were identified during any of the 13 ablations. Throughout 12 of the 13 percutaneous microwave ablations the patients remained in sinus rhythm, and during 11 of the 13 procedures patients had no changes to the EKG tracing. At the end of one procedure minimal ST-segment elevation was noted by the anesthesiologist. The patient was monitored for 24 hours, and three consecutive troponin measurements were negative. One patient had an episode of bradycardia, and a subsequent consultation from a cardiac electrophysiologist deemed the bradycardia normal due to the patient's device settings. There were no SIR class C or higher complications for any of the patients.

Conclusions: MW ablation, when performed in patients with implanted cardiac devices without programming mitigation, was safe with no associated significant arrhythmias or cardiac events in this retrospective single-center study.

Poster 73: The Use of Irreversible Electroporation for the Treatment of Epithelioid Hemangioendotheliomas of the Liver: A Case Series Report

M. Shnayder, R. Kuker, G. Narayanan; *University of Miami Miller School of Medicine, Miami, FL.*

Objectives: Epithelial hemangioendothelioma (EHE) is a rare vascular malignancy with limited treatment options. After EHE progression, 5-year overall survival is 24% (median survival 1.3 years). The purpose of this case series is to describe the tumor responsiveness and complication profile associated with percutaneous irreversible electroporation (IRE) for the treatment of hepatic EHE.

Methods: This retrospective study included 6 patients (4 female, 2 male; mean age 34.5 years) with biopsy-proven EHE who received percutaneous computed tomography (CT)-guided IRE. A total of 31 lesions (average diameter 28.1 mm) were treated with 6 lesions retreated (3 lesions with 2 retreatments and 3 lesions with 3 retreatments). The primary objective was to assess lesion responsiveness as determined by mRECIST criteria and percent change in size. Follow-up included CT or MRI within a range of 30 to 385 days (mean 104 days) thereafter. All adverse events (AEs) were recorded and graded according to the National Cancer Institute CTCAE V4.0.

Results: After initial treatment, 87% of lesions responded (14.8% complete response [CR], 85.2% partial response [PR]) by mRECIST criteria. 66.78% of retreated lesions responded (25% CR, 75% PR). In those lesions with CR on MRI, there was less restricted diffusion in the wall of the lesion in addition to a lack of enhancement. Average percent change in lesion size was -7.42% (SD 18.25) after initial treatment and -3.48% (SD 29.73) after retreatment. Ten lesions had more than a 25% reduction in lesion size from baseline. In this series, there were no treatment-related deaths and no 30-day mortality. Severe adverse events secondary to abdominal pain occurred in 14% (n=2) of treatments with an average length of stay of 1.14 days.

Conclusions: Percutaneous image-guided IRE appears to be a valuable tool for the treatment of the rare vascular tumor, EHE. IRE provides technically successful outcomes, no serious procedural complications, and minimal side effects. Prospective controlled trials will help clarify the role of IRE in the treatment algorithm of EHE patients and help evaluate the use of MRI diffusion imaging in assessing treatment response.

Poster 74: Treatment Of Malignant Inferior Vena Cava Obstruction With Gianturco Z Stents: A Single Center Thirteen Year Experience

Y. Epelboym, C. Fan, M. Stecker; *Radiology, Brigham & Women's Hospital, Chestnut Hill, MA.*

Objectives: To report technical and clinical outcomes in treating malignant inferior vena cava obstruction with Gianturco Z stents

Methods: In this IRB approved study, all patients undergoing treatment for malignant IVC obstruction with Gianturco Z stents from 1/1/2004 to 2/28/2017 were identified through a quality assurance database search. Exclusion criteria included procedures in which non-Gianturco Z stents were used as well as those in which stenting involved veins other than just the IVC. A retrospective review was performed including patient demographics, tumor primary, clinical indications, number and size of stents, technical success, clinical response, and complications

Results: Seventeen subjects (9 female, 8 male) were included. All subjects had lower extremity edema and 88% (15/17) had ascites as indication for treatment. IVC obstruction was caused by hepatic metastases (n = 9; 53%), peritoneal or retroperitoneal metastases (n = 6; 35%), primary hepatocellular carcinoma (n=1; 6%) and primary retroperitoneal sarcoma (n = 1; 6%). Technical success was 100%. The diameter of stents used were 15, 20, and 25 mm and a median of 2 stents (range 1-5) were used per procedure. Mean post treatment survival was 101 days (range 5-607 days), but median post treatment survival was only 28 days. Primary stent patency was 100%. One subject returned with a patent stent, but disease progression caudally, and received an additional stent 52 days later. Pressure gradients were available in 9 of 17 procedures. Mean pre- and post stent gradients were 17.5 mmHg (8-21 mmHg)

and 7.4 mmHg (0-18), respectively. Clinical follow up was available in 65% (11/17) of patients with a median time to follow up of 16 days (range 2-484 days). 64% (7/11) of patients demonstrated improved or resolved lower extremity edema while 36% had unchanged edema (4/11). There were no major or minor complications

Conclusions: Treatment of malignant IVC syndrome with Gianturco-Z stents is a safe procedure offering a high rate of stent patency with good clinical response in a majority of subjects

Poster 75: Ultrasound-Guided Percutaneous Microwave Ablation for Hepatic Alveolar Echinococcosis: A Preliminary Study

J. Guo, G. Hua, X. Zhang, F. Ye, L. Qi, R. Yang; *Interventional Ultrasound, Qinghai Provincial People's Hospital, Xining, China.*

Objectives: To evaluate safety and efficacy of ultrasound-guided percutaneous microwave ablation (MWA) for hepatic alveolar echinococcosis.

Methods: A total of 26 lumps of hepatic alveolar echinococcosis in 21 patients were treated with ultrasound-guided MWA from January 2016 to December 2017 in Qinghai Provincial People's Hospital. The 21 patients were selected based on the following inclusion criteria: (1) For single lesion: diameter ≤ 5 cm; (2) For Multiple lesions: diameter of each lesion ≤ 3 cm, and the lesions' number ≤ 3; (3) For palliative treatment: 5cm < single lesion diameter <10cm. Therapeutic efficacy was assessed by CT imaging, liver function laboratory examination, volume reduction rate, and complication at 1-month, 3-month and 6-month follow-up after MWA treatment.

Results: All of the procedure were technically successfully and the average volume reduction rate of the 26 lumps was 74.1% at 6-month follow-up. After the treatment, the patients'abdominal pain were relieved apparently. And liver functions were not affected by MWA. In addition, 21 lumps (80.8%) were completely ablated with obvious volume reduction and significant calcification (>70%) at 6-month follow-up, and no evidence of recurrence was demonstrated. 5 lumps (19.2%) were partially ablated, with volume reduction and partial calcification (> 50%). Besides, complications and metastasis were not observed.

Conclusions: Ultrasound-guided percutaneous microwave ablation for hepatic alveolar echinococcosis is safe and effective, without apparent complications and metastasis.

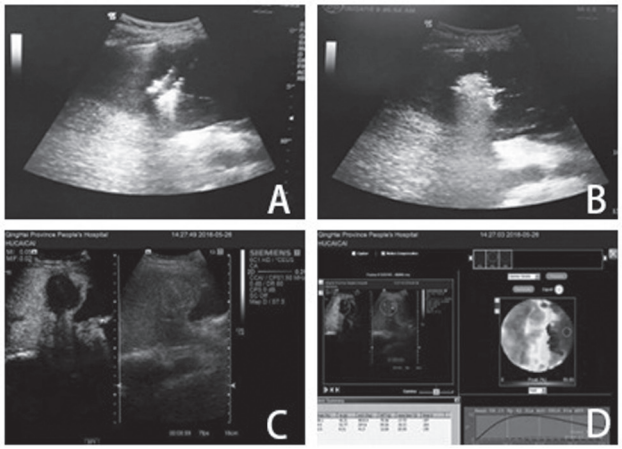

Figure 1. (A) Ultrasound-guided microwave ablation of hepatic alveolar echinococcosis. (B) Hyperechoic region covered the lesion. (C) CEUS showed no blood signal in the lesion. (D) CEUS quantitative analysis showed that the lesion was inactivated completely.

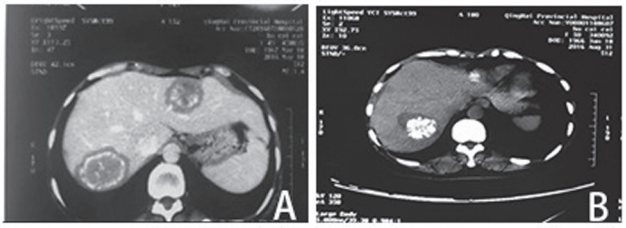

Figure 2. (A) Preoperative CT imaging of hepatic alveolar echinococcosis. (B) The lesions showed complete calcification and apparent volume reduction.

Poster 76: Ultrasound-Guided Radiofrequency Ablation of Morton's Neuroma as Alternative to Surgery

z.u. coskun; *radiology, Giresun medical school, Istanbul, Turkey.*

Objectives: To identify the effectivrness of ultrasound-guided radiofrequency ablation of Morton's neuroma as an alternative to surgical excision

Methods: 26 feet in 25 patients were studied. There were 6 men and 19 women with an average age of 52 years (range 33-73 years). All had tried previous methods of conservative management. Forty percent presented with 2nd space neuromas and 60% with 3rd space ones. All neoromas were seen on magnetic resonance imaging (mri) and ulrasound. Neuromas were ablated after insertion of the radiofrequency (rf) antenna under ultrasound controll. Patients were under deep sedation during the ablation period. Ablation durations were between 4 to 6 minutes acording to the size of the neuroma and under contunious ultrasound control all neuroma's mass were tried to be seen as occupied with gas formed by ablation. After procedures patients were recommended to take paracetamol medication acording to their pain sensatin for 3 to four days.

Results: Prior to treatment, all patients had pain on activity (VAS average:7.0, range 4-9). Post-treatment there was a statistically significant reduction in pain scores (post-RFA VAS average: 1.6, range 0-8, $p < 0.001$). The average overall symptom improvement was 78%. There were three minor complication of temporary nerve irritation. One neuroma (3.8%) have progressed to surgical excision; because of unchanged pain with no obvious cause. At 6 months, All the other feet had a satisfactory outcome.

Conclusions: Ultrasound-guided RFA is an effective and minimal invasive alternative for the treatment of Morton's neuroma in >96% of cases. Only <4% have proceeded to surgical excision. Beeing an outpatient procedure it is a cost and time effective method too

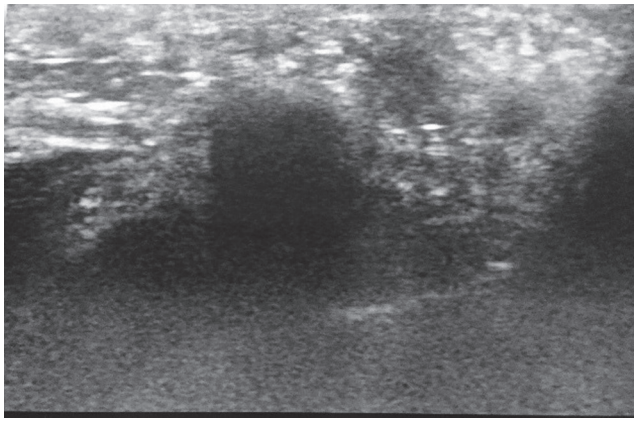

Axila Ultrasound image shows a hypoechoic solid mass between metacarpals

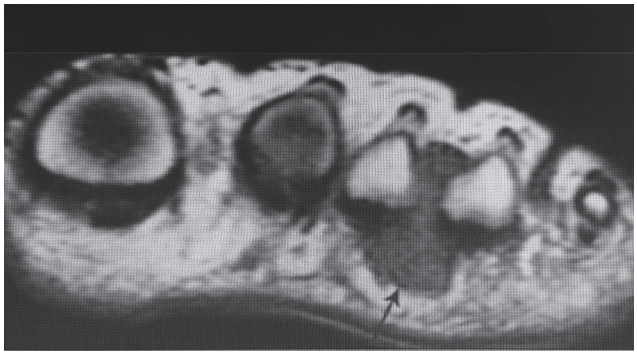

T1 axial mr image shows hypointense mass between 3rd and 4th metacarps

Poster 77: US-Guided Percutaneous Microwave Ablation Assisted by Three-Dimensional Visualization Operative Treatment Planning System and Percutaneous Renal Pelvis Tube Insertion with Intraductal Chilled Saline Perfusion in Urothelial Carcinoma of Renal Pelvis Patients with Isolated Kidney: A Preliminary Clinical Study

X. Li[1], F. Iiu[1], J. Yu[2], Z. Cheng[1], Z. Han[2], X. Yu[1], X. Zhang[3], F. Cao[4], D.E. Dupuy[5], P. Liang[1]; [1]*Chinese PLA General Hospital, Beijing, China;* [2]*Interventional ultrasound, PLA General Hospital, Beijing, China;* [3]*Department of Urology, Chinese PLA General Hospital, Beijing, China;* [4]*Department of Cardiovascular Medicine, Chinese PLA General Hospital, Beijing, China;* [5]*Department of Diagnotistic Imaging, Rhode Island Hospital, Providence, RI.*

Objectives: To assess the clinical effect of US-PMWA assisted by 3D visualization operative treatment planning system and PRPTI-ICSP for UCRP patients with isolated kidney.
Methods: Nine UCRP patients treated by the combination therapy were reviewed. The major outcomes for assessment were renal pelvis complications, local tumor recurrence, tumor-related survival rate and overall survival rate.
Results: Median follow-up period was 17 months. The mean diameter of tumor was 3.1cm±0.5cm. The mean volume of tumor was 8.6±1.5ml. The mean insertion number was 3.3±1.0. The mean session of tumor was 1.2±0.4. The mean time of ablation for per tumor was 531±41s. The mean saline volume used for the PRPTI-ICSP was 206±24ml per patient. Complete ablation were achieved in seven patients by one session and two patients by two. Two patients with local recurrence was detected at 8 and 15 months after ablation, and the 1- and 2- year local tumor progression rates were 11.1% and 22.2%, respectively. One patient aged 82 years old died of heart failure at 12 months after ablation, and tumor-related survival rate was 100%, while the overall survival rates were 88.9%. No severe complications occurred.
Conclusions: US-PMWA assisted by 3D visualization operative treatment planning system and PRPTI-ICSP with safe, convenient, effective and repetitive advantages would be an alternative technique for UCRP patients with isolated kidney, which improve the life quality and clinical efficiency.

Poster 78: Analysis of Therapeutic Effect of Transhepatic Arterial Embolization Combined with Microwave Ablation for Hepatic Epithelioid Hemangioendothelioma

J. Li, T. Zhu, X. Yang, Y. Zhang, J. Zheng; *Hepatic Disease and Oncology Minimally Invasive Interventional Center, Beijing Youan Hospital, Capital Medical University, Bei Jing, China.*

Objectives: To analyze the imaging signs of hepatic epithelioid hemangioendothelioma (HEHE) and the effect of transhepatic arterial embolization (TAE) combined with microwave ablation (MWA) in the treatment of HEHE
Methods: A retrospective analysis of 4 patients with HEHE diagnosed by pathological diagnosis of liver biopsy was performed. The patients underwent TAE, followed by MWA treatment.
Results: The tumors were multiple in 4 cases, and the diameter ranged from 0.6 to 7cm. The imaging signs were different. Plain scan of CT images showed hypodense. MRI scan showed hypointensity on T_1 weighed imaging (T_1WI), isointensity-hyperintensity on T_2 weighed imaging (T_2WI). The enhanced scan was mainly based on peripheral annular enhancement, or uneven enhancement. It can appear "halo sign", "capsule retraction sign" and so on. Digital subtraction angiography (DSA) showed tumor staining in the middle and late stages of the arteries. The tumor staining showed a strong staining in the parenchymal phase, but no central staining. After embolization, lipiodol appeared to be circular or partly deposited. 4 patients were followed up for 12-52 months after TAE combined with MWA, and 1 patients relapsed. There were no recurrences in the remaining 3 cases. No serious complications occurred.
Conclusions: The imaging signs of HEHE were peripheral annular or uneven enhancement. It can appear "halo sign", "capsule retraction sign" and so on. TAE combined with MWA is a safe, minimally invasive and effective method for the treatment of HEHE.

Poster 79: Histological Validation of Histotripsy-Induced Tissue Destruction Monitoring with Ultrasound Feedback

J. Macoskey[1], X. Zhang[1], T.L. Hall[2], J. Shi[3], E. Vlaisavljevich[4], F.T. Lee[5], C.A. Cain[1], Z. Xu[1]; [1]*Biomedical Engineering, University of Michigan, Ann Arbor, MI;* [2]*Biomedical Engineering, University of Michigan, Ann Arbor, MI;* [3]*Department of Pathology, University of Michigan, Ann Arbor, MI;* [4]*Virginia Tech University, Blacksburg, VA;* [5]*University of Wisconsin - Madison, Madison, WI.*

Objectives: Histotripsy is a noninvasive, non-thermal ultrasound ablation technique that uses high-pressure, microsecond-long pulses to generate acoustic cavitation to destroy cells in target tissues. With increasing number histotripsy pulses (i.e., dosage), the target tissue is gradually fractionated into a liquefied necrotic homogenate with no viable cells. As the target tissue becomes more fractionated, the cavitation-induced motion in the tissue changes, which can be detected with an ultrasound imaging feedback technique called bubble-induced color Doppler (BCD). This study analyzes the histological changes of tissue structures with various mechanical properties throughout histotripsy therapy and their correlations with BCD.
Methods: A 112-element, 500-kHz phased histotripsy array is used to generate volumetric lesions within ex vivo bovine liver with dosages between 30 and 1000 pulses-per-location. An L7-4 ultrasound probe is used to acquire BCD signals during all treatment sessions. The linear correlations between the change in BCD time-to-peak rebound velocity (t_{prv}) metric and three histological analytics are calculated using the Pearson correlation coefficient. Histological metrics used in this study represent weak (viable cell count), moderately-strong (remaining reticulin-stained type III), and strong (remaining trichrome-stained type I collagen) components of liver tissue, respectively.
Results: All BCD measurements indicated a mono-directional increase in tissue motion with increasing fractionation. Histological analysis revealed that hepatocytes are destroyed first during histotripsy therapy within the first 200 pulses (<3 min), followed by reticulin-stained type III collagen around 300-500 pulses (10-20 min), and finally trichrome-stained type I collagen between 500-1000 pulses (20-40 min). Only mild portal tract destruction was observed within the first 200 pulses. The change in BCD experienced a statistically significant ($p<0.001$) linear correlation with type III collagen destruction, indicating that structural components directly affect cavitation-induced tissue motion.
Conclusions: Here, we investigated the progression of histotripsy-induced tissue destruction from a histological perspective and found that ablation of structural components correlated with changes in cavitation-induced tissue motion throughout treatment.

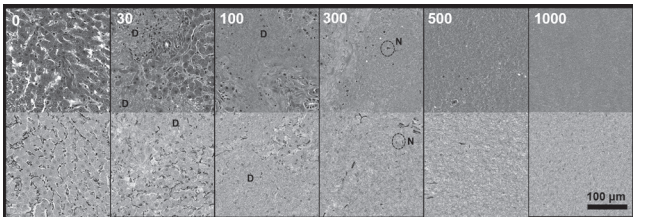

Representative histology of the liver tissue using Masson's trichrome (top row) and Gordon & Sweet's reticulin stain (bottom row) for normal liver (1st column) histotripsy dosages of 30 (2nd column), 100 (3rd column), 300 (4th column), and 1000 (5th column) pulses-per-location. Areas of destruction are marked with a D. Example remnant cell nuclei are marked with an N and a dashed-line circle. Complete tissue homogenization is observed at 1000 pulses-per-location.

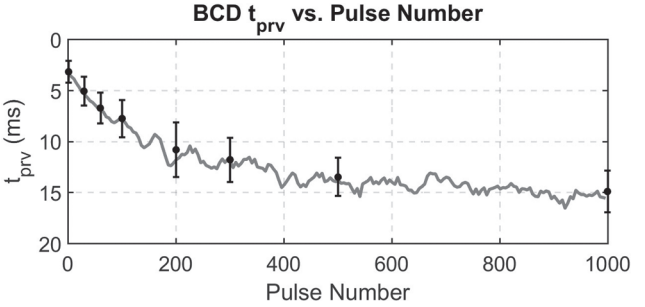

Mean BCD t_{prv} from six 1000-pulse treatments. Gray line indicates a 5-sample moving average. Black points indicate the t_{prv} values at the pulse numbers used to for histological analysis.

Poster 80: Preliminary Research of Advanced Esophageal Carcinoma Treated with Radioactive Gastric Tube with ^{125}I Seeds

H. Niu, X. Zhang, W. Sun, B. Wang, L. Sun, J. Wang, L. Hao; *Minimally invasive surgery, Affiliated Hospital of Shandong Academy of Medical Sciences, Shandong, China.*

Objectives: This study investigates the feasibility, safety and preliminary efficacy of gastric tube with ^{125}I seeds in the treatment of advanced esophageal carcinoma.
Methods: 13 patients of advanced esophageal carcinoma were selected. According to their preoperative CT images, we delineated the target areas in the TPS system, calculated the doses (prescription dose: 60 Gy, ^{125}I seeds radioactivity: 0.6 mCi) and estimated the number of ^{125}I seeds, then we selected the appropriate gastric tubes and fixed the ^{125}I seeds to the outside of the tubes. Under the guidance of C-arm

fluoroscopy X-ray machine, we placed the gastric tubes to the targeted area of the patients and followed up.

Results: All the ^{125}I gastric tubes were successfully planted in the patients. There was no perforation, bleeding or any other complications during the operation, and there was no chest pain, bleeding or pneumonia or any other related complications after the operation. Stooler's dysphagia scores of all the 13patients ranged from 2 to 3 one month after the operations, 8 of which decreased to 0~1 and 4 of which decreased to 1~2 four months after the operation.1patient died basic diseases 3month after the operations.

Conclusions: Gastric tube implanted with ^{125}I particles can provide nutritional support for the patients and inhibit growth of the tumor through radiation treatment inside the body. It is safe and practical for clinical use as a palliative treatment for advanced esophageal carcinoma.

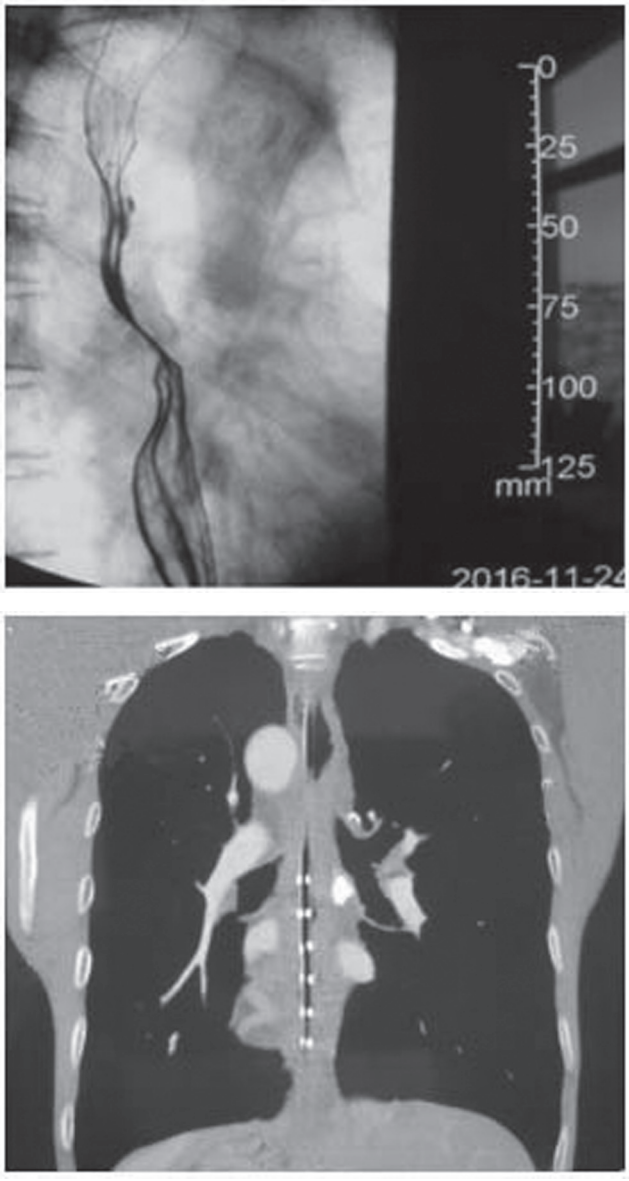

Poster 81: Reduced Non-Target Embolization and Increased Targeted Delivery of Embolization Particles in an Anatomical Arterial Flow Model Using a Novel Microcatheter

M. Tal[1], E. Miller[2], N. Holtzman[2], Y. Zipory[2], T. Dagan[2], O. Harbater[2];
[1]*Assuta Medical Center, Tel Aviv, Israel;* [2]*Accurate Medical Therapeutics LTD, Tel-Aviv, Israel.*

Objectives: The SeQure® microcatheter distal tip has micro pores, smaller than the Embolization beads, which enable a radial flow of contrast media only designed to utilize fluid dynamics for facilitating fluid dynamics was designed to facilitate a safer and more efficient embolization procedure. This paper is aimed to determine the effect of this novel catheter on Embolization safety and efficacy in a flow model, when compared to standard microcatheters.

Methods: Bench tests were conducted with a physiological flow simulator, which simulates the flow rates and pressures in anatomical arterial models with simulated tumors. Three SeQure® microcatheter models, 2.4, 2.7 and 2.8 Fr were comparatively tested against standard microcatheters during injection of microspheres in several sizes in the range of 75-700 micron. The test was performed on N=11 units from each tested SeQure® model (total of N=33 units). The parameters tested were the volume of embolic beads delivered to the target and non-target vessel during a full embolization process and the minimal injection flow rate causing beads to reflux for a vessel flow rate of 4±2 cc/min (near-stasis state). The reflux injection flow rate difference was calculated in percentages, in direct comparison between the SeQure® and a standard microcatheter.

Results: The SeQure® microcatheter delivered more than 3 times the amount of embolic material, while maintaining a reduced risk of reflux. The injection flow rate until reflux was higher when using the SeQure® microcatheter, compared to other commercial microcatheters. The difference in the reflux injection flow rates varied depending on the tested catheter model and beads sizes (Table 1). The lowest average flow rate difference was 77% for the 2.8Fr model when using 75-150 μm beads and the highest average difference was over 190% for the 2.7 Fr model when using 100-300 and 300-500 μm beads. The 2.4 Fr model showed better flow performance in smaller beads size (75-150 and 100-300 μm) than in the 300-500 μm beads. The 2.7 and 2.8 Fr models showed better flow performance in the 100-300 and 300-500 μm beads size than in the 75-150 μm. Beads in the size of 500-700 μm were only tested in the 2.8Fr model since it is the only model compatible for this bead size range.

Conclusions: The SeQure® microcatheter has shown in this model that it is capable of lowering the risks of beads reflux and non-target embolization and increasing the delivery of embolization particles.

Table 1: Summary of the average and standard deviation of the beads reflux flow rate difference between the Accurate Medical microcatheter and a standard microcatheter, for each tested bead size, and for different catheter models.

Beads Size	Catheter Size	Average Beads Reflux Flow Rate Difference	Standard Deviation of Beads Reflux Flow Rate Difference
75-150 μm	2.4 Fr	156%	45%
	2.7 Fr	96%	26%
	2.8 Fr	77%	22%
100-300 μm	2.4 Fr	150%	20%
	2.7 Fr	190%	48%
	2.8 Fr	185%	17%
300-500 μm	2.4 Fr	115%	27%
	2.7 Fr	194%	42%
	2.8 Fr	157%	55%
500-700 μm	2.8 Fr	137%	30%

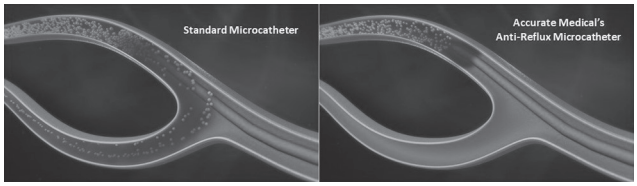

Figure 1: Left image – Non-target embolization in a standard microcatheter. Right image – Radial flow of contrast media through the Accurate Medical microcatheter distal tip micro pores reduces the risk of beads reflux and non-target embolization

Poster 82: Regional Transarterial Chemoembolization with Gelatin Sponge Microparticles for Treatment of Child-Pugh A Stage Hepatocellular Carcinoma Patients with Portal Vein Tumor Thrombosis : A Safety Study

Z. Yuewei; *Interventional Radiology Therapy Center, Beijing Tsinghua Changgung Hospital, Beijing, China.*

Objectives: Gelatin sponge particles (GSP) are widely recognized as temporary agents in embolization procedures involving hepatocellular carcinoma(HCC) and considered as an temporary agent to treat for liver cancer. However, the uniform and irregular gelfoam powders were shown to be associated with complications, such as biliary stricture, liver abscess, gallbladder infarction. In this study, TACE combined with gelatin sponge microparticles (GSMs), a new gelatin sponge material with a diameter of 350 to 560um, treat for Child-pugh A stage HCC patients with portal vein tumor thrombosis (PVTT). GSMs-TACE can be used to perform complete embolization of the regional tumor-feeding arteries and cause less damage to hepatic function. The results revealed the safety of GSMs-TACE treatment for Child-pugh A HCC patients with PVTT.

Methods: Between October 2010 to September 2017, 24 HCC patients with Child-pugh A and PVTT underwent GSMs-TACE were retrospectively analyzed. Statistical analysis, including the serum levels of albumin(ALB), alanine aminotransferase (ALT), aspartate aminotransferase (AST), total bilirubin(TBIL) and prothrombin time(PT) were performed before and 30d after GSMs-TACE. The National Cancer

Institute Common Terminology Criteria for adverse events were used to categorize complications.

Results: There were no significant differences in levels of ALB, ALT, AST, TBIL and PT between pre- and 30d post-GSMs-TACE (P> 0.05). No severe complications associated with GSMs-TACE procedure, including arterial vasospasm, pulmonary embolization, tumor rupture, upper gastrointestinal bleeding and bile duct damage, were observed in 30d after GSMs-TACE.

Conclusions: GSMs-TACE treament for HCC patients with Child-pugh A and PVTT was well tolerated with an acceptable safety profile.

Table 1 Changes of levels of ALB, ALT, AST, TBIL and PT in serum.

	pre- GSMs-TACE	30d post-GSMs-TACE	t	p
ALB(g/L)	39.73±5.79	37.73±6.01	1.661	0.112
ALT(U/L)	17.68±7.02	18.19±7.66	0.378	0.709
AST(U/L)	59.20±26.40	46.93±23.33	1.876	0.082
TBIL(μmol/L)	63.93±43.04	61.13±25.88	1.161	0.265
PT(s)	12.48±1.28	12.94±1.64	1.639	0.119

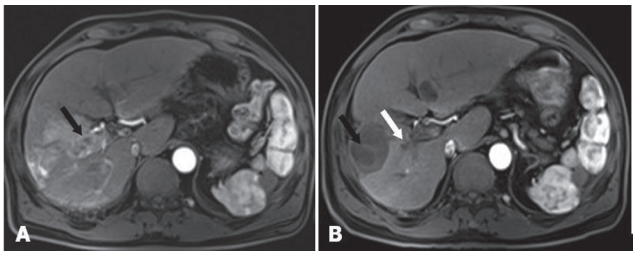

Fig A. A 65-year-old male patient with hepatocellular carcinoma and portal vein tumor thrombosis. MRI imaging shows a 6-cm enhanced tumor (black arrow) and portal vein tumor thrombus mass (white arrow) in the right hepatic lobe. Fig B. MRI at six-month after three GSMs-TACE procedures shows the nonenhanced tumor (black arrow) and portal vein tumor thrombus (white arrow), indicating a complete response by mRECIST criteria.

Poster 83: Risk Factors for Bile Duct Injury After Percutaneous Thermal Ablation of Malignant Liver Tumors: A Retrospective Case-Control Study

X. Xie[1], M. Lin[2]; [1]*Interventional Ultrasound, The First Affiliated Hospital, Sun Yat-sen University, Guangzhou, China;* [2]*Department of Medical Ultrasound, Institute of Diagnostic and Interventional Ultrasound, Guangzhou, China.*

Objectives: To evaluate the risk factors of intrahepatic bile duct injury after ablation of MLTs, and to evaluate the minimum safe distance for ablating tumors abutting bile ducts.

Methods: Sixty five patients with intrahepatic bile duct injury after ablation of MLTs, and 65 controls were recruited. Risk factors for intrahepatic bile duct injury were analyzed. Tumor location was recorded as ≤5 mm (group A), 5-10 mm (group B) and >10 mm (group C) from the right/left main duct or segmental bile duct.

Results: Ascites history(P<0.001), TACE treatment history(P=0.025), intrahepatic bile duct dilatation before ablation(P<0.001), and tumor location (P=0.000)were identified as significant risk factors for intrahepatic bile duct injury. Significant differences in the risk of intrahepatic bile duct injury were found between groups B and C (P=0.000), but not between groups A and B (P=0.751). Ascites history(P=0.002), and tumor location(P<0.001)were independent predictors with the OR (95% confidence interval) of 39.31(3.95-391.69) and 16.56 (5.87-46.71), respectively.

Conclusions: Bile duct injury after ablation of MLTs was the result of local treatment-related factors combined with the patients' general condition. The minimum safe distance for ablation of tumor abutting a bile duct was 10 mm.

Poster 84: The Role of a New Type of Curved Electrode with Controllable Direction for the Treatment of Tumors Behind Hepatic Vessels

A. Jiang, S. Wang, W. Yang, K. Zhao, H. Wu, X. Bai, K. Yan, M. Chen; *Ultrasound, Peking University Cancer Hospital, Beijing, China.*

Objectives: To investigate the value of a new type of curved electrode with controllable direction for the ablation of tumors behind great hepatic vessels.

Methods: In vitro experiment, 3cm conventional multipolar electrode (umbrella group), conventional monopolar (monopolar group) and new curved electrode (curved group) were used for performing ablation in bovine liver respectively (n=6). The ablation area, length and width, shape of ablative necrosis were calculated at the gross pathology samples. Then, 10 beagle dogs were used in the vivo experiment. Visual tumor target in the deep site of hepatic vessels was set up and the different electrodes were used for ultrasound guided liver ablation (n=6). The ablation area, target coverage rate and percentage of normal tissue injury were calculated respectively.

Results: In vitro, the mean ablation time of umbrella group and curved group were 8.5±3.6 min and 9.4±1.6 min respectively (p=0.715). The necrosis area had the shape of sphere in the umbrella group and semilunar in shape in the curved group. The average ablation area was 9.4±1.0 cm^2, the length 4.2±0.3cm and the width 3.8±0.4cm in the umbrella group and were 7.4±0.8cm^2, 4.2±0.6cm, 2.6±0.1cm in the curved group respectively. The ablation area and width of the two groups were statistically significant (p=0.009, p=0.000). In vivo, the average ablation area was 11.1±0.2 cm^2, the target tissue damage area was 7.1cm^2, the target coverage rate was 100%, and the percentage of normal tissue injury was 36.2±1.2% in the umbrella group. And the results were 8.7±0.3cm^2, 7.1cm^2, 100%, and 12.6±2.0% in the curved group, and were 9.3±1.1cm^2, 7.1cm^2, 80.9±1.7%, and 37.7±8.2% in the monopolar electrode group. The normal tissue damage area of curved group was smaller than that of umbrella group (p=0.000). The target coverage rate of curved group was better than that of monopolar group (p=0.000). After treatment, the rate of bleeding in the umbrella group was 3.3% (2/6), and there was no obvious bleeding in the curved group.

Conclusions: The novel curved electrode with controllable direction could achieve accurate targeted ablation, and is especially suitable for tumors with risky anatomical location in the liver.

Poster 85: Usability, Safety and Efficacy of a Novel Microcatheter for Reducing Non-Target Embolization

M. Tal[1], O. Harbater[2], N. Holtzman[2], T. Dagan[2], J. Cashdan[2], E. Miller[2]; [1]*Assuta Medical Center, Tel Aviv, Israel;* [2]*Accurate Medical Therapeutics LTD, Tel-Aviv, Israel.*

Objectives: The purpose of this paper is to evaluate the efficacy, safety and clinical usability of Accurate Medical's microcatheter. The device utilises fluid dynamics to minimise the risk of embolization bead reflux and non-target embolization and provides superior mechanical capabilities.

Methods: The usability, efficacy and safety of 26 units of Accurate Medical's microcatheters were evaluated in 12 female swines, by 4 experienced interventional radiologists. The devices were evaluated during standard embolization procedures which were carried out in the hepatic, renal and subclavian vasculatures. The manoeuvrability, mechanical characteristics and overall usability were recorded in questionnaires during the procedures. The safety of the Accurate microcatheter was evaluated through gross pathology and histopathological testing. Embolization efficacy assessment and identification of non-target embolization were performed using pre and post embolization angiography. In all tests, other commercial microcatheters were used for comparison.

Results: The embolization technique with Accurate Medical's microcatheter was identical to regular methods of use of other embolization microcatheters. Usability scores were near perfect, with a mean value of 4.97 (out of 5), with radiopacity, trackability and pushability scoring higher than a commercially available microcatheter. Post embolization angiographic evaluation of Accurate Medical's microcatheter's demonstrated that although reflux to close non-targeted vessels was observed during the embolization, those vessels remained open without any non-target embolization (Images 1 and 2). In the histopathological study, the scoring of different morphological parameters indicated comparable results between the Accurate microcatheter and another commercial microcatheter.

Conclusions: Accurate Medical's microcatheter showed superior mechanical performance compared to a commercial microcatheter and reduced non-target embolization in an animal model. Safety was demonstrated through a histopathological study. The microcatheters high performance capabilities ensure safer, more effective and more efficient embolization procedures. Clinical studies are needed to further quantify the catheter's performance.

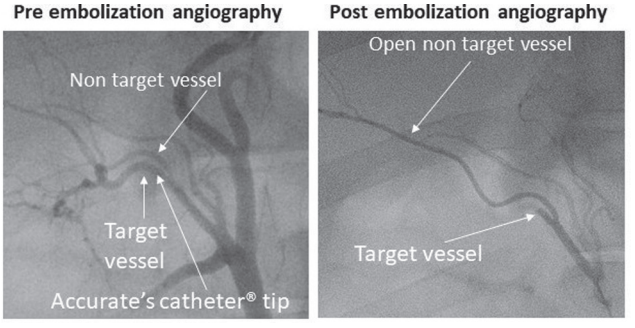

Image 1: Targeted embolization with the Accurate Medical microcatheter. Left image: Pre-embolization angiography. Right image: Post-embolization angiography showing the open non-target vessel.

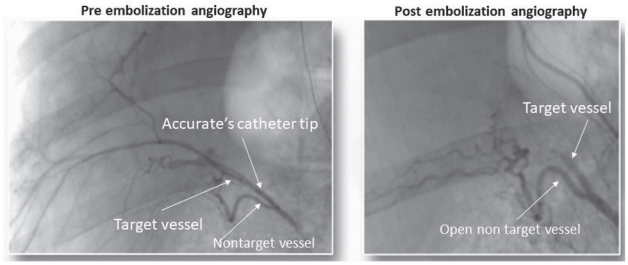

Image 2: Targeted embolization with the Accurate Medical microcatheter. Left image: Pre-embolization angiography. Right image: Post-embolization angiography showing the open non-target vessel.

Poster 86: Clinical Application of CT Guided Radiofrequency Ablation in the Treatment of Lung Metastatic Tumor

X. Zhang[1], Y. Xiao[2]; [1]*Radiology, The PLA general hospital, Bei Jing, China;* [2]*Interventional Division, Radiology, Chinese PLA General Hosipital, Beijing, China.*

Objectives: To discuss the clinical value of CT guided radiofrequency ablation in lung metastases diagnosis and treatment.
Methods: From June 2015 to June 2016, 69 patients were treated with CT-guided radiofrequency ablation in 83 lung metastatic lesions. 42 cases of male, 27 cases were female, aged 17.0 ~ 83.0, the median age is 46.0 years, all lesions diameter < 3 cm. In 58 cases, 17G radiofrequency ablation needle puncture was applied to the lesion directly under CT guidance, 11 patients was done the biopsy by 16G puncture needle before RF ablation. The ablation power range was 40 ~ 120W, and the ablation time was 12~25min, and the effect was evaluated by follow-up images.
Results: All operations were successfully carried out. 79 lesions was necrosis completely after RFA treatment(79/87,90.8%), postoperative row CT check regularly, 1 month shows an uniform consolidation shadow density of ablation zone, long-term follow-up volume are different degree of progressive narrowing, a fiber a funicular, nodular and hollow cylindrical shape change. Eight lesions were observed with nodular enhancement on the margins, after RFA ablation again, 7 of them were inactivated completely and 1 was still increasing. There were 12 patients with a small number of pneumothorax after operation, 6 patients with large number of pneumothorax, 8 patients with small hemorrhage, no serious complications.
Conclusions: The CT guided percutaneous radiofrequency ablation is safe and effective in the treatment of pulmonary metastasis, and has high clinical value.

Poster 87: Clinical Application of CT-Guided Radiofrequency Ablation Combined with Biopsy Synchronously to Multiple Small Nodules of Metastatic Tumors in Lung

X. He, Y. Xiao; *Radiology, Chinese PLA General Hospital, Beijing, China.*

Objectives: To investigate the therapeutic efficacy and safety of CT-guided radiofrequency ablation(RFA)combined with biopsy synchronously to multiple small nodules of metastatic tumors in lung.
Methods: In the past two years, 29 patients in our hospital with 52 lesions were divide into two groups(all the lesions were less than 1 centimeter). Group A 16 patients with 29 lesions were located in the lung periphery and far away from the blood vessels which underwent biopsy prior to RFA. Group B 13 patients with 23 lesions located in the middle and inner side of lung adjacent to the vasculatures underwent RFA prior to biopsy. The number of ablation nodules are 1 to 3. Two groups of patients were followed up in 1-12 months to observe the changes after ablation of ablation lesions.
Results: All the procedures were completed successfully. The intraoperative CT scanning showed the ablation zones were completely covered by the indicative 'halo sign' respectively. 1 of 16 patients in Group A was suffered a lot of hemoptysis with a volume of 200ml. 8 patients had slight or mild hemoptysis with the volumes from 10 to 50ml. One patient pneumothorax were developed during operation. Two patients had a delay slight pneumothorax. According to the pathologic results,4 patients proved to be metastatic squamous carcinomas,9 adenocarcinomas,and due to the small nodules, the malignant tumor cells were founded in the rest of 2 cases but the specific types were not distinguishable.,1 case has inflammatory cells infiltration, no tumor cells being found. Group B,2 of 13 patients had slight hemoptysis with the volume of less than 20ml,3 had developed pneumothorax,2 had a delay pneumothorax), 1 needed a drainage by catheter. Pathologic results demonstrated 3 metastatic squamous carcinoma,8 adenocarcinoma,and 2 was absent of evident tumor cells,only carbon deposition can be founded. Both patients in 2 groups had hypertensity ablation zones on their 1-month postoperative CT without enhancement. 3-and 6-postoperative CT illustrated a decrease of lesions,12-month postoperative CT showed the lesions turned to fibrous stripes.
Conclusions: The method of CT-guided radiofrequency ablation(RFA)combined with biopsy synchronously to multiple small nodules of metastatic tumors in lung are safe and effective,for the lesions located in the middle or inner side of lung,RFA prior to the biopsy can avoid a lot of hemoptysis and the biopsy results were not affected by ablation.

Poster 88: CT-Guided Conformal Cryoablation for NSCC

Y. Xiao[1], X. Zhang[1], Y. Wei[2], X. He[2]; [1]*Interventional Division, Radiology, Chinese PLA General Hosipital, Beijing, China;* [2]*Radiology, Chinese PLA General Hospital, Beijing, China.*

Objectives: To define the the efficacy and safty of this technique with 17G cryoprobes performing conformal cryoablation for NSCC with size < 3cm.
Methods: Totally 96 patients with NSCC confirmed pathologically with CT guided biopsy, among them 61 male patients and 35 female patients, the age from 49-82. The diameter of all lesions measured less than 3 cm. With the IG4 navigation system, CT-guided percutaneous conformal cryoablation was performed, and 2-4 probes of 17G were used according to the size and location of the lesion, the cryoprobes were inserted to the margin of the lesion to create double-needle clamping or bounding sphere cryoablation. Two freeze-thaw cycles (15-minute freeze, 3-minute thaw) was used. The procedure was performed with local anesthesia. CT scans were performed every 5 min during the procedure to monitor the formation of ice balls untill the GGO was found surrounding the tissues which present the ice ball covered the tumor completely. After the probes were removed, a CT scan (5 mm in thickness) was performed again to observe the potential complications.
Results: Two or four probes were inserted to the target successfully, severe complications were not observed in all of patients. 21 patients had hemoptysis, 18 patients had pneumothorax, and 9 of them were treated with close drainage. The enhanced CT scan was performed at month3, 6, 12, and 24 after operation for follow-up. 87 patients CT examination revealed the diameter of tumor was 1.91 cm±0.51, 1.52 cm±0.38, 1.39 cm±0.39, and 1.34 cm±0.36 respectively after operations, 6 patients with the stable size of the lesions without enhancement, 4 patients CT demonstrated there was recurrence.
Conclusions: CT-guided percutaneous conformal cryoablation of NSCC with IG4 guiding system is a safe and effective method, two to four probes symmetrically distributed on the edges of a lesion to create double-needle clamping or bounding sphere cryoablation which could ensure to destroy the lesion completely.

Poster 89: CT-Guided Hook-Wire Localization Facilitates Video-Assisted Thoracoscopic Surgery of Pulmonary Ground-Glass Nodules

C. Li, B. Liu, H. Jia, H. Meng; *Department of Radiology, Qilu Hospital of Shandong University, Jinan, China.*

Objectives: To investigate the efficiency and safety of utilizing CT guided hookwire to locate pulmonary ground-glass nodules (GGNs) prior to video-assisted thoracoscopic surgery (VATS).
Methods: This study was approved by the Ethics Committee of Qilu Hospital of Shandong University. Thirty consecutive patients (14 females and 16 males) underwent preoperative CT-guided hookwire placement from April 2016 to December 2017. The indications for CT-guided hookwire localizations were these patients with suspected malignant GGN: persistent GGN, part-solid GGN, or newly-presented GGN with extrathoracic malignant tumor history. A 21-G hook-wire system was employed to locate all the GGN lesions under CT guidance (Figure 1). VATS was performed immediately after hook-wire placement within 1h. Patients and nodules characteristics were recorded. And procedure time and complications were recorded. All the data were analyzed by SPSS 15.0 (SPSS Inc., Chicago, IL). Student's t test was used to analyze continuous variables. The $\chi 2$ test was used to compare categorical variables between groups
Results: The hook-wire was positioned successfully in all 30 pulmonary GGNs within mean time of 11 minutes (8-20 minutes, SD: 2.5). The 30 GGNs included 14 pure GGNs and 16 part-solid GGNs. The mean size of the GGNs was 0.8 cm (range 0.5 -1.8 cm) and the mean lesion distance to the pleural surface was 1.5 cm (range 0.2-5 cm). There were 8 nodules located in the right upper lobe, 4 in the right middle lobe, 5 in the right lower lobe, 8 in the left upper lobe and 5 in the left lower lobe. In 11 cases, the hook-wire directly penetrated the nodule. In the other 19 cases, the hookwire passed alongside the nodule less the 1.0cm from the GGN.The hookwire localization time of lower lobular GGN was significant longer than upper lobular GGN.In terms of complications, asymptomatic minimal pneumothorax was observed in 6 patients (20 %) without further interventions. Focal pulmonary haemorrhage along the puncture tract was seen in 5 cases. Pathologically, 12 part-solid GGNs were invasive adenocarcinoma; 8 part-solid GGN were MIA; 8 GGO were AAH. 8 GGO and 2 part-solid GGN were metastasis (1 from breast cancer and 1 from esophageal cancer). 2 were benign lesions (focal inflammation).

Conclusions: CT-guided pulmonary GGNs localisation prior to VATS could facilitate safe, accurate surgical guidance for the localisation of small GGNs.

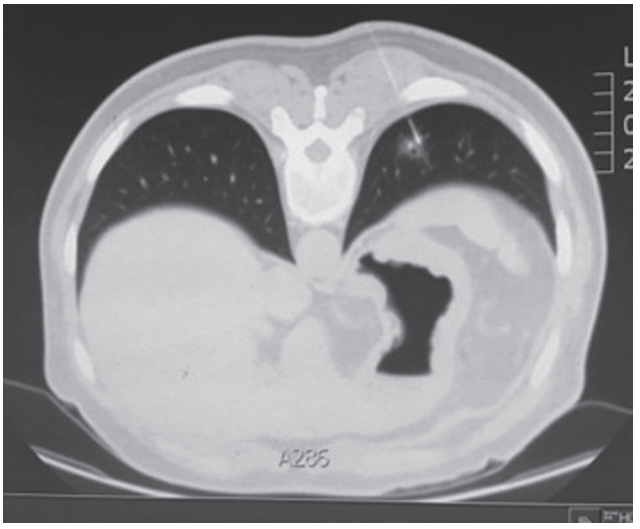

Figure 1. CT image of hook-wire localization of a 59-year man before VATS. The GGN was confirmed to be an invasive adenocarcinoma.

Poster 90: Radiofrequency Ablation and Particle Implantation Caused Increased Circulating Cell-Free DNA in Plasma but not Tumor Dissemination

X. He[1], Y. Xiao[2]; [1]*Radiology, Chinese PLA General Hospital, Beijing, China;* [2]*Interventional Division, Radiology, Chinese PLA General Hosipital, Beijing, China.*

Objectives: Radiofrequency ablation and particle implantation technologies are currently widely used for tumor treatment because they directly target local lesions through minimally invasive approach. However, whether the operation could increase the possibility of tumor dissemination has not been fully elucidated.
Methods: In this study, 12 patients with non-small cell lung cancer (NSCLC) who experienced radiofrequency ablation or particle implantation treatment were studied. For each patient, we collected a tumor tissue sample, as well as 2 plasma samples 2 hours before and after treatment for circulating cell-free DNA (cfDNA) extraction, and conducted next generation sequencing (NGS) of 416 cancer-related genes on these samples. Four of these patients were regularly followed up for 50 days and their plasma samples were collected for dynamic monitoring.
Results: Among the 12 patients, 7 patients with smaller lesions were treated by radiofrequency ablation and 5 patients with larger lesions were treated with particle implantation. The cfDNA quantification before and after treatment showed that cfDNA content increased (> 10%) in 7 (58.3%) patients, unchanged (=10%) in 4 patients (33.3%), and decreased (< 10%) in 1 patient (8.3%). NGS results of tumor tissues found that all 12 patients had tumor-specific gene alterations. However, in pre-treatment cfDNA, 7 patients with smaller lesions and received radiofrequency ablation had no detectable gene alterations, while 3 of 5 patients with larger lesions and received particle implantation were detected with tumor-specific mutations and the mutation allele frequency were decreased 2 hours after treatment. 4 patients that had been monitored for 50 days after treatment demonstrated significantly decreased cfDNA concentration.
Conclusions: The detection rate of ctDNA mutation is significantly correlated with tumor size. The increased cfDNA content in plasma after radiofrequency ablation and particle implantation may be due to the increase of cfDNA release in normal cells, rather than the dissemination of tumors.

Poster 91: Therapeutic Thoracentesis: IR & DR Attending Survey via ACR Engage & SIR Connect Online Forums

D.G. Mackey, A. Gill, G. McLennan, A. Malik, M. Shahin, A. Singleton, A. Gupta, N. Chauhan, C. Martin, P. Bayona Molano, A. Levitin; *Imaging Institute, VIR, Cleveland Clinic, Cleveland, OH.*

Objectives: Therapeutic thoracentesis is one of the most commonly performed image-guided procedures, and available online and in-print are quality resources regarding clinical decision making and technique. However, wide variation in practice preferences undoubtedly exists among practitioners, presenting challenges from a quality and outcomes study perspective. The purpose of this study is to survey physicians in an effort to begin to quantify variance surrounding this common procedure.
Methods: Between October 12, 2017 and January 8, 2018, approximately 44,200 attending-level Interventional Radiologists and Diagnostic Radiologists were electronically sent a 10-question survey regarding therapeutic thoracentesis via two popular online physician forums: ACR Engage (American College of Radiology) and SIR Connect (Society of Interventional Radiology).
Results: A total of 316 physicians (182 IR, 134 DR) answered the survey (0.7% response rate). For unilateral thoracentesis, 93 respondents (29%) reported a drainage volume cut-off of 1.5L, while 72 (23%) reported a 2L cutoff, and 65 (21%) reported no volume cutoff. For bilateral thoracentesis, 26 respondents (8.3%) reported a total 2L cutoff, while 228 (72.4%) reported that they do not usually perform bilateral thoracentesis in a single session. 213 (68%) respondents reported a preference for bedside thoracentesis for patients located in an ICU and/or Stepdown Unit setting. 277 (88%) respondents reported that the etiology of the effusion does not influence the volume they planned to drain. 230 (73%) respondents reported that patient symptoms are most likely to influence their decision to stop draining fluid, while 176 (56%) reported that their pre-determined drainage volume goal provides a similar level of influence in when to stop the procedure. 264 (84%) do not use pleural pressure measurements in stoppage decision making. 188 (60%) always order a chest radiograph of some kind after the procedure. 201 (66%) reported evacuated bottles as their suction device of choice for thoracentesis. 119 (39%) reported at least rarely placing tunneled thoracostomy tubes (Pleurex, Rocket, etc) in patients with transudative effusions, whereas 112 (37%) reported only doing so for patients with malignant or recurrent sterile inflammatory (autoimmune) effusions.
Conclusions: The response rate of 0.7% is below what has been typically reported as an acceptable rate of 10-15%. However, the total number of respondents (316) redeems the value of this study. Interestingly, practice preferences among Interventional and Diagnostic Radiologists varies greatly regarding certain thoracentesis-related clinical decisions, i.e how and whether to evaluate the post-thoracentesis patient with imaging, how much fluid to drain, perception of influences on procedural stoppage, and handling of exudative versus transudative effusions. Question(s) regarding management of acute versus chronic effusion would have been useful. Indeed, certain question designs proved unhelpful in discrimination analysis and clinical import. As expected, response rates fell as respondents neared the tenth question likely due to fatigue or distraction, with an average time of completion of the survey of 6 minutes 21 seconds. Rapid surveys such as this one can prove useful in studying clinically relevant practice topics. Well-designed and high yield questions are of utmost importance, requiring much forethought directed at response analysis. Additionally, providing incentive to the respondent in the survey invitation in the form of visualization of survey results after completion may yield better response rates when surveying a population likely interested in said results.

Poster 92: Using the Biosentry Trace Sealant Device Following Percutaneous Lung Biopsy with Seventeen G Trocar Placement: Does the Device Still Decrease Chest Tube and Pneumothorax Rates?

E. Joiner, W. Foss, Z. Cizman, g. fine, R. O'Hara, R. Hardman; *Radiology, University of Utah, Salt Lake City, UT.*

Objectives: To evaluate whether the use of a hydrogel tract sealant system during percutaneous lung biopsy using an 18 G core biopsy/17 G trocar decreases the rate of pneumothorax and chest tube placement.
Methods: Retrospective review of consecutive patients from August 2016-June 2017 were evaluated for Biosentry use. A comparison of patients from January 2015-July 2016 who would have been eligible for BioSentry™ device based on the biopsy tract length was used. A 17-gauge trocar was advanced into or adjacent to the lung lesion under CT guidance and 18-gauge core biopsies were obtained. Following the biopsy, if the tract to the lesion was at least 1.0 cm, a Biosentry tract sealant device was deployed. If the tract length was greater than 2.0 cm, the entire BioSentry™ device (BioSentry™; Surgical Specialties Corporation (US), Inc.) was deployed. If the tract length measured 1.0-2.0 cm, the BioSentry™ device was cut in half and used. CT images were acquired immediately after deployment of the device. One hour and three hour chest x-rays were acquired. Chest tube was placed by the interventional radiologist if the patient had greater than 10% pneumothorax, symptomatic pneumothorax, or enlarging pneumothorax. The rates of any pneumothorax and chest tube insertion were compared by Fisher exact test.
Results: BioSentry™ was used in 105 patients. Biopsy was performed without BioSentry™ in 386 patients; of these patients, 188 patients had a track length over 1 cm. The rate of pneumothorax evident on chest radiography was 20.9% (n=22) in the BioSentry group versus 37.7% (n=71) in the non-BioSentry group (p=0.0038). The rate of patients requiring chest tube insertion was 7.6% (n=8) in the BioSentry group compared to 12.8% (n=24) in the non-BioSentry group (p=0.2409).
Conclusions: The Biosentry self-expanding tract sealant device has been shown to decrease pneumothorax and chest tube rates when using a 19 G access trocar in lung biopsies. In this study, we have demonstrated a decreased chest tube rate when using the device with a 17 G trocar access as well. The Biosentry device can safely be used in larger lung biopsy cores, which are often needed with the expanded use of biomolecular tests for lung lesions.

Poster 93: Modelization of the Procoagulant and Proangiogenic Balance of Myeloma Plasma Cells

L. Papageorgiou[2], P. Van Dreden[1], S. Thouronde[3], A. Rousseau[1], S. Salta[3], I. Elalamy[2], G. Gerotziafas[2]; [1]*Clinical Research, Diagnostica Stago, Paris, France;* [2]*Service d'Hématologie Biologique, Hôpitaux Universitaires Est Parisien, Assistance Publique Hôpitaux de Paris., Paris, France;* [3]*Cancer Biology and Therapeutics, Centre de Recherche Saint-Antoine, INSERM U938, Institut Universitaire de Cancérologie (IUC), Université Pierre et Marie Curie (UPMC) Faculté de Médecine, Sorbonne Universities, Paris, France.*

Objectives: Introduction: Multiple myeloma is a clonal B-cell malignancy characterized by the accumulation of monoclonal plasma cells in the bone marrow and other tissues. The disease figures among malignancies which significantly increase the risk of venous thromboembolic disease. The interplay between Myeloma Plasma Cells (MPCs) with coagulation and angiogenesis is currently under investigation. It is already known that MPCs present an angiogenic activity through VEGF expression. Whether MPCs express procoagulant and/or anticoagulant proteins remains to be shown. Aim: We looked upon gene expression of tissue factor (TF), tissue factor pathway inhibitor 1 (TFPI1), tissue factor pathway inhibitor 2 (TFPI 2), vascular endothelial growth factor (VEGF A) and thrombomodulin (TM) by MPC.
Methods: Human MPCs (RPMI 8226) and Human Umbilical Vein Endothelial Cells (HUVECs) which were used as the control were cultured according to a standardized procedure. Total RNA was extracted and reversely transcribed as previously described. Briefly, 1 µg cDNA was PCR amplified using the Go TAq® qPCRMaster mix (Promega) and the Mx3000P qPCR system according to the manufacturer's protocol. Quantitative RT-PCR was used to measure the relative mRNA levels using TaqMan assays for VEGF-A, TFPI 1, TFPI 2, TF or TM (Sigma Aldrich). Ct values were normalized against the endogenous control B-Actine (from Sigma Aldrich). Relative mRNA expression was calculated using the method (1/PUISSANCE (2; (Ct (gene)-Ct (endogenous control))).
Results: MPCs exhibited a 4-fold higher TF expression as compared to HUVECs. MPCs showed a significantly lower TFPI1 and TFPI2 expression than HUVECs. In both MPCs and HUVECs the expression of TFPI 1 gene was more pronounced as compared to the expression of TF gene. In contrast, MPCs showed lower TFPI2 than TF expression. The TF/TFPI1 ratio was higher in MPCs, reflecting a potentially increased TF activity as opposed to HUVECs. MPCs expressed TM at similar levels as compared to those of HUVECs. Finally, VEGF expression was significantly higher in MPCs as compared to HUVECs. Results are summarized in Table 1.
Conclusions: Plasmocytes from human multiple myeloma cells are characterized by a marked proangiogenic potential driven by high gene expression of VEGF which is accompanied by increased expression of TF. Hence, TF expression seems to be at least partially compensated by expression of TFPI leading to the assumption that TF-dependent procoagulant properties of plasmocytes are restricted by a balanced increase in TFPI. These data indicate that TF expression by myeloma cells could be an additional pathway leading to cell proliferation rather than a procoagulant mechanism. The balance between TF and TFPI expression by myeloma cells could indicate their aggressiveness and could represent a potential therapeutic target.

Table 1. Relative mRNA expression TF, TFPI, VEGF and thrombomodulin by plasmocytes and normal HUVEC. Values are means±sd of 3 experiments. *p<0.05 versus HUVEC; $p<0.05 versus TF

	TF	TFPI-1	Ratio TF/TFPI-1	TFPI-2	Ratio TF/TFPI-2	VEGF A	THMD
MPCs (%)	0.18±0.01*	1.23±0.02*$	0.15*	0.02±0.001*	9*	37.7±5*	0.8±0.001
HUVECs (%)	0.05±0.001	30±5$	0.001	1±0.01$	0.05	0.2±0.001	1±0.001

Poster 94: New Biomarkers of Hypercoagulability for the Evaluation of Thromboembolic Risk in Ambulatory Patients with Lung Adenocarcinoma. ROADMAP-Cancer Associated Thrombosis Study

G. Gerotziafas[2], P. Van Dreden[1], A. Rousseau[1], I. Evmorfiadis[2], M. Grusse[1], A. Larsen[2], I. Elalamy[4], K. Syrigos[3]; [1]*Clinical research, Diagnostica Stago, Gennevilliers, France;* [2]*Cancer Biology and Therapeutics, Centre de Recherche Saint-Antoine, INSERM U938, Institut Universitaire de Cancérologie (IUC), Université Pierre et Marie Curie (UPMC) Faculté de Médecine, Sorbonne Universities, Paris, France;* [3]*Hellenic Cooperative Oncology Group, Athens, Greece;* [4]*Service d'Hématologie Biologique, Hôpitaux Universitaires Est Parisien, Assistance Publique Hôpitaux de Paris., Paris, France.*

Objectives: Background: The aim of this prospective longitudinal study was to identify the most clinically relevant hypercoagulability biomarkers in lung adenocarcinoma patients for elaboration of an improved risk assessment model (RAM) for venous thromboembolism (VTE).
Methods: Patients and Methods: 150 ambulatory patients with lung adenocarcinoma were prospectively enrolled. Thrombin generation, procoagulant phospholipid-dependent clotting time (Procoag-PPL), tissue factor activity (TFa), factor VIIa (FVIIa), factor V (FV), antithrombin (AT), D-Dimers (DDi), P-selectin and heparanase levels were assessed in platelet-poor plasma (PPP) at inclusion (baseline) and at the end of the 3rd chemotherapy cycle (3rd chemotherapy). Cox regression analysis was used to identify independent VTE predictors.
Results: Results: At baseline, patients had significantly attenuated thrombin generation, shorter Procoag-PPL, higher levels of TFa, D-Dimers and heparanase, and lower levels of FVIIa and P-selectin, compared to controls. A significant increase in Procoag-PPL, FV and FVIIa and a decrease of P-selectin levels were observed between baseline and 3rd chemotherapy. Hospitalization within the last 3 months prior to assessment, time since cancer diagnosis less than 6 months, mean rate index of thrombin generation (MRI) and Procoag-PPL were independently associated with symptomatic VTE. Accordingly, a prediction model including Prociag-PPL and MRI showed significant discriminating capacity (area under the curve/AUC: 0.84).
Conclusions: Conclusion: Ambulatory patients with lung adenocarcinoma may display pronounced blood hypercoagulability due to decreased Procoag-PPL, increased endothelial cell activation and increased degradation of fibrin. Incorporation of Procoag-PPL and MRI of thrombin generation may improve the accuracy of a VTE-RAM in the above setting.

Poster 95: Overall Survival in Fifty-Eight Patients with Metastatic Colorectal Hepatic Tumors Treated with Y90 and Correlation with KRAS

H. Kocharyan[1], A. Rastegarpour[1], C. Bailey[1], L. Karapetyan[2], K. Raval[1], A. Sucher[1], O. Intikhab[1], M. Thant[1], J. Critchfield[1]; [1]*Radiology, Detroit Medical Center, Lansing, MI;* [2]*Michigan State University, Lansing, MI.*

Objectives: We present the survival data of nine-year experience of Y90 treatments for metastatic colorectal cancer to the liver. We also investigated the association between the KRAS positivity and survival.
Methods: Retrospective survival analysis of all patients treated with Y90 Therasphere for metastatic colorectal cancer to the liver was done from 2008 to 2016 at Detroit Medical Center. Out of 69 patients 58 had data available for the overall survival calculated from the date of the treatment to the date of death or present date. The data analysis was performed with SPSS package using survival analysis with Kaplan-Meier and Log rank tools.
Results: Survival data was obtained from 58 patients with metastatic colorectal hepatic tumors undergoing treatment with Y90 therasphere embolization. The median survival was estimated to be 248 days with a standard error of 17.7 (95%CI: 213.2-282.8). None of the patients expired within 30 days of treatment, which by definition would have been considered to be treatment related mortality. 27 (46.6%) were male and 31 (53.4%) were female. The mean age of the patients at diagnosis was 59.9±12.9 years. The mean tumor burden was 29.4% with a standard deviation of 22.1. The total volume of treated liver tissue was 1330.0±689.4 mL. A single treatment was performed for 36 (62.1%) patients, while 22 (37.9%) had multiple treatments. The KRAS analysis results were available for 32 patients. It was negative in 25 (78.1) and positive in 7(21.9) patients. There was no significant difference in survival between KRAS positive and KRAS negative patients (p=0.637).
Conclusions: Our survival results after Y90 Therasphere are comparable to the previously reported data and confirm the survival benefit of Y90 in metastatic colorectal cancer to the liver. No correlation was found between KRAS positivity and survival.

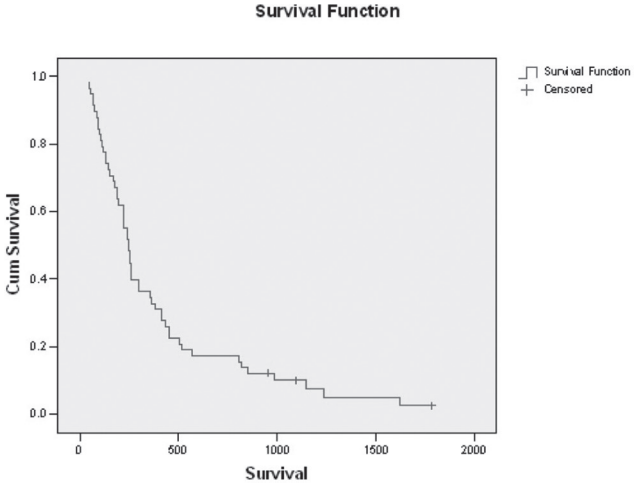

Poster 96: Correlation Between Survival and Response Measured by RECIST, mRECIST and WHO Criteria in Non Resectable HCC Patients Treated with Y90 Microspheres

H. Kocharyan[1], A. Rastegarpour[1], C. Bailey[1], L. Karapetyan[2], A. Sucher[1], O. Intikhab[1], J. Kallini[1], J. Critchfield[3]; [1]*Radiology, Detroit Medical Center, Lansing, MI;* [2]*Michigan State University, Lansing, MI;* [3]*Interventional Radiology, Detroit Metical Center, Detroit, MI.*

Objectives: In our study we aim to demonstrate a correlation between HCC survival and response rate measured by three different criteria in patients with unresectable HCC treated with Y90 microspheres.
Methods: Retrospective analysis of all patients treated with Y90 Therasphere for advanced HCC was done from 2008 to 2016 at Detroit Medical Center. Out of 96 patients 63 had data available for calculating both survival and the response at any time point from the first month follow up after the treatment through the 24th month. The survival was measured between the date of Y90 treatment and date of death. The response to the Y90 treatment was calculated by using RECIST, mRECIST and WHO criteria. The data analysis was performed using SPSS software package with Cox regression.
Results: Partial or complete response using RECIST (p=0.003), mRECIST (p=0.014), and WHO (p=0.015) criteria was directly related to survival for all three methods. The estimated Hazard Ratio for no tumor response to treatment was 2.63 for RECIST, 2.10 for mRECIST, and 3.21 for WHO criteria. Of the patients 46 (73.0%) were male and 17 (27.0%) were female. The mean age at diagnosis was 64.2±8.1 years. The mean tumor burden was 29.7±22.3%.
Conclusions: Statistically significant relationship was found between response rate measured with three different criteria and HCC survival in patients with unresectable HCC treated with Y90. The hazard ration of no response to treatment is highest with the WHO criteria.

Poster 97: Survival Analysis of Thirty-Five Patients with Metastatic Carcinoid Hepatic Tumors Treated with Y90

H. Kocharyan[1], A. Rastegarpour[1], C. Bailey[1], L. Karapetyan[2], K. Raval[1], A. Sucher[1], O. Intikhab[1], M. Thant[1], J. Critchfield[1]; [1]*Radiology, Detroit Medical Center, Lansing, MI;* [2]*Michigan State University, Lansing, MI.*

Objectives: Evaluate the survival outcomes of patients with metastatic carcinoid to the liver treated by Y90 radioembolization.
Methods: Retrospective survival analysis of all patients treated with Y90 Therasphere for metastatic colorectal cancer to the liver was done from 2008 to 2016 at Detroit Medical Center. Out of 53 patients 35 had data available for the overall survival calculated from the date of the treatment to the date of death or present date. The data analysis was performed with SPSS package using survival analysis with Kaplan-Meier and Log rank tools.
Results: Survival data was obtained from 35 patients with metastatic carcinoid hepatic tumors undergoing treatment with Y90 therasphere embolization. The median survival was estimated to be 597 days with a standard error of 210.4 (95%CI: 184.5-1009.5). Two patients expired within 30 days of treatment, which by definition was considered to be treatment related mortality. 18 (51.4%) were male and 17 (48.6%) were female. The mean age of the patients at diagnosis was 55.2±12.7 years. The mean tumor burden was 27.8% with a standard deviation of 22.0. A single treatment was performed for 16 (45.7%) patients, while 19 (54.3%) patients underwent multiple treatments. The mean treated liver volume was 1708.6±1294.5 mL.
Conclusions: Y90 radioemboliation demonstrates survival benefit in advanced carcinoid metastases to the liver and our results are compatible with previously reported results.

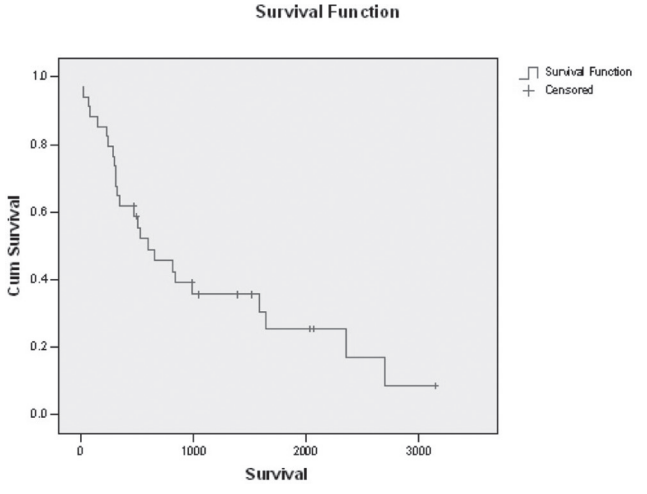

Poster 98: Response Outcomes of Metastatic Carcinoid Hepatic Tumors Treated with Y90 Measured by RECIST, mRECIST and WHO Criteria

H. Kocharyan[1], C. Bailey[1], K. Raval[1], L. Karapetyan[2], A. Rastegarpour[1], A. Sucher[1], O. Intikhab[1], M. Thant[1], J. Critchfield[1]; [1]*Radiology, Detroit Medical Center, Lansing, MI;* [2]*Michigan State University, Lansing, MI.*

Objectives: Evaluate the response after Y90 radioembolization in patients with carcinoid metastases to the liver measured by RECIST, mRECIST and WHO criteria.
Methods: Retrospective analysis of all patients treated with Y90 Therasphere for metastatic carcinoid cancers to the liver was done from 2008 to 2016 at Detroit Medical Center. Out of 53 patients 32 had data available for calculating the response at the last follow-up available, compared to the pretreatment baseline. The response to the Y90 treatment was calculated by using RECIST, mRECIST and WHO criteria. The data analysis was performed using SPSS software package with Chi-Square and Fisher exact tests.
Results: The mean follow-up was 12.0±9.8 months (range 1-24 months). Of 32 patients with metastatic carcinoid hepatic tumors undergoing treatment with Y90 therasphere embolization, complete response was noted in 1 case (3.1%) by RECIST and WHO criteria and 4 cases (12.5%) by mRECIST criteria. Partial response was seen in 10 cases (31.3%) by RECIST and WHO, and 7 cases (21.9%) by mRECIST criteria. Progression was noted in 1 case (3.1%) by RECIST and 2 cases (6.3%) by WHO criteria and no cases by mRECIST criteria. No significant difference was found in response when measured by different methods. 14 patients (43.8%) were male and 18 (56.3%) were female. The mean age of the patients at diagnosis was 55.5±10.3 years. The mean tumor burden was 25.5% with a standard deviation of 20.5.
Conclusions: Our study shows clinical benefit of Y90 trans-arterial radioembolization in advanced carcinoid patients with metastases to the liver. It is useful to note that no significant difference was found when utilizing RECIST, mRECIST or WHO criteria to measure the response.

Poster 99: Response Outcomes After Trans-Arterial Radioembolization with Y90 in Patients with Colorectal Cancer Metastases to the Liver Measured by RECIST, mRECIST and WHO Criteria

H. Kocharyan[1], K. Raval[1], L. Karapetyan[2], C. Bailey[1], A. Rastegarpour[1], A. Sucher[1], O. Intikhab[1], M. Thant[1], J. Critchfield[1]; [1]*Radiology, Detroit Medical Center, Lansing, MI;* [2]*Michigan State University, Lansing, MI.*

Objectives: Evaluate the response after Y90 trans-arterial radioembolization in patients with colorectal cancer metastases to the liver measured by RECIST, mRECIST and WHO criteria.
Methods: Retrospective analysis of all patients treated with Y90 Therasphere for metastatic colorectal cancers to the liver was done from 2008 to 2016 at Detroit Medical Center. Out of 69 patients 41 had data available for calculating the response at the last follow-up available, compared to the first available evaluation. The response to the Y90 treatment was calculated by using RECIST, mRECIST and WHO criteria. The data analysis was performed using SPSS software package with Chi-Square and Fisher exact tests.
Results: The mean follow-up was 9.1±8.0 months (range 1-24 months). Of 41 patients with metastatic colorectal hepatic tumors undergoing treatment with Y90 therasphere embolization, complete response was noted in 1 case (2.4%) by RECIST, mRECIST, and WHO criteria. Partial response was seen in 3 cases (7.3%) by RECIST and WHO criteria, and in 2 cases (4.9%) by mRECIST. Progression was noted in 14 cases (34.1%) by RECIST, 8 cases (19.5%) by mRECIST, and 17 cases (41.5%) by WHO criteria. 17 patients (41.5%) were male and 24 (58.5%) were female. No significant difference was found in response when measured by different methods. The mean age of the patients at diagnosis was 61.8±12.6 years. The mean tumor burden was 28.6% with a standard deviation of 18.7.
Conclusions: Our study shows clinical benefit of Y90 radioembolization in advanced colorectal cancer patients with metastases to the liver. It is useful to note that no significant difference was found when utilizing RECIST, mRECIST or WHO criteria to measure the response.

Author Index

T

U

V

W

X

Y

Z